



INERTIAL NAVIGATION SYSTEM AIDING USING VISION

THESIS

James O. Quarmyne, Second Lieutenant, USAF

AFIT-ENG-13-M-40

**DEPARTMENT OF THE AIR FORCE
AIR UNIVERSITY**

AIR FORCE INSTITUTE OF TECHNOLOGY

Wright-Patterson Air Force Base, Ohio

DISTRIBUTION STATEMENT A.
APPROVED FOR PUBLIC RELEASE; DISTRIBUTION UNLIMITED.

The views expressed in this thesis are those of the author and do not reflect the official policy or position of the United States Air Force, the Department of Defense, or the United States Government.

This material is declared a work of the U.S. Government and is not subject to copyright protection in the United States

AFIT-ENG-13-M-40

INERTIAL NAVIGATION SYSTEM AIDING USING VISION

THESIS

Presented to the Faculty
Department of Electrical and Computer Engineering
Graduate School of Engineering and Management
Air Force Institute of Technology
Air University
Air Education and Training Command
in Partial Fulfillment of the Requirements for the
Degree of Master of Science in Electrical Engineering

James O. Quarmyne, B.S.E.E.
Second Lieutenant, USAF

March 2013

DISTRIBUTION STATEMENT A.

APPROVED FOR PUBLIC RELEASE; DISTRIBUTION UNLIMITED.

INERTIAL NAVIGATION SYSTEM AIDING USING VISION

James O. Quarmyne, B.S.E.E.
Second Lieutenant, USAF

Approved:

Meir Pachter, PhD (Chairman)

Date

John F. Raquet, PhD (Committee Member)

Date

Kenneth A. Fisher, PhD (Committee Member)

Date

Abstract

The aiding of an INS using measurements over time of the line of sight of ground features as they come into view of an onboard camera is investigated. The objective is to quantify the reduction in the navigation states' errors by using bearings-only measurements over time of terrain features in the aircraft's field of view. INS aiding is achieved through the use of a Kalman Filter. The design of the Kalman Filter is presented and it is shown that during a long range, wings level cruising flight at constant velocity and altitude, a 90% reduction in the aided INS-calculated navigation state errors compared to a free INS, is possible.

*I dedicate this thesis to my loving wife, who supported me every step of the way.
I LOVE YOU!*

Table of Contents

	Page
Abstract	iv
Dedication	v
List of Figures	viii
List of Tables	x
List of Symbols	xi
List of Abbreviations	xiv
 1 Introduction	 1
1.1 Background	1
1.2 Motivation	2
1.3 Approach	3
 2 Literature Review	 4
2.1 Introduction	4
2.2 Reference Frames	4
2.2.1 Inertial Reference Frame	4
2.2.2 Earth-Centered, Earth-Fixed Inertial Reference Frame	4
2.2.3 Earth-fixed Reference Frame	5
2.2.4 Navigation Reference Frame	6
2.2.5 The Body Frame	7
2.2.6 Sensor Frame	8
2.3 Coordinate System Transformations	8
2.4 Inertial Navigation	11
2.5 Specific Force and Gravity	11
2.5.1 Specific Force	11
2.5.2 Gravity	12
2.6 INS Equation	13
2.6.1 INS Equations for Common Frames	14
2.6.1.1 Strapdown INS Equation in i-frame	14
2.6.1.2 Strapdown INS Equation in e-frame	14
2.6.1.3 Strapdown INS Equation in n-frame	14
2.7 SLAM	14
2.8 Camera Model	16

2.9	Recent Research	16
3	Methodology	19
3.1	Introduction	19
3.2	Development	19
3.2.1	Aircraft Trajectory	19
3.2.2	INS Alignment	19
3.2.3	Terrain Features Assumptions	19
3.3	Approach and Model Description	20
3.3.1	Dynamics	20
3.3.2	Modeling/Calibrating the Free INS	26
3.3.3	Measurement Equation	28
3.3.4	Synthesis of the Measurement Sent to the KF in Epoch n	38
3.4	Performance of Aided INS	40
3.4.1	Initialization of the KF	42
3.4.2	Kalman Filter	44
3.4.3	Summary	56
4	Simulation Results	58
4.1	Introduction	58
4.2	Simulation	58
5	Conclusion	64
	Appendix A: Simulation Results	65
	Appendix B: Ground Feature Calculations	73
	Bibliography	74

List of Figures

Figure	Page
2.1 The I-frame	5
2.2 The i-frame	6
2.3 The e-frame	7
2.4 The n-frame	8
2.5 The b-frame for Airplane	9
2.6 s-frame for INS Sensor and Camera	10
2.7 Relationship Between g , G and Earth's Rate of a Point Mass	12
2.8 Basic SLAM Problem	15
2.9 Pinhole Camera Geometry	16
3.1 Relationship between the body and inertial frame.	21
3.2 Measurement Geometry in General Position.	29
3.3 Showing the scenario set up.	41
3.4 INS Aiding Using a Kalman Filter	44
4.1 The development of the KF predicted standard deviation and realized position estimates of the unaided INS in the first three measurement epochs.	60
4.2 The development of the KF predicted standard deviation and realized position estimates of the aided INS for the first three measurement epochs.	61
A.1 The development of the KF predicted standard deviation and realized position estimate of the aided INS during a one hour flight.	65
A.2 The development of the KF predicted standard deviation and realized position estimates of the aided INS during a one hour flight for ground features arranged in a straight line.	66
A.3 The development of the KF predicted standard deviation and realized position estimates in the aided INS during a one hour flight for staggered ground features.	67

A.4	The development of velocity estimates in the aided INS during a one hour flight.	68
A.5	The development of attitude estimates in the aided INS during a one hour flight.	69
A.6	The calculated position of the first ground feature.	70
A.7	The geolocated second ground feature's position.	70
A.8	A zoomed in view of the development of the KF predicted standard deviation of the first ground feature's position in first seven measurement epochs.	71
A.9	A zoomed in view of the development of the KF predicted standard deviation of the second ground object's position in first seven measurement epochs.	71
A.10	Aircraft and ground objects' position estimates with KF predicted standard deviations.	72

List of Tables

Table	Page
4.1 Standard Deviations and Errors for Simulations	62
B.1 Ground Features on X-Axis: X Position	73
B.2 Ground Features on X-Axis: Y Position	73
B.3 Y Positions of Laterally Staggered Ground Features on Both Sides of X-Axis .	73

List of Symbols

Symbol	Page
C_b^a DCM from b to a Frame	10
h Altitude	19
v Velocity	19
x x Direction	19
y y Direction	19
z z Direction	19
y_p Inertial Frame y Position of Ground Feature	20
ψ Aircraft Yaw Angle	20
θ Aircraft Pitch Angle	20
ϕ Aircraft Roll Angle	20
$\delta \mathbf{x}$ Navigation Error State Vector	21
$\delta \mathbf{P}$ Position Error Vector	21
$\delta \mathbf{V}$ Velocity Error Vector	21
$\delta \mathbf{\Psi}$ Angle Error Vector	21
$\delta \mathbf{u}$ Disturbance Vector	21
b Indicates Body Frame	21
$^{(n)}$ Indicates Navigation Frame	23
$\vec{\mathbf{f}}$ Specific Force Measured by Accelerometer	23
$\vec{\mathbf{a}}$ Total Aircraft Acceleration	23
$\vec{\mathbf{g}}$ Specific Gravity Vector	23
$f_x^{(n)}$ Specific Force Measured by Longitudinal Accelerometer	23
$f_y^{(n)}$ Specific Force Measured by Lateral Accelerometer	23
$f_z^{(n)}$ Specific Force Measured by Vertical Accelerometer	23
g Acceleration of Gravity	23

a	Longitudinal Acceleration of Aircraft	23
t	Current Time	24
T	Duration of a Measurement Epoch	24
\mathbf{A}_a	Continuos-Time Dynamics Matrix	25
ΔT	Sampling Interval	25
l	Discrete Time Step Counter	25
L	Number of Bearing Measurements in an Epoch	25
\mathbf{A}_{ad}	Discrete-Time Dynamics Matrix	25
x_p	Inertial Frame x Position of Ground Feature	25
m	Number of Unknown Tracked Features	25
σ_a	Standard Deviation of the Uncertainty of the Accelerometer Bias	26
σ_g	Standard Deviation of the Uncertainty of the Gyroscope Bias	26
N	Number of Measurement Epochs	27
α	Accelerometer Bias Constant	27
β	Gyroscope Bias Constant	27
x_f	x Coordinate of Ground Feature on Camera Focal Plane	28
y_f	y Coordinate of Ground Feature on Camera Focal Plane	28
f	Focal Length	28
z_p	Ground Feature Elevation	30
c	Indicates Calculated Value from INS	31
m	Indicates a Measured Value	31
$\mathbf{H}(l)$	Time Dependent Measurement Matrix	33
u	Indicates Ground Feature's Position is Unknown	33
k	Indicates Ground Feature's Position is Known	34
\mathbf{z}	Measurements	36
σ	Error in One Pixel	37

x	True Navigation State	37
$\delta \mathbf{x}_F$	Navigation State Error of Free INS	37
(n)	Current Measurement Epoch	38
P	Covariance Matrix	42
$\hat{\delta \mathbf{x}}$	Kalman Filter Estimates	44
K	Kalman Gain	45
R	Measurement Uncertainty	45

List of Abbreviations

Abbreviation	Page
GPS Global Positioning System	1
INS Inertial Navigation Systems	1
LO Low Observable	2
HVT High Value Target	2
SLAM Simultaneous Localization and Mapping	3
CG center of gravity	7
DCM Direction Cosine Matrix	10
KF Kalman Filter	15
SS State Space	15
LOS Line Of Sight	17
UAVs Unmanned Aerial Vehicles	20
RHS Right Hand Side	32
LHS Left Hand Side	32
SIFT Scale-Invariant Feature Transform	64

Inertial Navigation System Aiding Using Vision

1 Introduction

1.1 Background

Navigation can be defined as the process of reading, and controlling the movement of a craft or vehicle from one place to another[1]. Navigation is achieved by comparing the navigator's position to known locations and this can be done in many different ways. These include but are not limited to an individual using a map, a vehicle using Global Positioning System (GPS), or an aircraft using an Inertial Navigation Systems (INS) in combination with a GPS to provide very precise navigation.

An aircraft using an Inertial Navigation Systems (INS) aided by GPS measurements is afforded very precise navigation. GPS is very accurate but may be occasionally denied due to outages. It is therefore prudent to have workarounds for situations where the precision available from GPS is denied. Aiding INS using the measurements of terrain features' bearings render the integrated navigation system less dependent on GPS. This is desirable since the vision-aided INS will be an autonomous navigation system which is self-contained and not susceptible to jamming and spoofing. The crucial issues of detection of ground features in a camera's field of view and the autonomous tracking of these features/image registration, [5], [7], and [6] are not addressed in this paper. The focus is on gaining an understanding of the INS aiding action afforded by bearings measurements over time of possibly unknown ground features.

In [12] it was shown using covariance analysis that the rate of growth of position uncertainty is significantly reduced when the aircraft uses terrain features bearing

measurements to aid the INS. The same applies to the uncertainty in velocity and the aircraft's Euler angles.

This paper focuses on the mechanization of the Kalman Filter (KF) for vision aided INS. It is shown that using the measurement over time of the bearings of ground features in an aircraft's field of view, a KF can significantly reduce the errors in the aircraft's navigation states in a GPS denied environment. A cross country navigation scenario using the concept of "bootstrapping" where new ground features as they come in the camera's field of view are sequentially geolocated and then tracked during their residence in the camera's field of view, is analyzed. The Kalman Filter is mechanized in the context of Simultaneous Localization and Mapping (SLAM).

It is shown that the synergetic action of the designed Kalman Filter and the geolocation algorithm makes SLAM possible and using the "bootstrapping" concept long range flight which entails INS aiding using bearing measurements of unknown ground features is feasible-this, provided that the image registration problem is solved.

1.2 Motivation

Consider a Low Observable (LO) aircraft carrying a LO munition on a mission into a territory to eliminate a High Value Target (HVT). The objective is to eliminate the target with as minimal collateral damage as possible, so precision is of utmost importance. The HVT is limited to a small area such that it takes approximately an hour to fly from the origin of the military base. The adversary actively uses anti-GPS technologies, thus denying the precision and accuracy of GPS. The aircraft has a navigation quality INS but the duration of the flight is long enough that the errors produced by the INS are too large for precise lock onto the HVT. The pilot needs a better navigation solution, but does not want to inform the enemy of the aircraft's presence by using active navigation techniques, such as radar. The autonomy of the INS is good for stealth but is not enough to provide precise navigation solution given the errors that accumulate over time.

The proposed solution is to use the bearing measurements of known and unknown ground features to aid the navigation provided by the INS. The aircraft uses its camera to geolocate ground features, track those features to aid the INS, and using that aided estimate geolocate new features as the original features leave the camera's FOV. This aiding scheme constrains the error enough to obtain target solution. The on board munition, with its lower quality INS, uses a similar visual scheme. It looks within the area given during the mission briefing for the HVT. The munition impacts the HVT and the aircraft leaves the scene without emitting any signal that will give away its location.

1.3 Approach

This paper will be structured such that each chapter will begin with a brief description of topics that will be forthcoming. Chapter 2 provides information on the various coordinate frames of reference that is used when working with an INS, the transformations between the coordinate frames, INS mechanization equations, a brief discussion of Simultaneous Localization and Mapping (SLAM) and concludes with recent research in the field. Chapter 3 shows the mathematical development of the 2-D case, including the dynamics and measurement model development, the state space representation and the use of the KF mechanization. This information is then extended to look at the 3-D case for both a horizontal flight and a vertical fall. Chapter 4 looks at the results of the covariance analysis. Finally, Chapter 5 summarizes the key points of the paper, focusing on the impact the INS aiding scheme provided.

2 Literature Review

2.1 Introduction

This section provides information on the various coordinate frames of reference that is used when working with INS. Section 2.2 discusses the different coordinate frames of reference. Section 2.3 discusses the transformations between the various coordinate frames. Section 2.4 discusses the fundamentals of inertial navigation, including a brief discussion of the sensors used and how they work. Section 2.6 discusses the fundamental INS equation and the INS equations for some common frames. Section 2.7 discusses SLAM. Section 2.8 discusses the camera model that will be used as a sensor. Finally, Section 2.9 reviews recent research that contributed to this paper.

2.2 Reference Frames

2.2.1 Inertial Reference Frame. The Inertial Reference Frame which is also known as the “true” inertial frame is denoted as the I-frame. The I-frame is located in the sky and it is in this frame that Newton’s laws apply. All reference frames used in this paper follow the right handed reference system. The I-frame is shown in Figure 2.1.

2.2.2 Earth-Centered, Earth-Fixed Inertial Reference Frame. The Earth-centered, Earth-Fixed (ECEF) inertial reference frame, as the name imply, has its origin fixed to the center of the earth. It is denoted as the i-frame and moves with the earth relative to the I-frame. With the Earth modelled as an ellipsoid, the axes of the i-frame are partially fixed to the I-frame and are defined as follows:

- x_i -axis \triangleq along the Equator and pointing towards the first star in the Aries
- z_i -axis \triangleq points towards the North Pole
- y_i -axis \triangleq along the Equator, and completing the right handed reference system

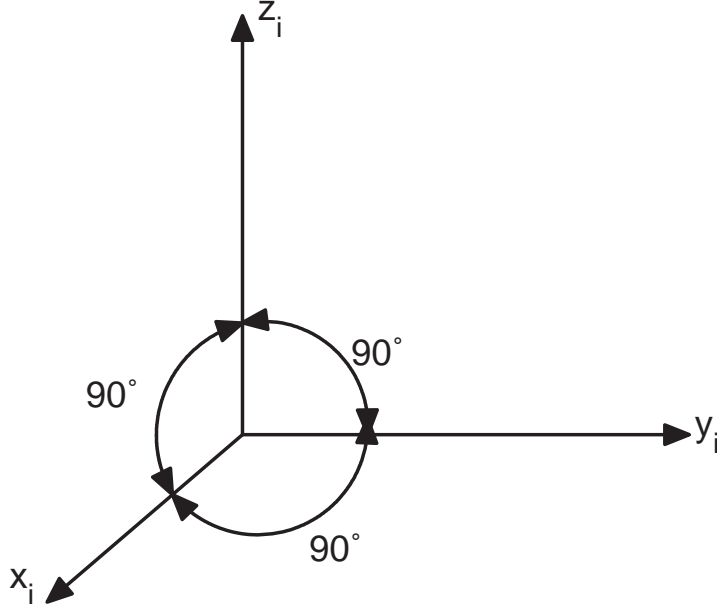


Figure 2.1: The I-frame

The i-frame in the earth model is shown in Figure 2.2.

2.2.3 Earth-fixed Reference Frame. The Earth-fixed reference frame has its origin fixed to an arbitrary point on the surface of the Earth. The axes of the e-frame are defined as follows:

- x_e -axis points to the North
- y_e -axis points to the east
- z_e -points to the gravitational center of the Earth.

The e-frame is shown in Figure 2.3. Since the e-frame is fixed to an arbitrary point on the surface of the earth, it moves at the earth rate. The rotation between the i-frame and the e-frame is denoted by θ_{ie}^e , where θ_{ie}^e is given by:

$$\theta_{ie}^e = \omega_e(t - t_0)$$

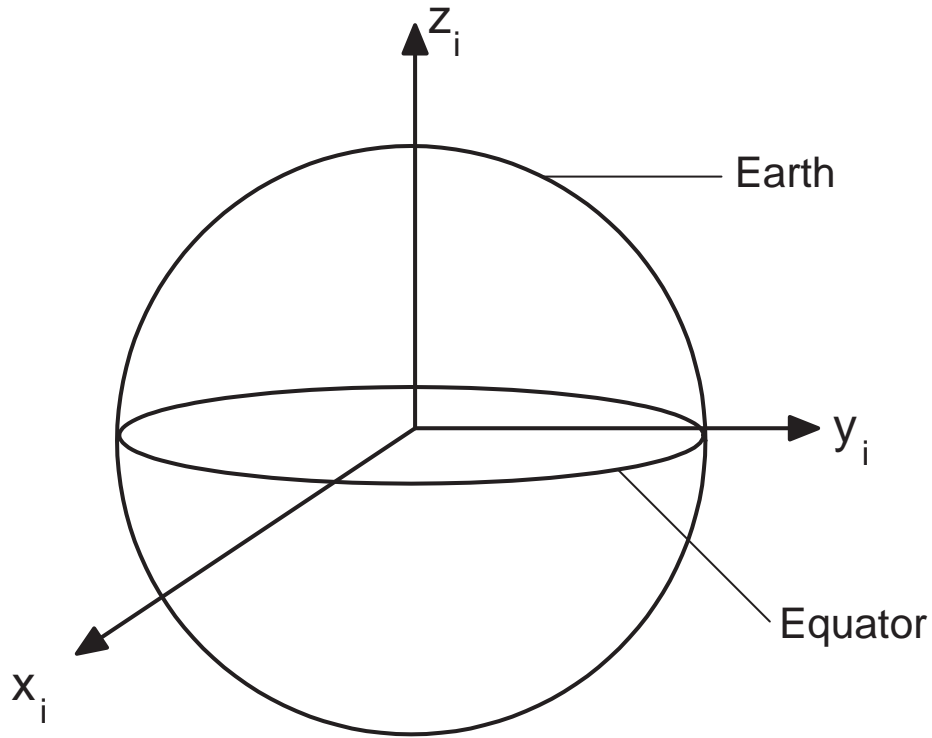


Figure 2.2: The i-frame

and ω_e is the sidereal rate of the earth $\approx 360^\circ/\text{day}$

2.2.4 Navigation Reference Frame. The navigation frame, also known as the local level frame is denoted as the n-frame. The origin of this reference frame is located on a plane which is tangential to the surface of the Earth, where $z = 0$ is for the surface of the Earth. The e-frame is fixed to the earth, but the n-frame is not. The axes of the n-frame are defined as follows:

- x_n -axis \triangleq points from the origin to the North pole
- y_n -axis \triangleq points to the west
- z_n -axis \triangleq points down away from the center of the Earth

Figure 2.4 shows the n-frame in the Earth model.

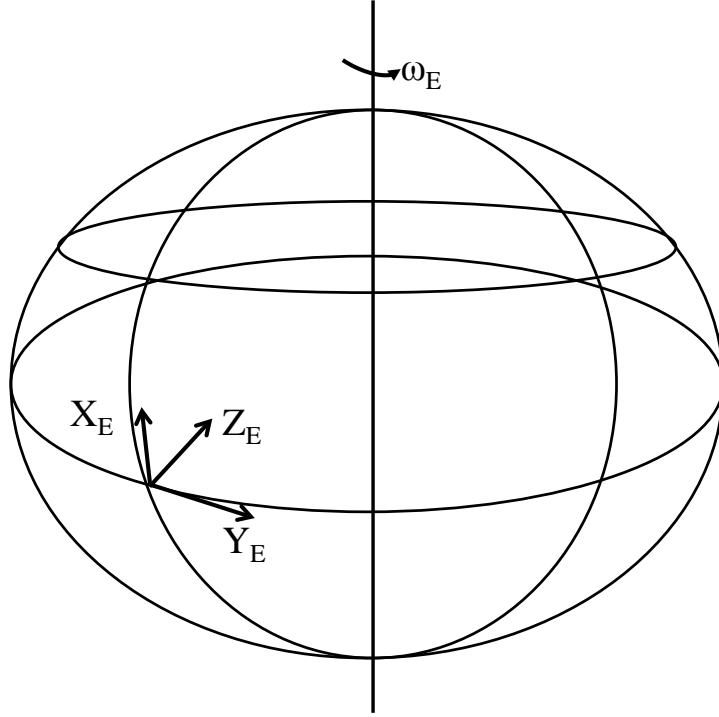


Figure 2.3: The e-frame

2.2.5 The Body Frame. The body frame, denoted as the b-frame is rigidly attached to the body of a vehicle (airplane, car, ship, etc.). The origin is located somewhere on the body, either the center of gravity (CG) or something measurable. The axes do not change with changes to an aircraft's trajectory or orientation of a car. Due to the fact that an aircraft loses fuel in the cause of flight and the center of gravity will consequently change, the origin of the body frame will be fixed to the origin of the camera in this paper. The body axes are defined as follows:

- x_b -axis \triangleq points out of the nose of the aircraft
- y_b -axis \triangleq points out of the left wing of the aircraft
- z_b -axis \triangleq points out of the top of the aircraft

Figure 2.5 shows the body frame for an airplane.

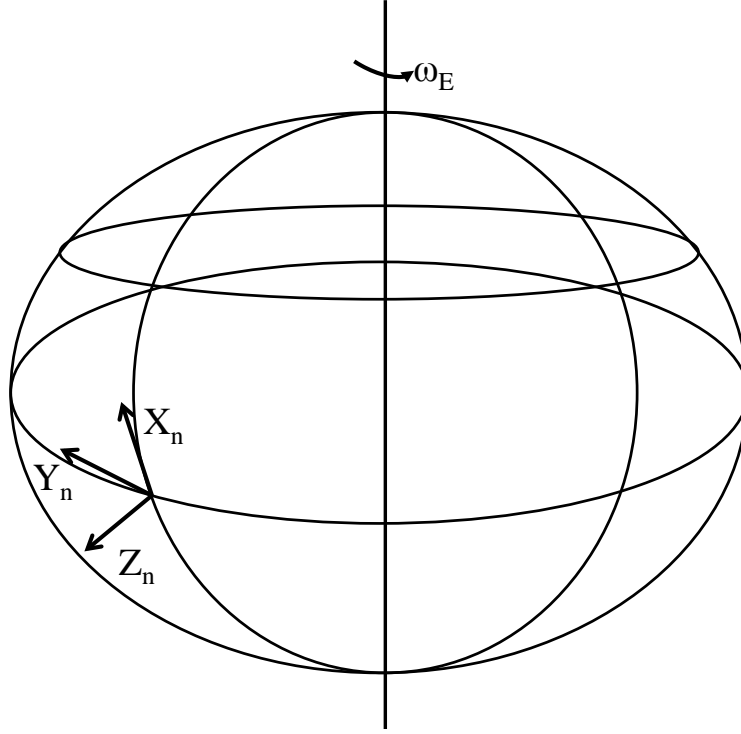


Figure 2.4: The n-frame

2.2.6 Sensor Frame. The sensor frame, denoted as the s-frame is defined by the designer using the right handed reference system. It is completely up to the designer to define the origin and axes of the s-frame. Figure 2.6 shows two sensors (INS and camera) with their respective s-frames in relation to the b-frame of an object whose origin is at the CG. Again, for reasons discussed in sub-section 2.2.5 the origin of the body frame will be co-located with the origin of the camera frame in this paper.

2.3 Coordinate System Transformations

In INS computations, it is often convenient to convert the different frames to a single frame (often the navigation frame) for easy calculations. In order to transform points and vectors from one frame to the other, there is the need to perform either translation, rotation, or both. Translation is an $n \times 1$ vector that relates the origins of two frames of

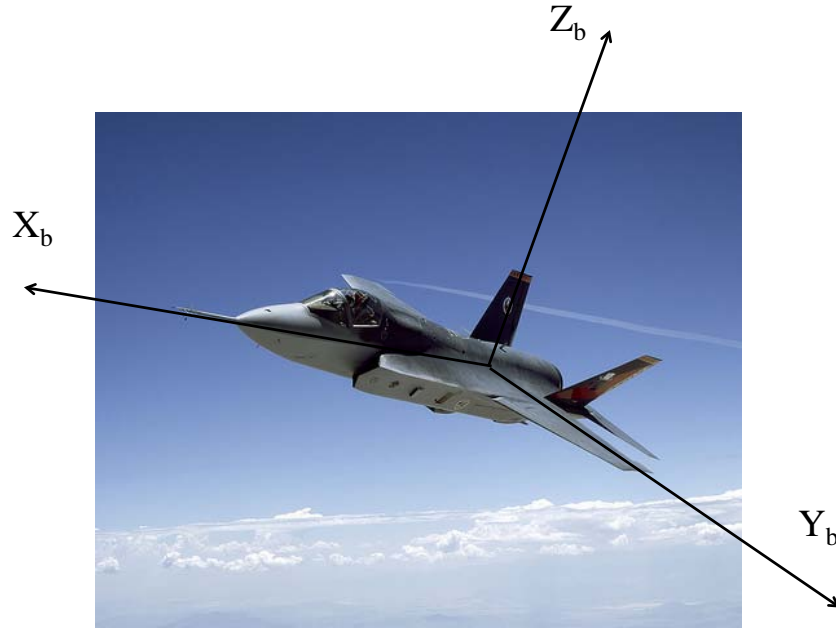


Figure 2.5: The b-frame for Airplane

interest. The translation of a point P , from a-frame to b-frame in the a-frame is denoted by P_{ab}^a . Rotations on the other hand are defined with respect to the orthogonal right-handed axis set. Rotation of a set of axes in one frame to another frame can be done in one of three ways, namely:

1. Euler angles (ϕ, θ, ψ) : This is a transformation of one frame to another by three successive rotations about three different axes taken in turn [13]. It is worth noting that the order of rotation matters; rotation in the order (ϕ, θ, ψ) is different from rotation in the order (θ, ψ, ϕ) .
2. Quaternions (4×1 vector): The quaternion attitude representation allows a transformation from one coordinate frame to another to be effected by a single rotation about a vector defined in the reference frame. The quaternion is a

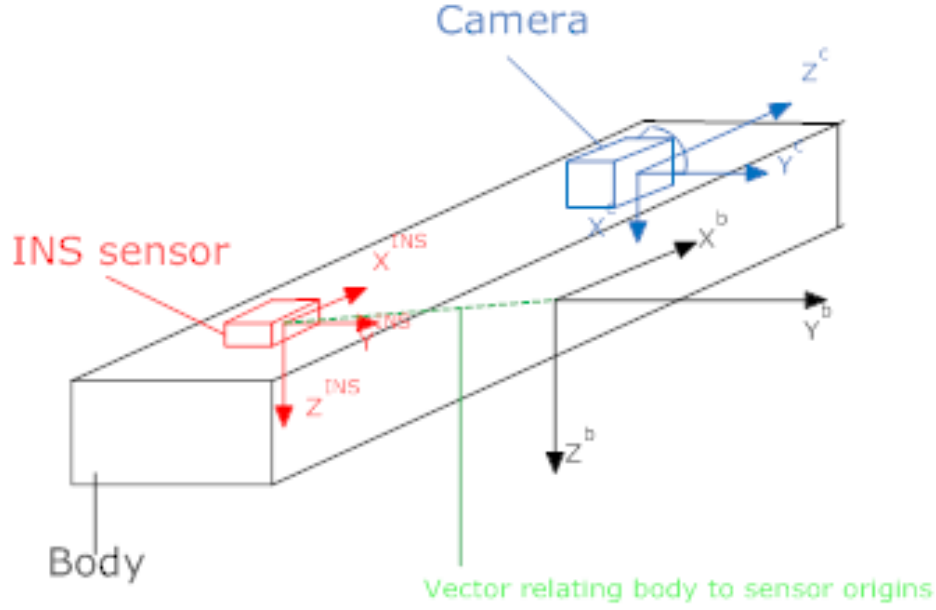


Figure 2.6: s-frame for INS Sensor and Camera

four-element vector representation, the elements of which are functions of the orientation of this vector and the magnitude of the rotation.

3. Direction Cosine Matrix (DCM) (3×3 matrix): The Direction Cosine Matrix (DCM), is a 3×3 matrix, the columns of which represent unit vectors in body axes projected along the reference axes. The DCM from a b-frame to an a-frame is denoted by C_b^a , which is written as follows:

$$C_b^a = \begin{bmatrix} C_{11} & C_{12} & C_{13} \\ C_{21} & C_{22} & C_{23} \\ C_{31} & C_{32} & C_{33} \end{bmatrix} \quad (2.1)$$

Where the element in the i th row and the j th column represents the cosine of the angle between the i -axis of the a-frame and the j -axis of the b-frame.

This paper uses DCM for coordinate system transformations. For right-handed, orthonormal reference frames, some DCM rules are as follows:

$$\begin{aligned} \text{Det}(C_b^a) &= |C_b^a| = 1 \\ (C_b^a)^{-1} &= (C_b^a)^T = C_a^b \\ C_c^a &= C_b^a C_c^b \end{aligned}$$

2.4 Inertial Navigation

This section provides an overview of the basic principles of inertial systems. To navigate, knowledge of the measurements of specific force and angular rates are required. These measurements are provided by an INS, which consists of accelerometers and gyros. Accelerometers measure specific force, while gyros measure angular rate. An INS is a self-contained and nonjammable navigation instrument that provides redundancy for radio navigation systems that can experience interference or be jammed; however, an INS does suffer from drift, the unbounded growth of errors over time. Even, with perfect alignment, accelerometer biases and gyro drift causes the errors in INS to grow over time [10].

2.5 Specific Force and Gravity

2.5.1 Specific Force. From Newton's Second Law of Motion, the force, F_I acting on a body of mass m , moving with an acceleration of \ddot{p}_I in the inertial frame is given by:

$$F_I = m\ddot{p}_I \quad (2.2)$$

Accelerometers, as was mentioned earlier, measure specific force, f_I , and it is defined as the inertial force, F_I , per unit mass m , required to produce the acceleration \ddot{p}_I . This relationship is given by Equation 2.3.

$$f_I \triangleq \frac{F_I}{m} \approx f_i \quad (2.3)$$

Examples of inertial forces include spring force, friction, lift, thrust, and support.

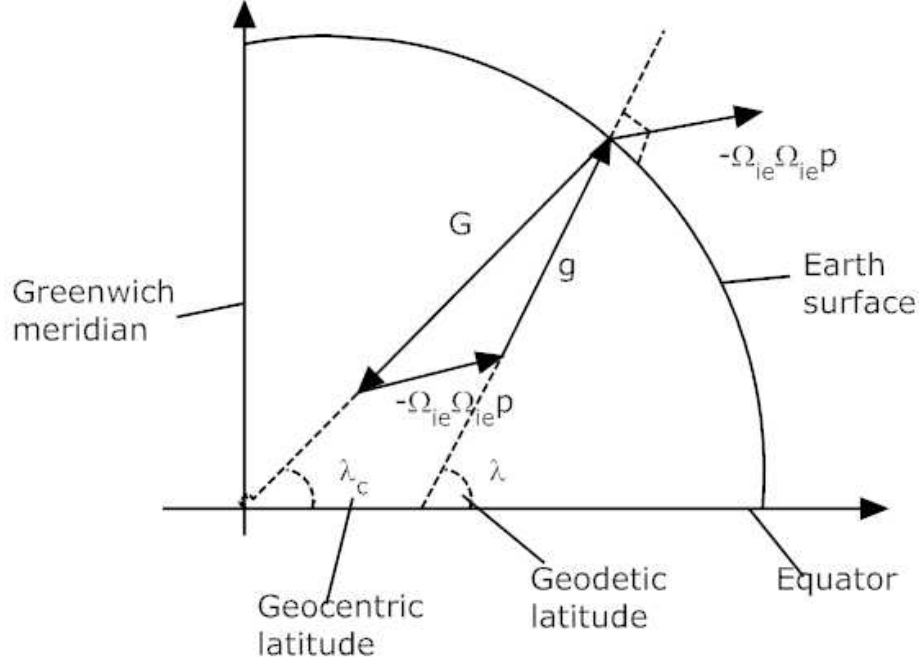


Figure 2.7: Relationship Between g , G and Earth's Rate of a Point Mass

2.5.2 *Gravity.* The acceleration \ddot{p}_I , acting on a particle in a gravitational field is given by the fundamental equation of inertial navigation as:

$$\ddot{p}_I = f_i + G_i \quad (2.4)$$

Gravity g , is then defined by equation 2.5 below.

$$g = G(p) - \Omega_{ie}\Omega_{ie}p \quad (2.5)$$

where G is the Earth's gravitational force acting on the particle at position p and Ω_{ie} is the centrifugal force pulling outward due to the rotation of the earth. It is worth noting that gravity is not an inertial force. This relationship is as depicted in Figure 2.7.

This effect is not very significant, since the centrifugal force is only a fraction of the gravitational force:

$$\|\Omega_{ie}\Omega_{ie}p\| \approx \frac{1}{300} \|G(p)\| \quad (2.6)$$

2.6 INS Equation

Consider relating the time derivative of vectors in rotating reference frames. From vector addition:

$$\mathbf{r}_{a_0p}^a = \mathbf{r}_{a_0b_0}^a + \mathbf{r}_{b_0p}^a \quad (2.7)$$

where $\mathbf{r}_{a_0p}^a$ and $\mathbf{r}_{a_0b_0}^a$ and it is the desire to find $\mathbf{r}_{b_0p}^a$ in the b -frame:

$$\mathbf{r}_{b_0p}^b = \mathbf{C}_a^b \mathbf{r}_{b_0p}^a = \mathbf{C}_a^b (\mathbf{r}_{a_0p}^a - \mathbf{r}_{a_0b_0}^a) = \mathbf{C}_a^b \mathbf{r}_{a_0p}^a + \mathbf{r}_{b_0a_0}^b \quad (2.8)$$

For short-hand, write as

$$\mathbf{p}^b = \mathbf{C}_a^b \mathbf{p}^a + \mathbf{r}_{ba}^b \quad (2.9)$$

Taking the time derivative of \mathbf{p}^b yields:

$$\frac{d}{dt}(\mathbf{p}^b) \triangleq \mathbf{v}^b = \frac{d}{dt}(\mathbf{C}_a^b) \mathbf{p}^a + \mathbf{C}_a^b \frac{d}{dt}(\mathbf{p}^a) + \frac{d}{dt}(\mathbf{r}_{ba}^b) \quad (2.10)$$

$$= \mathbf{C}_a^b \boldsymbol{\Omega}_{ab}^a \mathbf{p}^a + \mathbf{C}_a^b \frac{d}{dt}(\mathbf{p}^a) + \frac{d}{dt}(\mathbf{r}_{ba}^b) \quad (2.11)$$

$$\mathbf{v}^b = \frac{d}{dt}(\mathbf{r}_{ba}^b) + \mathbf{C}_a^b (\boldsymbol{\Omega}_{ab}^a \mathbf{p}^a + \mathbf{v}^a) \quad (2.12)$$

where $\frac{d}{dt}(\mathbf{r}_{ba}^b)$ accounts for the relative velocity between the a -frame and b -frame,

$\mathbf{C}_a^b \boldsymbol{\Omega}_{ab}^a \mathbf{p}^a$ is the instantaneous velocity of p relative to the b -frame due to the relative rotation of the a -frame, and $\mathbf{C}_a^b \mathbf{v}^a$ is the instantaneous velocity of p in the a -frame

transformed into b -frame. Taking another time derivative of Eq. 2.12 results in:

$$\frac{d}{dt}(\mathbf{v}^b) \triangleq \mathbf{a}^b = \frac{d^2}{dt^2} \mathbf{r}_{ba}^b + \frac{d}{dt} \left[\mathbf{C}_a^b (\boldsymbol{\Omega}_{ab}^a \mathbf{p}^a + \mathbf{v}^a) \right] \quad (2.13)$$

$$= \ddot{\mathbf{r}}_{ba}^b + \frac{d\mathbf{C}_a^b}{dt} (\boldsymbol{\Omega}_{ab}^a \mathbf{p}^a + \mathbf{v}^a) + \mathbf{C}_a^b \frac{d(\boldsymbol{\Omega}_{ab}^a \mathbf{p}^a + \mathbf{v}^a)}{dt} \quad (2.14)$$

$$= \ddot{\mathbf{r}}_{ba}^b + \left(\dot{\mathbf{C}}_a^b \boldsymbol{\Omega}_{ab}^a \right) (\boldsymbol{\Omega}_{ab}^a \mathbf{p}^a + \mathbf{v}^a) + \mathbf{C}_a^b (\dot{\boldsymbol{\Omega}}_{ab}^a \mathbf{p}^a + \boldsymbol{\Omega}_{ab}^a \mathbf{v}^a) + \mathbf{C}_a^b \mathbf{a}^a \quad (2.15)$$

$$\mathbf{a}^b = \ddot{\mathbf{r}}_{ba}^b + \mathbf{C}_a^b [(\dot{\boldsymbol{\Omega}}_{ab}^a \boldsymbol{\Omega}_{ab}^a + \boldsymbol{\Omega}_{ab}^a \dot{\boldsymbol{\Omega}}_{ab}^a) \mathbf{p}^a + 2\boldsymbol{\Omega}_{ab}^a \mathbf{v}^a + \mathbf{a}^a] \quad (2.16)$$

Eq. 2.16 represents the fundamental relationship for an INS.

2.6.1 INS Equations for Common Frames. The previous section dealt with INS equations for some arbitrary frames. This section will briefly provide the strapdown INS equations for the following frames:

2.6.1.1 Strapdown INS Equation in *i*-frame. In the *i*-frame, Eq. 2.16 reduces to

$$\frac{d^2 p_i}{dt^2} = C_b^i f_b + g_i \quad (2.17)$$

2.6.1.2 Strapdown INS Equation in *e*-frame. In the *e*-frame, Eq. 2.16 reduces to

$$\frac{d^2 p_e}{dt^2} = C_b^e f_b + g_e - 2\Omega_{ie}^e v_e \quad (2.18)$$

2.6.1.3 Strapdown INS Equation in *n*-frame. In the *n*-frame, Eq. 2.16 reduces to

$$\frac{d^2 p_n}{dt^2} = C_b^n f_b + g_n - (2\Omega_{ie}^n v_n + \Omega_{en}^n) v_n \quad (2.19)$$

2.7 SLAM

Maps are needed to depict an environment for planning and navigation. They may or may not be readily available depending on the environment of interest. In the case that they are not readily available (due to topographical changes or an unfamiliar indoor environment), the techniques of SLAM come in very handy. SLAM is a process by which a mobile robot or an autonomous vehicle can build a map of an environment and at the same time use this map to deduce its location [2]. The essential SLAM problem is shown in Figure 2.8 [2]

To understand SLAM, consider a mobile robot having an onboard sensor, a camera for example, moving through an unknown environment with no *a priori* information about the environment. The robot probabilistically estimates its own position and uses the onboard camera to estimate the position of unknown landmarks. It is a recursive process

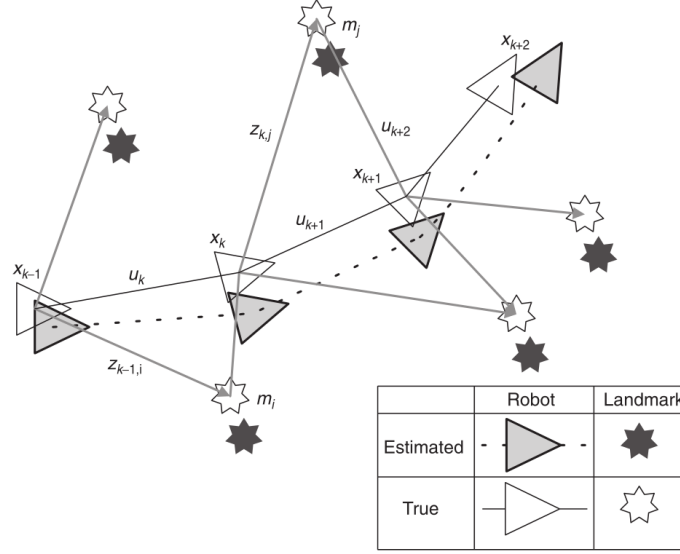


Figure 2.8: **Basic SLAM Problem.** The essential problem of SLAM requires the simultaneous estimation of both robot or autonomous vehicle and landmark positions. Neither position is truly known[2].

where the robot uses its position to estimate the position of unknown ground features and then uses the estimates of the ground features to estimate its own position. This recursive process is typically achieved through the use of a Kalman Filter (KF).

With the introduction of each additional unknown ground feature, the states used in the State Space (SS) equation of the KF increases depending on the type information required by the KF for its estimation. In this paper, the x and y positions of stationary ground features are the information of interest so with the addition of an unknown ground feature whose position is to be estimated, the states in the SS of the KF increase by two. This is because stationary ground features are at zero elevation, so only the x and y positions of the ground features are considered. Likewise, with the drop of ground feature by the sensor (camera) because it is no longer in its FOV the states in the SS of the KF decrease by two.

2.8 Camera Model

In this paper, the camera will be modelled as the basic pinhole camera where it is assumed that there are no camera distortions. Camera calibration will therefore not be considered. The basic pinhole camera is shown in Figure 2.9. The focal length of the

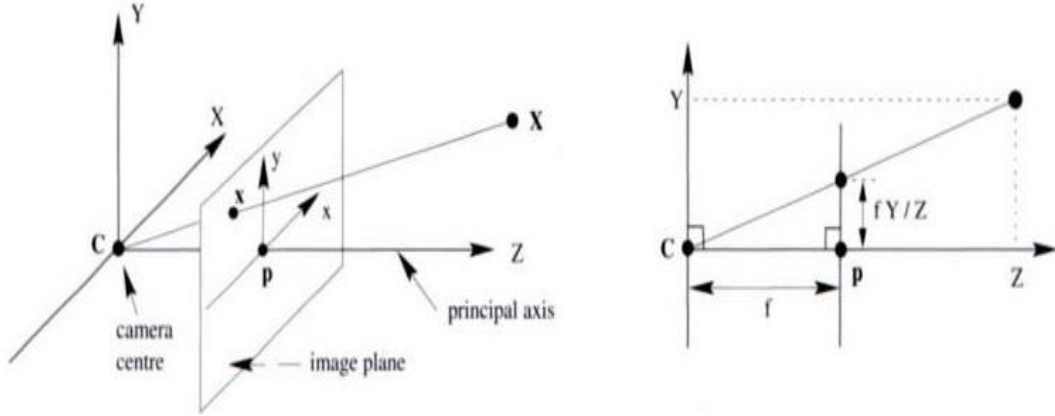


Figure 2.9: **Pinhole Camera Geometry.** C is the camera center and p the principal point. The camera center is placed at the coordinate origin [4].

camera is f . Features are considered as points which are projected in space onto an image plane. A point in space with coordinates $\mathbf{X} = (X, Y, Z)^T$ is projected onto the image plane. From the geometry, it can be computed by similar triangles that $(X, Y, Z)^T$ maps onto the point $(fX/Z, fY/Z, f)^T$ on the image plane[4]. Ignoring the final image coordinate, it can be seen that

$$(X, Y, Z)^T \mapsto (fX/Z, fY/Z)^T \quad (2.20)$$

2.9 Recent Research

In [10], Pachter et. al researched the idea of using bearings-only measurements for aiding INS. This was a theoretical work, where no simulations or empirical data were used to substantiate the theory. The significance of this research was the development of the

mathematics for observing the Line Of Sight (LOS) angle measurements to a ground feature over time and using that information to update an INS. The update was theorized to constraining the unbounded errors developed by an INS if it were allowed to operate freely.

In [3], Giebner aided an aircraft INS using visual measurements when the aircraft flies in a circular orbit around a several ground features. A KF was used to achieve the aiding and this was done both in simulation and in an actual test environment. It was found that the uncertainty in the aircraft's position after six minutes of flight time, was reduced from 350 meters, in the unaided INS case, down to 50 meters, in the aided INS case, when the visual measurements were combined with barometric altimeter readings.

In [9], Pachter and Mutlu explored the observability of a vision-aided INS. The bearing measurements used were time dependent because the position of the ground feature(s) being tracked by the aircraft changed with time. The time dependent measurement matrix prompted the use of observability Grammian. It was determined that using the bearings-only visual measurements of a single ground feature to aid the INS, the observability Grammian was rank deficient, making the INS aiding action incomplete. In order for full rank observability Grammian and thereby have complete INS aiding action, a second ground feature had to be simultaneously tracked. Complete INS aiding action means all of the navigation states receive some improvement from the measurement when compared to the unaided INS.

In [2], Durrant-Whyte and Bailey provided the origins of SLAM. It was shown how various filter methods can be used to implement SLAM using the limited information in a robot's environment. The uncertainty of detected features, as well as the navigation estimate, was shown to be dependent on the number of measurements taken. The more measurements that were taken, the less the uncertainty. In a scenario where a robot was remotely piloted through an indoor environment, a pilot with no visual access of the robot,

the robot autonomously returned to its starting point using map that it build up during the navigation process.

In [14], Veth looked at the fusion of imaging and inertial sensors for navigation. A statistical feature projection technique was developed which utilizes inertial measurements to predict vectors in the feature space between images. The feature matches and inertial measurements were used to estimate the navigation trajectory on-line using an extended Kalman filter.

This paper is a continuation of [12]. In [12] it was shown using covariance analysis that the rate of growth of position uncertainty is significantly reduced when the aircraft uses terrain features bearing measurements to aid the INS. The same applies to the uncertainty in velocity and the aircraft's Euler angles. The method used for geolocating new ground features were crude, where only the aircraft position was used in the geolocation process. This paper will look at a more accurate method (include the other navigation states in the geolocation of ground features) of calculating the covariances and implement a KF in a simulation analysis to substantiate the theory.

3 Methodology

3.1 Introduction

This chapter is broken up into three main sections. Section 3.2 discusses the navigation scenario that is considered for the dynamics model development. Section 3.3 discusses the approach that is taking in calibrating the unaided INS with small angle assumptions, measurement model development, the measurement equations that are sent to the KF, and how the calculations are accomplished. Section 3.4 discusses the performance of the aided INS, which includes the KF and its initialization at the beginning of each epoch.

3.2 Development

The navigation scenario is as follows:

3.2.1 Aircraft Trajectory. The aircraft is flying wings-level at a constant altitude h . The ground speed of the aircraft is constant and the aircraft flies in the positive x_n direction.

3.2.2 INS Alignment. The initial INS alignment is considered to be “perfect”. That is, at the start of the flight at altitude h and velocity v in the positive x_n direction, the exact aircraft’s position, velocity, and attitude are known with very small errors. The emphasis is on the contribution of the inertial instruments’ errors to the INS navigation state errors. In this respect it is assumed that the x , y , and z accelerometers are of the same quality; also the x , y , and z gyroscopes are of the same quality and the instruments’ measurement error is modeled as a random bias.

3.2.3 Terrain Features Assumptions. At all time two ground features need to be tracked for observability [9]. Thus, it is assumed that the position of the first two ground

features to come into the aircraft camera's field of view are known. The position of subsequent features are not known but these are geolocated as they come into the camera's field of view à la SLAM. Bearing measurements to these newly acquired features are subsequently taken, hence the "bootstrapping" concept. Obviously, for vision-aided navigation to be possible, one cannot fly over featureless terrain and the features need to be more or less regularly spaced. Hence, without loss of generality it is assumed that the features are nominally equally spaced in the positive x_n direction and are at zero, a.k.a. known, elevation. Two scenarios are considered. First the ground features are arranged in a perfect straight line along the aircraft's trajectory, and second, the ground features are laterally staggered y_p meters about the x_n axis. Thus, in the first navigation scenario, y_p is zero meters and all the terrain features are on the x_n axis. The Earth is assumed flat and nonrotating. This assumption is reasonable considering the relatively short range and/or the tactical grade specification of the gyros and accelerometers of small Unmanned Aerial Vehicles (UAVs) for which this autonomous navigation system is being developed.

Kalman filtering in a SLAM scenario where the aircraft uses inertial navigation is considered. Our novel approach to SLAM is rooted in the theory of inertial navigation, as opposed to robotics or computer science.

3.3 Approach and Model Description

3.3.1 Dynamics. The navigation n-frame is the Earth fixed "inertial" (x_n, y_n, z_n) frame. The aircraft's body axes are (x_b, y_b, z_b) . The aircraft's and camera's position in the navigation frame is (x, y, z) , with ψ , θ , and ϕ as its Euler angles. A strapdown [13] INS arrangement is considered. When flying over a non-rotating and flat Earth as shown in Figure 3.1, the INS error dynamics can be considerably simplified [11], [12], [13]. The simplified dynamics of the INS errors in state space notation, also known as the error

equations, are $\delta\dot{\mathbf{x}} = \mathbf{A}\delta\mathbf{x} + \mathbf{\Gamma}\delta\mathbf{u}$, where the navigation error state vector $\delta\mathbf{x}$ given by

$$\delta\mathbf{x} = [\delta\mathbf{P} \quad \delta\mathbf{V} \quad \delta\mathbf{\Psi}]^T \quad (3.1)$$

are the errors in the navigation state's position $\delta\mathbf{P}$, velocity $\delta\mathbf{V}$, and angles $\delta\mathbf{\Psi}$, and the disturbances $\delta\mathbf{u}$ are the three accelerometers' and the three rate gyroscopes' random biases

$$\delta\mathbf{u} = [\delta f_x^b \quad \delta f_y^b \quad \delta f_z^b \quad \delta\omega_x^b \quad \delta\omega_y^b \quad \delta\omega_z^b]^T \quad (3.2)$$

The superscript ^b indicates that the body frame of reference is being used. The errors in

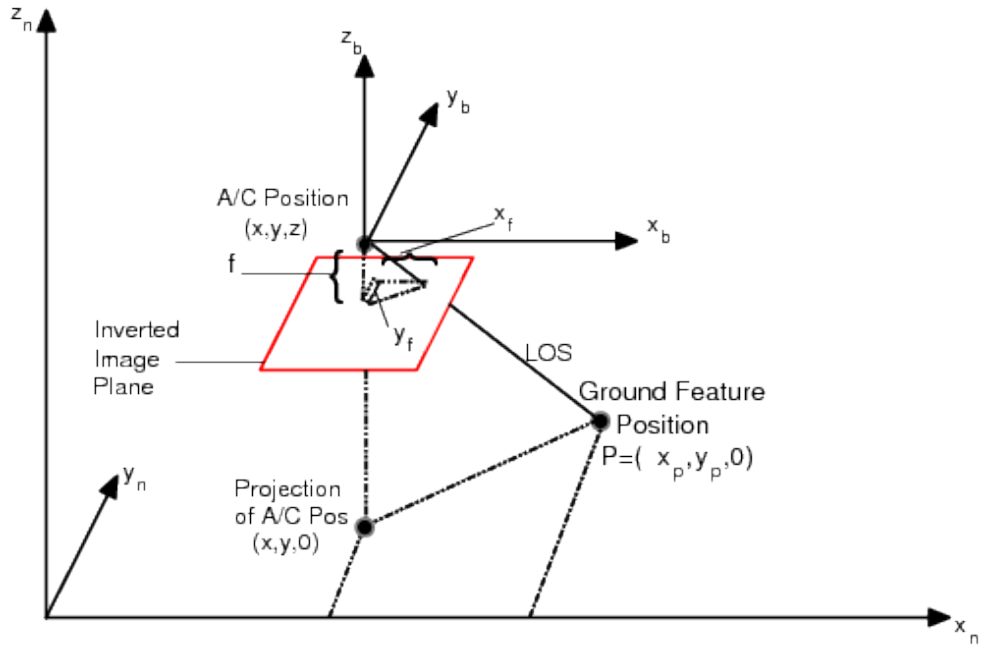


Figure 3.1: Level Flight at Constant Altitude Along the x_n -axis

the angles, $\delta\mathbf{\Psi}$, are given by

$$\delta\mathbf{\Psi} = -\delta\mathbf{C}_b^n \mathbf{C}_n^b \quad (3.3)$$

and

$$\delta\mathbf{\Psi} = \delta\mathbf{\Psi} \times \quad (3.4)$$

where \mathbf{C}_n^b is the DCM and $\delta\mathbf{\Psi}$ is the skew symmetric matrix formed from the angle errors vector $\delta\mathbf{\Psi}$ according to Eq. (3.4).

For small Euler angles ψ, θ, ϕ , the DCM

$$\mathbf{C}_b^n(\psi, \theta, \phi) = \begin{bmatrix} 1 & -\psi & \theta \\ \psi & 1 & -\phi \\ -\theta & \phi & 1 \end{bmatrix} \quad (3.5)$$

and therefore its perturbation

$$\delta\mathbf{C}_b^n = \begin{bmatrix} 0 & -\delta\psi & \delta\theta \\ \delta\psi & 0 & -\delta\phi \\ -\delta\theta & \delta\phi & 0 \end{bmatrix} \quad (3.6)$$

For constant altitude flight in the direction of the x_n axis, the nominal $\mathbf{C}_n^b = \mathbf{I}_3$. Thus, using Eq. (3.3) the following is calculated

$$\delta\mathbf{\Psi} = \begin{bmatrix} 0 & \delta\psi & -\delta\theta \\ -\delta\psi & 0 & \delta\phi \\ \delta\theta & -\delta\phi & 0 \end{bmatrix} \quad (3.7)$$

and since $\delta\mathbf{\Psi} = \delta\mathbf{\Psi} \times$ the errors in the aircraft's Euler angles are recovered

$$\delta\mathbf{\Psi} = [-\delta\phi \quad -\delta\theta \quad -\delta\psi]^T \quad (3.8)$$

Hence, the navigation state's error vector is

$$\delta\mathbf{x} = [\delta x \quad \delta y \quad \delta z \quad \delta v_x \quad \delta v_y \quad \delta v_z \quad -\delta\phi \quad -\delta\theta \quad -\delta\psi]^T \quad (3.9)$$

and the INS error state equations are

$$\delta\dot{\mathbf{x}} = \begin{bmatrix} \mathbf{0}_{3 \times 3} & \mathbf{I}_{3 \times 3} & \mathbf{0}_{3 \times 3} \\ \mathbf{0}_{3 \times 3} & \mathbf{0}_{3 \times 3} & \mathbf{F}_{3 \times 3}^{(n)} \\ \mathbf{0}_{3 \times 3} & \mathbf{0}_{3 \times 3} & \mathbf{0}_{3 \times 3} \end{bmatrix} \delta\mathbf{x} + \begin{bmatrix} \mathbf{0}_{3 \times 3} & \mathbf{0}_{3 \times 3} \\ \mathbf{C}_n^b & \mathbf{0}_{3 \times 3} \\ \mathbf{0}_{3 \times 3} & -\mathbf{C}_n^b \end{bmatrix} \delta\mathbf{u} \quad (3.10)$$

where $\mathbf{F}^{(n)} = \mathbf{f}^{(n)} \times$ is the skew symmetric matrix form of the specific force vector $\mathbf{f}^{(n)}$. The superscript $^{(n)}$ indicates that the inertial navigation frame of reference is being used. The specific force measured by the accelerometer $\vec{\mathbf{f}}$, total aircraft acceleration $\vec{\mathbf{a}}$, and the specific gravity vector $\vec{\mathbf{g}}$ are related according to Eq. 2.4 by $\vec{\mathbf{f}} = \vec{\mathbf{a}} - \vec{\mathbf{g}}$, that is, $\mathbf{f}^{(n)} = \mathbf{a}^{(n)} - \mathbf{g}^{(n)}$. During wings level flight

$$\mathbf{a}^{(n)} = \begin{pmatrix} a \\ 0 \\ 0 \end{pmatrix}, \quad \mathbf{g}^{(n)} = \begin{pmatrix} 0 \\ 0 \\ -g \end{pmatrix}$$

Therefore the nominal specific force components during constant altitude, wings level flight are $f_x^{(n)} = a$, $f_y^{(n)} = 0$ and $f_z^{(n)} = g$, where g is the acceleration of gravity and a is the longitudinal acceleration of the aircraft. Thus,

$$\mathbf{f}^{(n)} = \begin{pmatrix} f_x^{(n)} \\ f_y^{(n)} \\ f_z^{(n)} \end{pmatrix} = \begin{pmatrix} a \\ 0 \\ g \end{pmatrix} \quad (3.11)$$

Eqs. (3.10) and (3.11) represent the dynamics of the navigation state's error, $(\delta\mathbf{P}, \delta\mathbf{V}, \delta\mathbf{\Psi})$, under the assumption that the Earth is flat and non-rotating. The meaning of the angular errors' vector $\delta\mathbf{\Psi}$, that is, its relationship to the Euler angles' errors, is determined by the aircraft's trajectory, that is, the nominal DCM \mathbf{C}_b^n . In the special case of wings level flight when the body and navigation frames are aligned as shown in Figure 3.1, the angular errors are the Euler angles. However, having negative angle error states is unorthodox. In order for the navigation state error to be

$$\delta\mathbf{x} = [\delta x \quad \delta y \quad \delta z \quad \delta v_x \quad \delta v_y \quad \delta v_z \quad \delta\phi \quad \delta\theta \quad \delta\psi]^T \quad (3.12)$$

the dynamics Eq. (3.10) is modified as follows

$$\delta\dot{\mathbf{x}} = \begin{bmatrix} \mathbf{0}_{3 \times 3} & \mathbf{I}_{3 \times 3} & \mathbf{0}_{3 \times 3} \\ \mathbf{0}_{3 \times 3} & \mathbf{0}_{3 \times 3} & -\mathbf{F}_{3 \times 3}^{(n)} \\ \mathbf{0}_{3 \times 3} & \mathbf{0}_{3 \times 3} & \mathbf{0}_{3 \times 3} \end{bmatrix} \delta\mathbf{x} + \begin{bmatrix} \mathbf{0}_{3 \times 3} & \mathbf{0}_{3 \times 3} \\ \mathbf{C}_n^b & \mathbf{0}_{3 \times 3} \\ \mathbf{0}_{3 \times 3} & \mathbf{C}_n^b \end{bmatrix} \delta\mathbf{u} \quad (3.13)$$

and for “perfect” INS alignment with very small uncertainties,

$$\delta \mathbf{x}(\mathbf{0}) = \begin{pmatrix} \delta \mathbf{P}(\mathbf{0}) \\ \delta \mathbf{V}(\mathbf{0}) \\ \delta \mathbf{\Psi}(\mathbf{0}) \end{pmatrix}_{9 \times 1}$$

where

$$(\delta \mathbf{P}_x^{(b)}(\mathbf{0}), \delta \mathbf{P}_y^{(b)}(\mathbf{0}), \delta \mathbf{P}_z^{(b)}(\mathbf{0}) \sim N(\mathbf{0}_{3 \times 1}, 1 \times 10^{-6} \mathbf{I}_3)$$

$$(\delta \mathbf{V}_x^{(b)}(\mathbf{0}), \delta \mathbf{V}_y^{(b)}(\mathbf{0}), \delta \mathbf{V}_z^{(b)}(\mathbf{0}) \sim N(\mathbf{0}_{3 \times 1}, 1 \times 10^{-16} \mathbf{I}_3)$$

$$(\delta \mathbf{\Psi}_\phi^{(b)}(\mathbf{0}), \delta \mathbf{\Psi}_\theta^{(b)}(\mathbf{0}), \delta \mathbf{\Psi}_\psi^{(b)}(\mathbf{0}) \sim N(\mathbf{0}_{3 \times 1}, 1 \times 10^{-8} \mathbf{I}_3)$$

Since this is wings level, constant altitude flight, in the direction of the x_n axis, the nominal, true navigation variables are

$$x = x_0 + v_x t + \frac{1}{2} a t^2, y = 0, z = h, \phi = \theta = \psi = 0. \text{ These variables are}$$

non-dimensionalized as follows

$$\begin{array}{lll} x \rightarrow \frac{x}{h}, & y \rightarrow \frac{y}{h}, & z \rightarrow \frac{z}{h}, \\ v_x \rightarrow \frac{v_x}{v}, & v_y \rightarrow \frac{v_y}{v}, & v_z \rightarrow \frac{v_z}{v}, \\ \delta f_x \rightarrow \frac{\delta f_x}{g}, & \delta f_y \rightarrow \frac{\delta f_y}{g}, & \delta f_z \rightarrow \frac{\delta f_z}{g}, \\ \delta \omega_x^b \rightarrow h \frac{\delta \omega_x^b}{v}, & \delta \omega_y^b \rightarrow h \frac{\delta \omega_y^b}{v}, & \delta \omega_z^b \rightarrow h \frac{\delta \omega_z^b}{v}, \\ t \rightarrow t \frac{v}{h}, & T \rightarrow T \frac{v}{h}, & \end{array}$$

where t is the current time, and T is the length of a measurement epoch.

The non-dimensional parameters are

$$g \triangleq \frac{hg}{v^2} \quad \text{and} \quad a \triangleq \frac{ha}{v^2}$$

During cruise, $a \equiv 0$. If, for example,

$$h = 1000[m], \quad v = 100 \left[\frac{m}{sec} \right], \quad g = 10 \left[\frac{m}{sec^2} \right],$$

the non-dimensional parameter $g = 1$. Since the ground features are spaced 1 [km] apart, the duration of a nondimensional measurement epoch $T = 1$.

It is assumed that the sensor errors are constant, albeit random biases that are Gaussian distributed. This allows the state error vector to be augmented with the disturbance vector $\delta \mathbf{u}$; the augmented state is

$$\delta \mathbf{x}_a = \begin{pmatrix} \delta \mathbf{x} \\ \dots \\ \delta \mathbf{u} \end{pmatrix}_{15 \times 1} \quad (3.14)$$

and the dynamics matrix is augmented by the $\mathbf{\Gamma}$ matrix, as shown

$$\mathbf{A}_a = \begin{bmatrix} \mathbf{A} & \mathbf{\Gamma} \\ \mathbf{0}_{6 \times 9} & \mathbf{0}_{6 \times 6} \end{bmatrix}_{15 \times 15} \quad (3.15)$$

One obtains a dynamic system in “free fall”. When converted to discrete time, $\mathbf{A}_a \rightarrow \mathbf{A}_{ad} = e^{\mathbf{A}_a \Delta T}$, where ΔT is the sampling interval. The augmented discrete time state dynamics become

$$\delta \mathbf{x}_a(l+1) = \mathbf{A}_{ad} \delta \mathbf{x}_a(l), \quad l = 0, \dots, L-1 \quad (3.16)$$

where l is the discrete time step counter and L is the total time during a measurement epoch during which the two ground features are being tracked. The non-dimensional time step is $\Delta T = \frac{T}{L} := \Delta T \frac{v}{h}$. The discrete-time dynamics matrix \mathbf{A}_{ad} can be analytically derived.

This dynamics equation applies as long as the ground objects’ positions (x_p, y_p) are known. Assuming the ground objects are stationary, but their position is not known, two additional states, the x and y horizontal coordinates of the tracked ground objects, must be added to the navigation state for each tracked ground object whose position will be estimated on the fly. If the number of unknown ground features being tracked is m , then

the augmented navigation state is

$$\delta \mathbf{x}_a := \begin{pmatrix} \delta \mathbf{x}_a \\ \vdots \\ \delta x_{p1} \\ \vdots \\ \delta y_{pm} \end{pmatrix}_{(15+2m) \times 1} \quad (3.17)$$

and

$$\mathbf{A}_{ad} := \begin{bmatrix} \mathbf{A}_{ad} & \mathbf{0}_{15 \times 2m} \\ \mathbf{0}_{2m \times 15} & \mathbf{I}_{2m \times 2m} \end{bmatrix}_{(15+2m) \times (15+2m)} \quad (3.18)$$

If, for example, one unknown ground feature is being tracked, as is the case during the second measurement epoch, then the dimension of the augmented navigation state's error is 17. Two unknown ground features are being tracked during the measurement epoch $n \geq 3$, whereupon the dimension of the navigation state's error is 19. On one hand, state augmentation reduces the degree of observability, which decreases the strength of INS aiding action. On the other hand, however, the inclusion of additional features to be tracked increases the number of measurement equations, which helps wash out the bearing angles measurement error.

3.3.2 Modeling/Calibrating the Free INS. With the dynamics from Subsection 3.3.1, the values for the standard deviation σ_a and σ_g , the uncertainty in the bias of the accelerometers and gyroscopes, respectively, are set such that the free INS is a $1 \frac{km}{hr}$ navigation system. Since the dynamics are not forced, that is, there is no controlled input, the calibration is performed by using the solution to the Lyapunov difference equation

$$\mathbf{P}(l+1) = \mathbf{A}_{ad} \mathbf{P}(l) \mathbf{A}_{ad}^T, \quad 0 \leq l \leq LN-1 \quad (3.19)$$

with the initial covariance matrix

$$\mathbf{P}(\mathbf{0}) = \begin{bmatrix} \mathbf{0}_{9 \times 9} & \mathbf{0} & \mathbf{0} \\ \mathbf{0} & \text{diag}(\sigma_a^2, \sigma_a^2, \sigma_a^2) & \mathbf{0} \\ \mathbf{0} & \mathbf{0} & \text{diag}(\sigma_g^2, \sigma_g^2, \sigma_g^2) \end{bmatrix}_{15 \times 15} \quad (3.20)$$

Note: During 1 *hr* the number of measurement epochs is $N = 360$.

Since the Lyapunov difference equation is linear, there is a linear relationship between the uncertainty in the sensors' biases variances and the ensuing uncertainty in the aircraft's x position:

$$P_{1,1}(LN) = \alpha \sigma_a^2 + \beta \sigma_g^2 \quad (3.21)$$

where the coefficients α and β are constants. Therefore, Eq. (3.19) is solved for one non-dimensional hour twice to calculate the values of the constants α and β . The first time, σ_a is set to 1 and σ_g is set to 0. The second time, σ_a is set to 0 and σ_g is set to 1. Then assigning the errors in the accelerometers and gyroscopes an equal role in the uncertainty of the aircraft's position at the nondimensional time 360, the values for the nondimensionalized variances of the sensors' biases are calculated as

$$\sigma_a = \frac{1}{\sqrt{2\alpha}} = 1.0912 \times 10^{-5} \quad (3.22)$$

$$\sigma_g = \frac{1}{\sqrt{2\beta}} = 9.0935 \times 10^{-8} \quad (3.23)$$

Using the calculated σ_a and σ_g , the errors of the free INS, $\delta \mathbf{x}_a$ are generated through the solution of the linear difference equation (3.16) with

$$\delta \mathbf{x}_a(\mathbf{0}) = \begin{pmatrix} \delta \mathbf{P}(\mathbf{0}) \\ \delta \mathbf{V}(\mathbf{0}) \\ \delta \mathbf{\Psi}(\mathbf{0}) \\ \delta \mathbf{f}(\mathbf{0}) \\ \delta \omega(\mathbf{0}) \end{pmatrix}_{15 \times 1} \quad (3.24)$$

where

$$\begin{aligned}
(\delta \mathbf{P}_x^{(b)}(\mathbf{0}), \delta \mathbf{P}_y^{(b)}(\mathbf{0}), \delta \mathbf{P}_z^{(b)}(\mathbf{0})) &\sim N(\mathbf{0}_{3 \times 1}, 1 \times 10^{-6} \mathbf{I}_3) \\
(\delta \mathbf{V}_x^{(b)}(\mathbf{0}), \delta \mathbf{V}_y^{(b)}(\mathbf{0}), \delta \mathbf{V}_z^{(b)}(\mathbf{0})) &\sim N(\mathbf{0}_{3 \times 1}, 1 \times 10^{-16} \mathbf{I}_3) \\
(\delta \Psi_\phi^{(b)}(\mathbf{0}), \delta \Psi_\theta^{(b)}(\mathbf{0}), \delta \Psi_\psi^{(b)}(\mathbf{0})) &\sim N(\mathbf{0}_{3 \times 1}, 1 \times 10^{-8} \mathbf{I}_3) \\
(\delta \mathbf{f}_x^{(b)}(\mathbf{0}), \delta \mathbf{f}_y^{(b)}(\mathbf{0}), \delta \mathbf{f}_z^{(b)}(\mathbf{0})) &\sim N(\mathbf{0}_{3 \times 1}, \sigma_a^2 \mathbf{I}_3) \\
(\delta \omega_x^{(b)}(\mathbf{0}), \delta \omega_y^{(b)}(\mathbf{0}), \delta \omega_z^{(b)}(\mathbf{0})) &\sim N(\mathbf{0}_{3 \times 1}, \sigma_g^2 \mathbf{I}_3)
\end{aligned}$$

Thus, it is assumed that the initial uncertainty in the aircraft position is ca. 1 [m], the uncertainty in its velocity is ca. 10^{-3} [mm/sec], and the uncertainty in pitch, roll, and yaw is a ca. 20 arc seconds. The ensuing navigation state error of the free INS is given by the solution of Eq. (3.16) solved over the planning horizon $360L - 1$. These are the errors of an unaided/free INS and will serve as a benchmark to be compared to the errors when, using SLAM the INS is aided by the measurement over time of the bearings of terrain features.

3.3.3 Measurement Equation. The relationship of the inertial position and attitude of the aircraft to that of the ground object/feature P is

$$\begin{bmatrix} x \\ y \\ z \end{bmatrix} = \begin{bmatrix} x_p \\ y_p \\ z_p \end{bmatrix} - \frac{|R_{LOS}|}{\sqrt{x_f^2 + y_f^2 + f^2}} \mathbf{C}_b^n \begin{bmatrix} x_f \\ y_f \\ -f \end{bmatrix} \quad (3.25)$$

where x_f and y_f are the projections of the ground feature's respective x and y coordinates onto the focal plane of the camera and f is the camera's focal length - see Figure 3.2. For

the case when the aircraft flies wings level at a constant altitude in the direction of the x_n axis and the Euler angles are small, the DCM for relating the body frame to the navigation frame is given in Eq. (3.5). The relationship (3.25) has the appearance of three equations but in fact has the strength of two independent equations. The first two equations in the

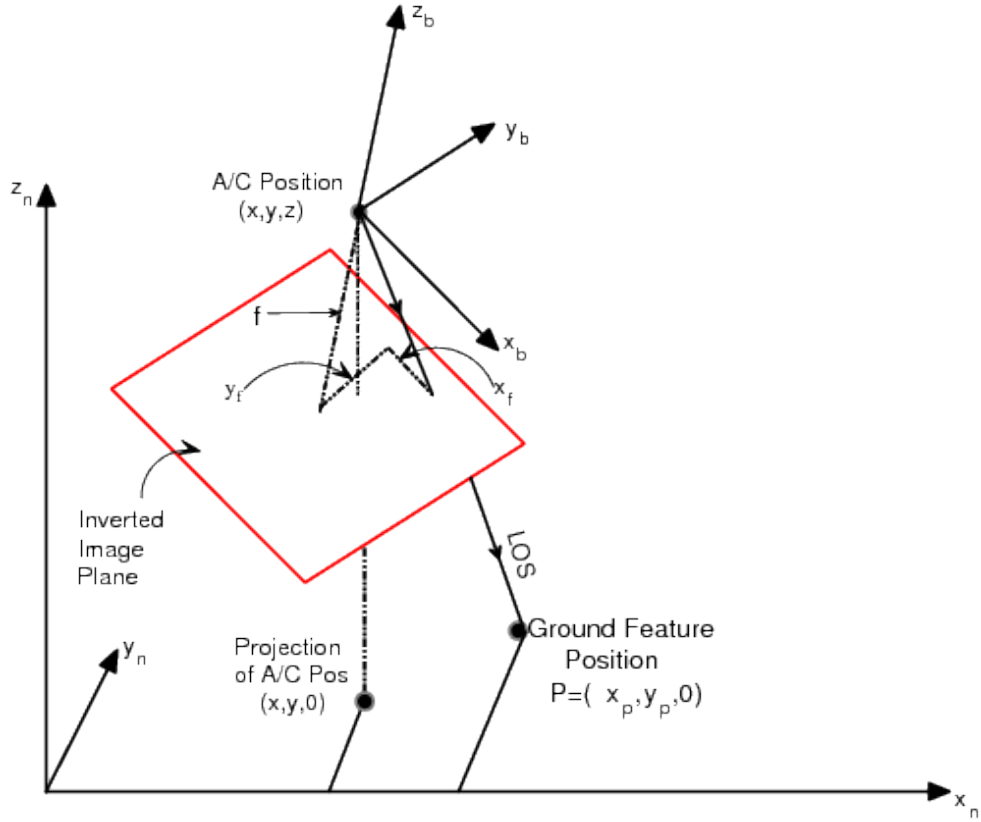


Figure 3.2: Measurement Geometry in General Position.

relationship given by Eq. (3.25) are non-linearly dependent on the third. Now, the third equation yields

$$z_p - z = \frac{|R_{LOS}|}{\sqrt{x_f^2 + y_f^2 + f^2}} \begin{bmatrix} 0 & 0 & 1 \end{bmatrix} \mathbf{C}_b^n \begin{bmatrix} x_f \\ y_f \\ -f \end{bmatrix}$$

and thus

$$\frac{|R_{LOS}|}{\sqrt{x_f^2 + y_f^2 + f^2}} = \frac{z_p - z}{\begin{bmatrix} 0 & 0 & 1 \end{bmatrix} \mathbf{C}_b^n \begin{bmatrix} x_f \\ y_f \\ -f \end{bmatrix}} \quad (3.26)$$

Substituting Eq. (3.26) into Eq. (3.25) yields the two measurement equations for the three dimensional case:

$$\begin{bmatrix} x \\ y \end{bmatrix} = \begin{bmatrix} x_p \\ y_p \end{bmatrix} - \frac{z_p - z}{\begin{bmatrix} 0 & 0 & 1 \end{bmatrix} \mathbf{C}_b^n \begin{bmatrix} x_f \\ y_f \\ -f \end{bmatrix}} \begin{bmatrix} 1 & 0 & 0 \\ 0 & 1 & 0 \end{bmatrix} \mathbf{C}_b^n \begin{bmatrix} x_f \\ y_f \\ -f \end{bmatrix}$$

Multiplying out the matrices yields

$$\begin{bmatrix} x \\ y \end{bmatrix} = \begin{bmatrix} x_p \\ y_p \end{bmatrix} - (z_p - z) \frac{1}{-f - \theta x_f + \phi y_f} \begin{bmatrix} x_f - \psi y_f - f\theta \\ y_f + x_f\psi + f\phi \end{bmatrix}$$

and nondimensionalizing such that

$$x_f \rightarrow \frac{x_f}{f}, \quad y_f \rightarrow \frac{y_f}{f}$$

yields

$$\begin{bmatrix} x \\ y \end{bmatrix} = \begin{bmatrix} x_p \\ y_p \end{bmatrix} - (z_p - z) \frac{1}{-1 - \theta x_f + \phi y_f} \begin{bmatrix} x_f - \psi y_f - \theta \\ y_f + x_f\psi + \phi \end{bmatrix}$$

Thus, two separate nonlinear measurement equations are obtained

$$x_p - x = -(z_p - z) \frac{x_f - \psi y_f - \theta}{1 + \theta x_f - \phi y_f} \quad (3.27)$$

$$y_p - y = -(z_p - z) \frac{y_f + \psi x_f + \phi}{1 + \theta x_f - \phi y_f} \quad (3.28)$$

Due to the small angles assumption, the denominator in Eqs. (3.27) and (3.28) can be moved up such that

$$x_p - x \approx -(z_p - z)(x_f - \psi y_f - \theta)(1 - \theta x_f + \phi y_f) \quad (3.29)$$

$$y_p - y \approx -(z_p - z)(y_f + x_f\psi + \phi)(1 - \theta x_f + \phi y_f) \quad (3.30)$$

Since the aircraft is using ground objects to aid its INS, it can be assumed, without loss of generality, that the terrain elevation is known and $z_p = 0$. Due to the small values of the

angles, when the former fraction is distributed out, the products of the angles are negligible, yielding

$$x_p - x = z[x_f - \theta(1 + x_f^2) + \phi x_f y_f - \psi y_f] \quad (3.31)$$

$$y_p - y = z[y_f - \theta x_f y_f + \phi(1 + y_f^2) + \psi x_f] \quad (3.32)$$

Next, perturb the states and the measurements

$$\begin{aligned} x &= x_c - \delta x & y &= y_c - \delta y & z &= z_c - \delta z \\ \theta &= \theta_c - \delta \theta & \phi &= \phi_c - \delta \phi & \psi &= \psi_c - \delta \psi \\ x_p &= x_{pc} - \delta x_p & y_p &= y_{pc} - \delta y_p \\ x_f &= x_{fm} - \delta x_f & y_f &= y_{fm} - \delta y_f \end{aligned}$$

where the subscript c indicates the navigation states components provided by the free INS and the subscript m indicates measured quantities. The calculation of the “nominal” position (x_{pc}, y_{pc}) of a geolocated ground feature will be discussed in the sequel. Inserting the perturbation equations into the measurement Eqs. (3.31) and (3.32) yields

$$\begin{aligned} x_{pc} - x_c + \delta x - \delta x_p &= (z_c - \delta z) \left(x_{fm} - \delta x_f - (\theta_c - \delta \theta)(1 + x_{fm}^2 - 2x_{fm}\delta x_f + \delta x_f^2) \right. \\ &\quad \left. + (\phi_c - \delta \phi)(x_{fm} - \delta x_f)(y_{fm} - \delta y_f) - (\psi_c - \delta \psi)(y_{fm} - \delta y_f) \right) \end{aligned}$$

Due to the small error in the measurements and the small angles, the products of these terms can be neglected.

$$\begin{aligned} x_{pc} - x_c + \delta x - \delta x_p &= (z_c - \delta z) \left(x_{fm} - \delta x_f - (\theta_c - \delta \theta)(1 + x_{fm}^2) \right. \\ &\quad \left. + (\phi_c - \delta \phi)x_{fm}y_{fm} - (\psi_c - \delta \psi)y_{fm} \right) \end{aligned}$$

Similarly, in the second measurement equation

$$\begin{aligned} y_{pc} - y_c + \delta y - \delta y_p &= (z_c - \delta z) \left(y_{fm} - \delta y_f - (\theta_c - \delta \theta)(x_{fm} - \delta x_f)(y_{fm} - \delta y_f) + (\phi_c - \delta \phi) \right. \\ &\quad \left. (y_{fm}^2 - 2y_{fm}\delta y_f + \delta y_f^2) + (\psi_c - \delta \psi)(x_{fm} - \delta x_f) \right) \\ &= (z_c - \delta z) \left(y_{fm} - \delta y_f - (\theta_c - \delta \theta)x_{fm}y_{fm} + (\phi_c - \delta \phi)(1 + y_{fm}^2) \right. \\ &\quad \left. + (\psi_c - \delta \psi)x_{fm} \right) \end{aligned}$$

Moving all the error terms to the Right Hand Side (RHS) of the equation and all the non-error terms to the Left Hand Side (LHS) yields

$$\begin{aligned}
x_{pc} - x_c - z_c[x_{fm} - \theta_c(1 + x_{fm}^2) + \phi_c x_{fm} y_{fm} - \psi_c y_{fm}] = \\
- \delta x - \delta z[x_{fm} - \theta_c(1 + x_{fm}^2) + \phi_c x_{fm} y_{fm} - \psi_c y_{fm}] \\
+ \delta\theta(1 + x_{fm}^2)z_c - \delta\phi x_{fm} y_{fm} z_c + \delta\psi y_{fm} z_c + \delta x_p - z_c \delta x_f
\end{aligned} \tag{3.33}$$

and

$$\begin{aligned}
y_{pc} - y_c - z_c[y_{fm} - \theta_c x_{fm} y_{fm} + \phi_c(1 + y_{fm}^2) + \psi_c x_{fm}] = \\
- \delta y - \delta z[y_{fm} - \theta_c x_{fm} y_{fm} + \phi_c(1 + y_{fm}^2) + \psi_c x_{fm}] \\
+ \delta\theta x_{fm} y_{fm} z_c - \delta\phi(1 + y_{fm}^2)z_c - \delta\psi x_{fm} z_c + \delta y_p - z_c \delta y_f
\end{aligned} \tag{3.34}$$

Finally, nondimensionalizing such that

$$x_p \rightarrow \frac{x_p}{h} \quad y_p \rightarrow \frac{y_p}{h} \quad z_p \rightarrow \frac{z_p}{h},$$

we also note that the nominal nondimensional altitude is $z = 1$. In addition, for the purpose of covariance and Kalman Filtering analysis, set all of the calculated and measured values on the RHS equal to the nominal/true values. This causes all of the angles to go to zero, simplifying the measurement Eqs. (3.33) and (3.34). Also, on the RHS set $x_{fm} := x_f$ and $y_{fm} := y_f$, where, in view of the nondimensionalization, and since in the KF mechanization in each measurement epoch t is the time elapsed from the beginning of the epoch, $x_f = x_p - t$, $y_f = y_p - t$ - see Figure 3.1. Hence, for the first ground object, $x_{f1}(t) = 1 - t$, $y_{f1}(t) = y_{p1}$ and for the second ground object $x_{f2}(t) = 2 - t$, $y_{f2}(t) = y_{p2}$.

Thus, Eqs. (3.33) and (3.34) yield the linearized measurement equations

$$\begin{aligned}
x_{pc} - x_c - z_c[x_{fm} - \theta_c(1 + x_{fm}^2) + \phi_c x_{fm} y_{fm} - \psi_c y_{fm}] = \\
- \delta x - x_f \delta z + \delta\theta(1 + x_f^2) - x_f y_f \delta\phi + y_f \delta\psi + \delta x_p - \delta x_f
\end{aligned} \tag{3.35}$$

and

$$\begin{aligned}
y_{pc} - y_c - z_c[y_{fm} - \theta_c x_{fm} y_{fm} + \phi_c(1 + y_{fm}^2) + \psi_c x_{fm}] = \\
- \delta y - \delta z y_f + x_f y_f \delta\theta - \delta\phi(1 + y_f^2) - x_f \delta\psi + \delta y_p - \delta y_f
\end{aligned} \tag{3.36}$$

Hence, the time dependent observation matrix $\mathbf{H}(l)$ during a measurement epoch with one unknown ground feature is

$$\mathbf{H}_u(l) = \begin{bmatrix} -1 & 0 \\ 0 & -1 \\ -x_f & -y_f \\ 0 & 0 \\ 0 & 0 \\ 0 & 0 \\ -x_f y_f & -(1 + y_f^2) \\ 1 + x_f^2 & x_f y_f \\ y_f & -x_f \\ 0 & 0 \\ 0 & 0 \\ 0 & 0 \\ 0 & 0 \\ 0 & 0 \\ 0 & 0 \\ 1 & 0 \\ 0 & 1 \end{bmatrix}^T \quad (3.37)$$

where the subscript $_u$ indicates that the position of the ground object being tracked is unknown. The nondimensional measurement error is $[\delta x_f, \delta y_f]^T$.

Since, for the sake of observability [9], in each measurement epoch two ground objects will be tracked, there will be two subscripts 1 and 2. The first corresponds to the ground object that is closer to the aircraft and the second to the ground object that is further away. In the first measurement epoch it is assumed that both ground objects are

known. If both ground objects are known, the observation matrix is

$$\mathbf{H}_{kk}(l) = \begin{bmatrix} -1 & 0 & -1 & 0 \\ 0 & -1 & 0 & -1 \\ -x_{f1} & -y_{f1} & -x_{f2} & -y_{f2} \\ 0 & 0 & 0 & 0 \\ 0 & 0 & 0 & 0 \\ 0 & 0 & 0 & 0 \\ -x_{f1}y_{f1} & -(1 + y_{f1}^2) & -x_{f2}y_{f2} & -(1 + y_{f2}^2) \\ 1 + x_{f1}^2 & x_{f1}y_{f1} & 1 + x_{f2}^2 & x_{f2}y_{f2} \\ y_{f1} & -x_{f1} & y_{f2} & -x_{f2} \\ 0 & 0 & 0 & 0 \\ 0 & 0 & 0 & 0 \\ 0 & 0 & 0 & 0 \\ 0 & 0 & 0 & 0 \\ 0 & 0 & 0 & 0 \\ 0 & 0 & 0 & 0 \end{bmatrix}^T \quad (3.38)$$

where the subscript k indicates that the position of the ground object is known. In the second measurement epoch a new ground feature is acquired so that in the field of view of the camera there is one known and one unknown ground object. When there is one known

and one unknown ground object, the observation matrix is

$$\mathbf{H}_{ku}(l) = \begin{bmatrix} -1 & 0 & -1 & 0 \\ 0 & -1 & 0 & -1 \\ -x_{f1} & -y_{f1} & -x_{f2} & -y_{f2} \\ 0 & 0 & 0 & 0 \\ 0 & 0 & 0 & 0 \\ 0 & 0 & 0 & 0 \\ -x_{f1}y_{f1} & -(1+y_{f1}^2) & -x_{f2}y_{f2} & -(1+y_{f2}^2) \\ 1+x_{f1}^2 & x_{f1}y_{f1} & 1+x_{f2}^2 & x_{f2}y_{f2} \\ y_{f1} & -x_{f1} & y_{f2} & -x_{f2} \\ 0 & 0 & 0 & 0 \\ 0 & 0 & 0 & 0 \\ 0 & 0 & 0 & 0 \\ 0 & 0 & 0 & 0 \\ 0 & 0 & 0 & 0 \\ 0 & 0 & 0 & 0 \\ 0 & 0 & 1 & 0 \\ 0 & 0 & 0 & 1 \end{bmatrix}^T \quad (3.39)$$

Finally, starting at measurement epoch three when neither ground object's position is known, the observation matrix

$$\mathbf{H}_{uu}(l) = \begin{bmatrix} -1 & 0 & -1 & 0 \\ 0 & -1 & 0 & -1 \\ -x_{f1} & -y_{f1} & -x_{f2} & -y_{f2} \\ 0 & 0 & 0 & 0 \\ 0 & 0 & 0 & 0 \\ 0 & 0 & 0 & 0 \\ -x_{f1}y_{f1} & -(1 + y_{f1}^2) & -x_{f2}y_{f2} & -(1 + y_{f2}^2) \\ 1 + x_{f1}^2 & x_{f1}y_{f1} & 1 + x_{f2}^2 & x_{f2}y_{f2} \\ y_{f1} & -x_{f1} & y_{f2} & -x_{f2} \\ 0 & 0 & 0 & 0 \\ 0 & 0 & 0 & 0 \\ 0 & 0 & 0 & 0 \\ 0 & 0 & 0 & 0 \\ 0 & 0 & 0 & 0 \\ 0 & 0 & 0 & 0 \\ 1 & 0 & 0 & 0 \\ 0 & 1 & 0 & 0 \\ 0 & 0 & 1 & 0 \\ 0 & 0 & 0 & 1 \end{bmatrix}^T \quad (3.40)$$

Two ground objects, P_1 and P_2 are tracked. The measurements \mathbf{z} given to the Kalman Filter during the n th measurement epoch at each time step, $l=1, 2=L$, are generated from

the LHS of Eqs. (3.35) and (3.36) as

$$\mathbf{z} = \begin{pmatrix} x_{p1c} - x_c - z_c(x_{fm1} - \theta_c(1 + x_{fm1}^2) + \phi_c x_{fm1} y_{fm1} - \psi_c y_{fm1}) \\ y_{p1c} - y_c - z_c(y_{fm1} - \theta_c x_{fm1} y_{fm1} + \phi_c(1 + y_{fm1}^2) + \psi_c x_{fm1}) \\ x_{p2c} - x_c - z_c(x_{fm2} - \theta_c(1 + x_{fm2}^2) + \phi_c x_{fm2} y_{fm2} - \psi_c y_{fm2}) \\ y_{p2c} - y_c - z_c(y_{fm2} - \theta_c x_{fm2} y_{fm2} + \phi_c(1 + y_{fm2}^2) + \psi_c x_{fm2}) \end{pmatrix} \quad (3.41)$$

where

$$\mathbf{x}_{f1}(t) = 1 - t, \quad \mathbf{x}_{f2}(t) = 2 - t, \quad t = l\Delta T, \quad 1 \leq l \leq L$$

and

$$\begin{aligned} \mathbf{x}_{fm1} &= \mathbf{x}_{f1}(t) + \xi_1, & \mathbf{x}_{fm2} &= \mathbf{x}_{f2}(t) + \xi_2, \\ \xi_1 &\sim N(0, \sigma^2), & \xi_2 &\sim N(0, \sigma^2), \\ \mathbf{y}_{fm1} &= \mathbf{y}_{f1} + \eta_1, & \mathbf{y}_{fm2} &= \mathbf{y}_{f2} + \eta_2, \\ \eta_1 &\sim N(0, \sigma^2), & \eta_2 &\sim N(0, \sigma^2) \end{aligned}$$

where $\sigma = \frac{1}{3} \times 10^{-3}$ (for a 9 mega pixels camera with an aspect ratio of 1). The calculated navigation state is output by the free INS and given by

$$\mathbf{x}_c = \mathbf{x}_F = \mathbf{x} + \delta\mathbf{x}_F$$

where \mathbf{x} is the true (nondimensional) navigation state given by

$$\mathbf{x} = [t \ 0 \ 1 \ 1 \ 0 \ 0 \ 0 \ 0 \ 0]^T$$

and $\delta\mathbf{x}_F$ is the navigation state error of the free INS. Thus, the sequence $\delta\mathbf{x}_F$ is obtained as follows:

$$\delta\mathbf{x}_F(l+1) = \mathbf{A}_{ad}\delta\mathbf{x}_F(k), \quad \delta\mathbf{x}_a(\mathbf{0}) = \begin{pmatrix} \delta\mathbf{P}(\mathbf{0}) \\ \delta\mathbf{V}(\mathbf{0}) \\ \delta\mathbf{\Psi}(\mathbf{0}) \\ \delta\mathbf{f}(\mathbf{0}) \\ \delta\omega(\mathbf{0}) \end{pmatrix}_{15 \times 1}$$

$$l = 0, \dots, LN - 1$$

where

$$(\delta \mathbf{P}_x^{(b)}(\mathbf{0}), \delta \mathbf{P}_y^{(b)}(\mathbf{0}), \delta \mathbf{P}_z^{(b)}(\mathbf{0})) \sim N(\mathbf{0}_{3 \times 1}, 1 \times 10^{-6} \mathbf{I}_3)$$

$$(\delta \mathbf{V}_x^{(b)}(\mathbf{0}), \delta \mathbf{V}_y^{(b)}(\mathbf{0}), \delta \mathbf{V}_z^{(b)}(\mathbf{0})) \sim N(\mathbf{0}_{3 \times 1}, 1 \times 10^{-16} \mathbf{I}_3)$$

$$(\delta \mathbf{\Psi}_\phi^{(b)}(\mathbf{0}), \delta \mathbf{\Psi}_\theta^{(b)}(\mathbf{0}), \delta \mathbf{\Psi}_\psi^{(b)}(\mathbf{0})) \sim N(\mathbf{0}_{3 \times 1}, 1 \times 10^{-8} \mathbf{I}_3)$$

$$(\delta \mathbf{f}_x^{(b)}(\mathbf{0}), \delta \mathbf{f}_y^{(b)}(\mathbf{0}), \delta \mathbf{f}_z^{(b)}(\mathbf{0})) \sim N(\mathbf{0}_{3 \times 1}, \sigma_a^2 \mathbf{I}_3)$$

$$(\delta \omega_x^{(b)}(\mathbf{0}), \delta \omega_y^{(b)}(\mathbf{0}), \delta \omega_z^{(b)}(\mathbf{0})) \sim N(\mathbf{0}_{3 \times 1}, \sigma_g^2 \mathbf{I}_3)$$

During a measurement epoch x_{p1c} , x_{p2c} , y_{p2c} , and y_{p1c} which feature in measurements \mathbf{z} given to the KF are held constant. At the end of the measurement epoch they are updated for the next measurement epoch. They are calculated according to Tables B.1 - B.3 in Appendix B.

3.3.4 Synthesis of the Measurement Sent to the KF in Epoch n . In epoch 1, $x_{p1c} = 1$, $y_{p1c} = -y_p$, and $x_{p2c} = 2$, $y_{p2c} = y_p$. In epoch 2, $x_{p1c} = 2$, $y_{p1c} = y_p$.

Consider measurement epoch n , $3 \leq n \leq N$, $N=360$. In total, $n + 1$ ground features are used. $n - 1$ new ground features are geolocated.

The meaning of $x_{pc}^{(n)}$ and $y_{pc}^{(n)}$ used during epoch $n \geq 2$ to calculate the measurement given to the KF - we refer to Eq. (3.41): they are kept constant during the measurement epoch (n) and were calculated at the conclusion of epoch ($n - 1$) using Eqs. (3.27) and (3.28) and setting therein $z_p \equiv 0$:

$$x_{p2c}^{(n)} = x + z \frac{x_f - \psi y_f - \theta}{1 + \theta x_f - \phi y_f} \quad (3.42)$$

$$y_{p2c}^{(n)} = y + z \frac{y_f + \psi x_f + \phi}{1 + \theta x_f - \phi y_f} \quad (3.43)$$

Since the scenario considered is wings level flight at constant altitude, in Eqs. (3.42) and (3.43) set

$$\begin{aligned}x &= n - 1 + \delta x_F|_{n-1} - \hat{\delta x}|_{n-1}, \\y &= \delta y_F|_{n-1} - \hat{\delta y}|_{n-1}, \\z &= 1 + \delta z_F|_{n-1} - \hat{\delta z}|_{n-1}, \\\psi &= \delta \psi_F|_{n-1} - \hat{\delta \psi}|_{n-1}, \\\theta &= \delta \theta_F|_{n-1} - \hat{\delta \theta}|_{n-1}, \\\phi &= \delta \phi_F|_{n-1} - \hat{\delta \phi}|_{n-1}\end{aligned}$$

and since at the end of an epoch the newly acquired ground feature's $x_f = 2$, $y_f = \pm y_p$, in Eqs. (3.42) and (3.43) set

$$\begin{aligned}x_f &= 2 + \xi, \quad \xi \sim N(0, \sigma^2), \\y_f &= \pm y_p + \eta, \quad \eta \sim N(0, \sigma^2)\end{aligned}$$

where

$$\begin{aligned}\sigma &= \frac{1}{3} \times 10^{-3}, \\\delta x_F|_{n-1} &\equiv \delta x_F((n-1)L), \quad \delta y_F|_{n-1} \equiv \delta y_F((n-1)L)\end{aligned}$$

whereas

$$\hat{\delta x}|_{n-1} \equiv \hat{\delta x}^{(n-1)}(L), \quad \hat{\delta y}|_{n-1} \equiv \hat{\delta y}^{(n-1)}(L)$$

and the same applies to the navigation states z, ψ, θ, ϕ . In addition, at the end of the measurement epoch $n - 1$, set

$$\begin{aligned}x_{p1c}^{(n)} &:= x_{p2c}^{(n-1)} - \hat{\delta x}_{p2}^{(n-1)}(L), \\y_{p1c}^{(n)} &:= y_{p2c}^{(n-1)} - \hat{\delta y}_{p2}^{(n-1)}(L), \\n &= 3, \dots, 360\end{aligned}$$

Also, at the end of the measurement epoch 1 set

$$x_{p1c}^{(2)} = 2, \quad y_{p1c}^{(2)} = 0$$

Also, during measurement epoch n , at time l , in Eq. (3.41)

$$\begin{aligned} x_c &= t + \delta x_F(t), & y_c &= \delta y_F(t), & z_c &= 1 + \delta z_F(t), \\ \theta_c &= \delta \theta_F(t), & \phi_c &= \delta \phi_F(t), & \psi_c &= \delta \psi_F(t) \end{aligned}$$

where

$$t = n - 1 + \Delta T * l, \quad l = 1, \dots, L, \quad \Delta T = 1/L$$

and

$$\begin{aligned} x_{f1m} &= x_{f1} + \xi_1, \quad \xi_1 \sim N(0, \sigma^2), \\ x_{f2m} &= x_{f2} + \xi_2, \quad \xi_2 \sim N(0, \sigma^2), \\ y_{f1m} &= \pm y_p + \eta_1, \quad \eta_1 \sim N(0, \sigma^2), \\ y_{f2m} &= \mp y_p + \eta_2, \quad \eta_2 \sim N(0, \sigma^2) \end{aligned}$$

where, during the measurement epoch (n)

$$x_{f1} = 1 - l\Delta T, \quad x_{f2} = 2 - l\Delta T, \quad l = 1, \dots, L$$

3.4 Performance of Aided INS

The performance of the aided INS is evaluated for the nominal scenario described in Section 3.2 and illustrated in Figure 3.3. The aircraft is flying wings-level, at a constant speed with ground features spaced at one kilometer apart. The first two ground features are known and the aircraft starts one kilometer behind the first ground feature. In the observation matrices \mathbf{H} ,

$$x_{f1}(t) = 1 - t, \quad x_{f2}(t) = 2 - t, \quad 0 \leq t \leq 1$$

If ground features are arranged in a straight line on the positive x_n axis, then in the \mathbf{H} matrix

$$y_{f1}(t) = y_{f2}(t) = 0$$

However, if the ground features are laterally staggered at equal distance y_p about the positive x_n axis, then in the \mathbf{H} matrix

$$y_{f1}(t) = y_p \quad y_{f2}(t) = -y_p$$

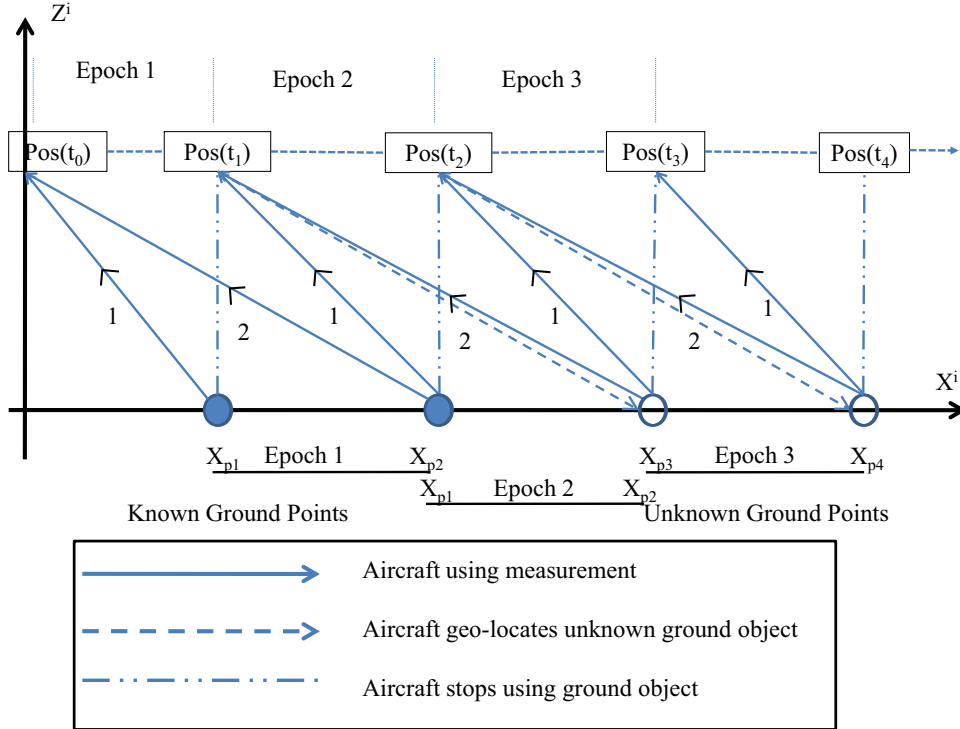


Figure 3.3: In the first measurement epoch the two ground objects' position are known, but in the second measurement epoch there is one known and one unknown ground object, where the unknown object's position was estimated by the aircraft at the end of the first epoch. From epoch 3 onward both ground objects' locations are estimated using the aircraft's navigation state at the end of the preceding epoch and therefore are not exactly known.

3.4.1 Initialization of the KF. In the first measurement epoch the Kalman Filter is initialized according to Eq. (3.44)

$$(\hat{\delta \mathbf{x}}_a^+ (\mathbf{0}))^{(1)} = \mathbf{0}_{15 \times 1} \quad (3.44)$$

while the covariance matrix is initialized as $(\mathbf{P}(\mathbf{0}))^{(1)}$ by using \mathbf{P} as in the equation following Eq. (3.24) where it is assumed that the position, velocity, and orientation are known with an uncertainty of $a = 1 \times 10^{-6}$, $b = 1 \times 10^{-16}$, and $c = 1 \times 10^{-8}$, respectively as in, Eq. (3.45).

$$(\mathbf{P}(\mathbf{0}))^{(1)} = \begin{bmatrix} A & \mathbf{0} & \mathbf{0} & \mathbf{0} & \mathbf{0} \\ \mathbf{0} & B & \mathbf{0} & \mathbf{0} & \mathbf{0} \\ \mathbf{0} & \mathbf{0} & C & \mathbf{0} & \mathbf{0} \\ \mathbf{0} & \mathbf{0} & \mathbf{0} & D & \mathbf{0} \\ \mathbf{0} & \mathbf{0} & \mathbf{0} & \mathbf{0} & E \end{bmatrix}_{15 \times 15} \quad (3.45)$$

where

$$A = \text{diag}(a, a, a)$$

$$B = \text{diag}(b, b, b)$$

$$C = \text{diag}(c, c, c)$$

$$D = \text{diag}(\sigma_a^2, \sigma_a^2, \sigma_a^2)$$

$$E = \text{diag}(\sigma_g^2, \sigma_g^2, \sigma_g^2)$$

The superscripts in $(\delta \hat{\mathbf{x}}_a^+ (\mathbf{0}))^{(1)}$ and $(\mathbf{P}(\mathbf{0}))^{(1)}$ represents the epoch number (epoch 1 in this case). The three accelerometer and the three gyroscope set are of the same quality: the random biases in the sensors are

$$\begin{aligned} \delta f_x^b &\sim N(0, \sigma_a^2) & \delta f_y^b &\sim N(0, \sigma_a^2) & \delta f_z^b &\sim N(0, \sigma_a^2) \\ \delta \omega_x^b &\sim N(0, \sigma_g^2) & \delta \omega_y^b &\sim N(0, \sigma_g^2) & \delta \omega_z^b &\sim N(0, \sigma_g^2) \end{aligned}$$

In each measurement epoch the KF is re-initialized. Since in measurement epoch n , $n \geq 2$, one navigates off a newly acquired ground feature, the KF is being re-initialized as

follows: In epoch $n = 2$ the KF state is a 17×1 vector initialized as

$$(\hat{\delta x}(0)_{15 \times 1})^{(2)} = (\hat{\delta x}(L)_{15 \times 1})^{(1)}, \quad \delta \hat{x}_{p2}(0) = 0, \quad \delta \hat{y}_{p2}(0) = 0,$$

$$\text{and } (\mathbf{P}(0))^{(2)} = \begin{bmatrix} (\mathbf{P}(L)_{15 \times 15})^{(1)} & \mathbf{p}_{15 \times 2}^{(2)} \\ (\mathbf{p}_{2 \times 15}^{(2)})^T & \mathbf{\Pi}_{2 \times 2}^{(2)} \end{bmatrix}_{17 \times 17}$$

where the covariance of the position error of the newly acquired ground feature and their cross correlation terms are calculated using Eqs. (3.31) and (3.32). The ground position x_p and y_p are isolated from Eqs. (3.31) and (3.32) as follows:

$$x_p = x + z[x_f - \theta(1 + x_f^2) + \phi x_f y_f - \psi y_f] \quad (3.46)$$

$$y_p = y + z[y_f - \theta x_f y_f + \phi(1 + y_f^2) + \psi x_f] \quad (3.47)$$

Perturbing Eq (3.46) yields

$$\begin{aligned} \delta x_{p2} = & \delta x + \delta z[x_f - \theta(1 + x_f^2) + \phi x_f y_f - \psi y_f] + z[\delta x_f - \delta \theta(1 + x_f^2) - 2x_f \theta \delta x_f + x_f y_f \delta \phi \\ & + \phi x_f \delta y_f + \phi \delta x_f y_f - y_f \delta \psi - \psi \delta y_f] \end{aligned}$$

Setting $z = 1$, $\psi = \theta = \phi = 0$, $x_f = 2$, $y_f = \pm y_p$, $\delta x_f = \xi$, and $\delta y_f = \eta$, where

$$\xi \sim N(0, \sigma^2), \quad \eta \sim N(0, \sigma^2)$$

we obtain: at the beginning of epoch 2 the error in the newly acquired feature's position

$$\delta x_{p2}(0) = \delta x + 2\delta z - 5\delta \theta \pm 2y_p \delta \phi \mp y_p \delta \psi + \xi \quad (3.48)$$

Similarly, perturbing Eq. (3.47) yields

$$\begin{aligned} \delta y_{p2} = & \delta y + \delta z[y_f - \theta x_f y_f + \phi(1 + y_f^2) + \psi x_f] + z[\delta y_f - x_f y_f \delta \theta - \theta x_f \delta y_f - \theta y_f \delta x_f \\ & + 2y_f \phi \delta y_f + \delta \phi(1 + y_f^2) + \psi \delta x_f + x_f \delta \psi] \end{aligned}$$

That is, at the beginning of epoch 2 the error in the newly acquired feature's position

$$\delta y_{p2}(0) = \delta y \pm y_p \delta z \mp 2y_p \delta \theta + (1 + y_p^2) \delta \phi + 2\delta \psi + \eta \quad (3.49)$$

Eqs. (3.48) and (3.49), can be re-written to give the x and y position of the second ground feature at the beginning of an epoch as

$$\delta x_{p2}^{(n)}(0) = \delta x(L)^{(n-1)} + 2\delta z(L)^{(n-1)} - 5\delta\theta(L)^{(n-1)} \pm 2y_p\delta\phi(L)^{(n-1)} \mp y_p\delta\psi(L)^{(n-1)} + \xi \quad (3.50)$$

$$\begin{aligned} \delta y_{p2}^{(n)}(0) = & \delta y(L)^{(n-1)} + \delta\phi(L)^{(n-1)} + 2\delta\psi(L)^{(n-1)} \pm y_p\delta z(L)^{(n-1)} \mp 2y_p\delta\theta(L)^{(n-1)} \\ & + y_p^2\delta\phi(L)^{(n-1)} + \eta \end{aligned} \quad (3.51)$$

3.4.2 Kalman Filter: The INS aiding scheme is as illustrated in Figure 3.4. The

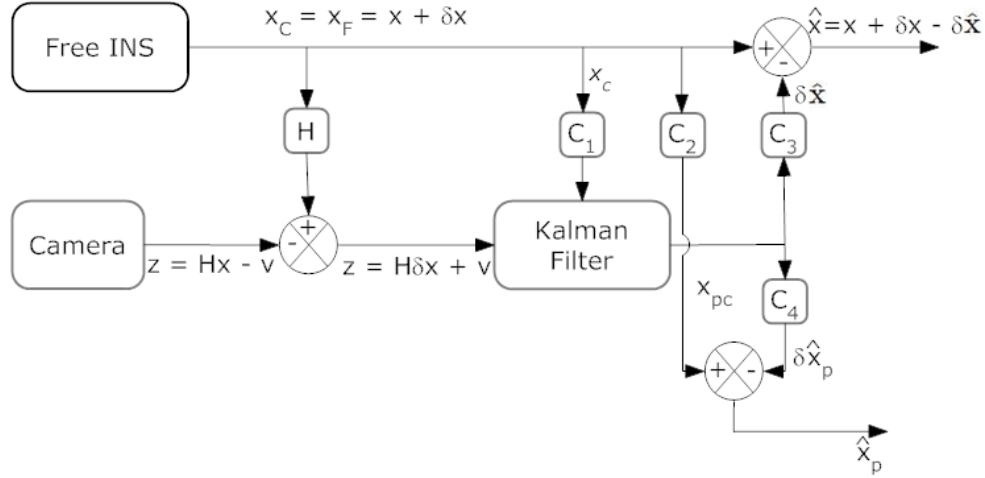


Figure 3.4: INS Aiding Using a Kalman Filter

free INS outputs the calculated navigation state, \mathbf{x}_c , which is the sum of the true navigation state, \mathbf{x} and the errors in the navigation states of the free INS, $\delta\mathbf{x}$. The aircraft's camera generates a noise corrupted measurement of the free INS navigation state and upon linearizing the measurement equation a measurement of the navigation state's error is obtained, as shown in Figure 3.4. The results of this operation gives the measurement \mathbf{z} , which is provided to the KF. Using this information, the KF calculates an estimate $\hat{\delta\mathbf{x}}$ of the free INS navigation state error $\delta\mathbf{x}$, which is subtracted from the free INS navigation state $\mathbf{x}_F = \mathbf{x} + \delta\mathbf{x}$ to yield the calculated “clean” navigation state $\mathbf{x}_c = \mathbf{x} + \delta\mathbf{x} - \hat{\delta\mathbf{x}}$. Thus in

effect, the KF removes the error from the calculated navigation state, as shown in Figure 3.4.

In the measurement epoch 1, the positions of both tracked ground features are assumed known. Therefore, in epoch 1 the observation matrix $\mathbf{H}_{\mathbf{k}\mathbf{k}}(l)_{4 \times 15}$, and the dynamics matrix $\mathbf{A}_{\mathbf{ad}}_{15 \times 15}$ are used. For both scenarios (ground features in a straight line and staggered), the one hour flight duration results in 360 nondimensionalized seconds resulting in 360 epochs. Each non-dimentionalized second is 10 [s]. Sampling at 0.2 [Hz] results in $L = 2$ bearing measurements in each measurement epoch. In the first epoch, the error state estimate is propagated for two steps. The propagate equations of the Kalman filter [8] are as follows:

$$\hat{\mathbf{x}}_{l+1}^- = \mathbf{A}_{\mathbf{ad}} \hat{\mathbf{x}}_l^+ \quad (3.52)$$

$$\mathbf{P}_{l+1}^- = \mathbf{A}_{\mathbf{ad}} \mathbf{P}_l^+ \mathbf{A}_{\mathbf{ad}}^T \quad (3.53)$$

and the error state estimate is updated using the update equations of the Kalman filter [8]

$$\hat{\mathbf{x}}_{l+1}^+ = \hat{\mathbf{x}}_{l+1}^- + \mathbf{K}_{l+1} [\mathbf{Z}_{l+1} - \mathbf{H}_{l+1} \hat{\mathbf{x}}_{l+1}^-] \quad (3.54)$$

where the Kalman gain \mathbf{K} is given by

$$\mathbf{K}_{l+1} = \mathbf{P}_{l+1}^- \mathbf{H}_{l+1}^T [\mathbf{H}_{l+1} \mathbf{P}_{l+1}^- \mathbf{H}_{l+1}^T + \mathbf{R}]^{-1} \quad (3.55)$$

and

$$\mathbf{P}_{l+1}^+ = (\mathbf{I} - \mathbf{K}_{l+1} \mathbf{H}_{l+1}) \mathbf{P}_{l+1}^- \quad (3.56)$$

In Eq. (3.55) \mathbf{R} is the covariance matrix of the bearings angles' measurement error. It corresponds to one pixel measurement error in the camera's focal plane:

$$x_{fm} = x_f + \delta x_f, \quad y_{fm} = y_f + \delta y_f$$

$$\begin{pmatrix} \delta x_{f1} \\ \delta y_{f1} \\ \delta x_{f2} \\ \delta y_{f2} \end{pmatrix} \sim N(0, \mathbf{R})$$

For a small UAV, a 9 Mega pixel camera with an aspect ratio of 1 is assumed and therefore $\sigma = \frac{1}{3} \times 10^{-3}$ (error in 1 pixel) and the nondimensional measurement error covariance matrix

$$\mathbf{R} = \begin{bmatrix} \frac{1}{9} & 0 & 0 & 0 \\ 0 & \frac{1}{9} & 0 & 0 \\ 0 & 0 & \frac{1}{9} & 0 \\ 0 & 0 & 0 & \frac{1}{9} \end{bmatrix} \times 10^{-6} \quad (3.57)$$

At the conclusion of the first two steps/the first measurement epoch, the first ground object is dropped from consideration, and a new, unknown ground object is brought in as shown in Figure 3.3. In the second measurement epoch, the second ground object from epoch 1 becomes the ground object 1 in epoch 2, whose position is perfectly known so that at the beginning of epoch 2, $(\hat{\delta x}_{p2}(0))^{(2)} = 0$, $(\hat{\delta y}_{p2}(0))^{(2)} = 0$, and the newly acquired ground object becomes ground object 2, whose position during the measurement epoch 2 is $2 + \delta x(L)_1$, where $\delta x(L)_1$ is the x-component of the free INS's position's error at the end of the first measurement epoch. Thus the next time block requires the use of the augmented dynamics matrix $\mathbf{A}_{ad17 \times 17}$ from Eq. (3.18) and the observation matrix $\mathbf{H}_{ku}(l)_{4 \times 17}$.

At the start of the second measurement epoch, the error state's covariance matrix at the end of epoch 1, $(\mathbf{P}(L))^{(1)}$, is transitioned from a 15×15 to a 17×17 matrix, while including the correct cross-covariance terms. This is done as follows: when transitioning from two known ground features to one known and one unknown ground feature, the new covariance matrix at the beginning of measurement epoch 2 is

$$(\mathbf{P}(0))^{(2)} = \begin{bmatrix} (\mathbf{P}(L)_{15 \times 15})^{(1)} & \mathbf{P}_{15 \times 2}^{(2)} \\ (\mathbf{p}_{2 \times 15}^{(2)})^T & \mathbf{\Pi}_{2 \times 2}^{(2)} \end{bmatrix}_{17 \times 17} \quad (3.58)$$

where the elements of the matrix block $\mathbf{p}_{15 \times 2}^{(2)}$ are obtained using Eqs. (3.50) and (3.51) as follows:

$$\begin{aligned}
p_{16,1}^{(2)} &= \mathbf{E} \left(\delta x(L)_{p2}^{(1)} \cdot \delta x(0)_{p2}^{(2)} \right) \\
&= \mathbf{E} \left(\delta x(L)_{p2}^{(1)} \cdot (\delta x(L)^{(1)} + 2\delta z(L)^{(1)} - 5\delta\theta(L)^{(1)} \pm 2y_p\delta\phi(L)^{(1)} \mp y_p\delta\psi(L)^{(1)} + \xi) \right) \\
&= \mathbf{P}(L)_{1,1}^{(1)} + 2\mathbf{P}(L)_{3,1}^{(1)} - 5\mathbf{P}(L)_{8,1}^{(1)} \pm 2y_p\mathbf{P}(L)_{7,1}^{(1)} \mp y_p\mathbf{P}(L)_{9,1}^{(1)} \\
p_{16,2}^{(2)} &= \mathbf{E} \left(\delta y(L)_{p2}^{(1)} \cdot \delta x(0)_{p2}^{(2)} \right) \\
&= \mathbf{E} \left(\delta y(L)_{p2}^{(1)} \cdot (\delta x(L)^{(1)} + 2\delta z(L)^{(1)} - 5\delta\theta(L)^{(1)} \pm 2y_p\delta\phi(L)^{(1)} \mp y_p\delta\psi(L)^{(1)} + \xi) \right) \\
&= \mathbf{P}(L)_{1,2}^{(1)} + 2\mathbf{P}(L)_{3,2}^{(1)} - 5\mathbf{P}(L)_{8,2}^{(1)} \pm 2y_p\mathbf{P}(L)_{7,2}^{(1)} \mp y_p\mathbf{P}(L)_{9,2}^{(1)} \\
&\vdots \\
p_{16,i}^{(2)} &= \mathbf{P}(L)_{1,i}^{(1)} + 2\mathbf{P}(L)_{3,i}^{(1)} - 5\mathbf{P}(L)_{8,i}^{(1)} \pm 2y_p\mathbf{P}(L)_{7,i}^{(1)} \mp y_p\mathbf{P}(L)_{9,i}^{(1)}
\end{aligned}$$

for $i=1, \dots, 15$

Similarly,

$$p_{17,i}^{(2)} = \mathbf{P}(L)_{2,i}^{(1)} + \mathbf{P}(L)_{7,i}^{(1)} + 2\mathbf{P}(L)_{9,i}^{(1)} \pm y_p\mathbf{P}(L)_{3,i}^{(1)} \mp 2y_p\mathbf{P}(L)_{8,i}^{(1)} + y_p^2\mathbf{P}(L)_{7,i}^{(1)}$$

for $i=1, \dots, 15$

The first and second diagonal terms of the matrix $\mathbf{\Pi}(0)_{2 \times 2}^{(2)}$ are the respective uncertainty in the x and y position of the new ground object, and it is obtained using Eqs. (3.50) and (3.51) as follows:

$$\mathbf{\Pi}(0)_{1,1}^{(2)} = \mathbf{P}(0)_{16,16}^{(2)}$$

where

$$\begin{aligned}
\mathbf{P}(0)_{16,16}^{(2)} &= \mathbf{E} \left(\delta x(0)_{p2}^{(2)} \cdot \delta x(0)_{p2}^{(2)} \right) \\
&= \mathbf{E} \left((\delta x(L)^{(1)} + 2\delta z(L)^{(1)} - 5\delta\theta(L)^{(1)} \pm 2y_p\delta\phi(L)^{(1)} \mp y_p\delta\psi(L)^{(1)} + \xi) \cdot (\delta x(L)^{(1)} \right. \\
&\quad \left. + 2\delta z(L)^{(1)} - 5\delta\theta(L)^{(1)} \pm 2y_p\delta\phi(L)^{(1)} \mp y_p\delta\psi(L)^{(1)} + \xi) \right)
\end{aligned}$$

$$\begin{aligned}
&= \mathbf{P}(L)_{1,1}^{(1)} + 4\mathbf{P}(L)_{3,3}^{(1)} + 25\mathbf{P}(L)_{8,8}^{(1)} + 4\mathbf{P}(L)_{1,3}^{(1)} - 10\mathbf{P}(L)_{1,8}^{(1)} - 20\mathbf{P}(L)_{3,8}^{(1)} + 4y_p^2\mathbf{P}(L)_{7,7}^{(1)} \\
&\quad + y_p^2\mathbf{P}(L)_{9,9}^{(1)} \pm 4y_p\mathbf{P}(L)_{1,7}^{(1)} \mp 2y_p\mathbf{P}(L)_{1,9}^{(1)} \pm 8y_p\mathbf{P}(L)_{3,7}^{(1)} \mp 4y_p\mathbf{P}(L)_{3,9}^{(1)} \mp 20y_p\mathbf{P}(L)_{7,8}^{(1)} \\
&\quad \pm 10y_p\mathbf{P}(L)_{8,9}^{(1)} - 4y_p^2\mathbf{P}(L)_{7,9}^{(1)} + \sigma_\xi^2
\end{aligned}$$

$$\mathbf{\Pi}(0)_{2,2}^{(2)} = \mathbf{P}(0)_{17,17}^{(2)}$$

where

$$\begin{aligned}
\mathbf{P}(0)_{17,17}^{(2)} &= \mathbf{E}\left(\delta y(0)_{p^2}^{(2)} \cdot \delta y(0)_{p^2}^{(2)}\right) \\
&= \mathbf{E}\left((\delta y(L)^{(1)} + \delta\phi(L)^{(1)} + 2\delta\psi(L)^{(1)} \pm y_p\delta z(L)^{(1)} \mp 2y_p\delta\theta(L)^{(1)} + y_p^2\delta\phi(L)^{(1)} + \eta) \right. \\
&\quad \left. \cdot (\delta y(L)^{(1)} + \delta\phi(L)^{(1)} + 2\delta\psi(L)^{(1)} \pm y_p\delta z(L)^{(1)} \mp 2y_p\delta\theta(L)^{(1)} + y_p^2\delta\phi(L)^{(1)} + \eta)\right) \\
&= \mathbf{P}(L)_{2,2}^{(1)} + \mathbf{P}(L)_{7,7}^{(1)} + 4\mathbf{P}(L)_{9,9}^{(1)} + 2\mathbf{P}(L)_{2,7}^{(1)} + 4\mathbf{P}(L)_{2,9}^{(1)} + 4\mathbf{P}(L)_{7,9}^{(1)} \pm 2y_p\mathbf{P}(L)_{3,7}^{(1)} \\
&\quad \mp 4y_p\mathbf{P}(L)_{7,8}^{(1)} + 2y_p^2\mathbf{P}(L)_{2,7}^{(1)} \pm 2y_p^3\mathbf{P}(L)_{3,7}^{(1)} \mp 4y_p^3\mathbf{P}(L)_{7,8}^{(1)} + 2y_p^2\mathbf{P}(L)_{7,7}^{(1)} + y_p^4\mathbf{P}(L)_{7,7}^{(1)} \\
&\quad \pm 4y_p\mathbf{P}(L)_{3,9}^{(1)} \mp 8y_p\mathbf{P}(L)_{8,9}^{(1)} + 4y_p^2\mathbf{P}(L)_{7,9}^{(1)} \pm y_p\mathbf{P}(L)_{2,3}^{(1)} \mp 2y_p\mathbf{P}(L)_{2,8}^{(1)} \pm y_p\mathbf{P}(L)_{2,3}^{(1)} \\
&\quad + y_p^2\mathbf{P}(L)_{3,3}^{(1)} - 2y_p^2\mathbf{P}(L)_{3,8}^{(1)} \mp 2y_p\mathbf{P}(L)_{2,8}^{(1)} - 2y_p^2\mathbf{P}(L)_{3,8}^{(1)} + 4y_p^2\mathbf{P}(L)_{8,8}^{(1)} + \sigma_\eta^2
\end{aligned}$$

Finally, the off-diagonal terms of the matrix block $\mathbf{\Pi}_{2 \times 2}$ are obtained as follows:

$$\mathbf{\Pi}_{1,2} = \mathbf{\Pi}_{2,1} = \mathbf{P}(0)_{16,17}^{(2)}$$

where

$$\begin{aligned}
\mathbf{P}(0)_{16,17}^{(2)} &= \mathbf{E}\left(\delta x(0)_{p^2}^{(2)} \cdot \delta y(0)_{p^2}^{(2)}\right) \\
&= \mathbf{E}\left((\delta x(L)^{(1)} + 2\delta z(L)^{(1)} - 5\delta\theta(L)^{(1)} \pm 2y_p\delta\phi(L)^{(1)} \mp y_p\delta\psi(L)^{(1)} + \xi) \cdot (\delta y(L)^{(1)} \right. \\
&\quad \left. + \delta\phi(L)^{(1)} + 2\delta\psi(L)^{(1)} \pm y_p\delta z(L)^{(1)} \mp 2y_p\delta\theta(L)^{(1)} + y_p^2\delta\phi(L)^{(1)} + \eta)\right) \\
&= \mathbf{P}(L)_{1,2}^{(1)} + 2\mathbf{P}(L)_{3,2}^{(1)} - 5\mathbf{P}(L)_{8,2}^{(1)} + \mathbf{P}(L)_{1,7}^{(1)} + 2\mathbf{P}(L)_{3,7}^{(1)} - 5\mathbf{P}(L)_{7,8}^{(1)} + 2\mathbf{P}(L)_{1,9}^{(1)} + 4\mathbf{P}(L)_{3,9}^{(1)} \\
&\quad - 10\mathbf{P}(L)_{8,9}^{(1)} \pm y_p\mathbf{P}(L)_{1,3}^{(1)} \mp 2y_p\mathbf{P}(L)_{1,8}^{(1)} + y_p^2\mathbf{P}(L)_{1,7}^{(1)} \pm 2y_p\mathbf{P}(L)_{3,3}^{(1)} \mp 4y_p\mathbf{P}(L)_{3,8}^{(1)} \\
&\quad + 2y_p^2\mathbf{P}(L)_{3,7}^{(1)} \mp 5y_p\mathbf{P}(L)_{3,8}^{(1)} \pm 10y_p\mathbf{P}(L)_{8,8}^{(1)} - 5y_p^2\mathbf{P}(L)_{7,8}^{(1)} \pm 2y_p\mathbf{P}(L)_{2,7}^{(1)} \pm 2y_p\mathbf{P}(L)_{7,7}^{(1)} \\
&\quad \pm 4y_p\mathbf{P}(L)_{7,9}^{(1)} + 2y_p^2\mathbf{P}(L)_{3,7}^{(1)} - 4y_p^2\mathbf{P}(L)_{7,8}^{(1)} \pm 2y_p^3\mathbf{P}(L)_{7,7}^{(1)} \mp y_p\mathbf{P}(L)_{2,9}^{(1)} \mp y_p\mathbf{P}(L)_{7,9}^{(1)} \\
&\quad \mp 2y_p\mathbf{P}(L)_{9,9}^{(1)} - y_p^2\mathbf{P}(L)_{3,9}^{(1)} + 2y_p^2\mathbf{P}(L)_{8,9}^{(1)} \mp y_p^3\mathbf{P}(L)_{7,9}^{(1)}
\end{aligned}$$

where, recall, ξ and η are the uncertainties caused by the error in the LOS angle measurements. It is because of the correlation of the errors in the aircraft navigation state x and the new ground object's position state x_{p2} that the first row and column from $(\mathbf{P}(L))_{15 \times 15}^{(1)}$ are used in the calculation of their respective positions in $(\mathbf{P}(0))_{17 \times 17}^{(2)}$. Since there is no correlation between the LOS error of the camera and any of the INS navigation or bias states, σ^2 is not added in the calculations of any of the entries of the covariance matrix except $\mathbf{P}(0)_{16,16}^{(2)}$ and $\mathbf{P}(0)_{17,17}^{(2)}$. The same holds true for the navigation state y and the new state y_{p2} . The covariance matrix is then propagated in the same manner as in the first epoch, following Eqs. (3.53)-(3.56), with the proper substitution of the initial covariance, $(\mathbf{P}^+(0))_{17 \times 17}^{(2)}$ for $(\mathbf{P}(2))_{15 \times 15}^{(1)}$, dynamics, $\mathbf{A}_{ad17 \times 17}$ for $\mathbf{A}_{ad15 \times 15}$, and observation matrices, \mathbf{H}_{ku} for \mathbf{H}_{kk} .

The state estimate is transitioned by augmenting the state estimate at the last measurement step L with zeros as

$$(\delta \hat{x}_a^+(0))^{(2)} = \begin{pmatrix} (\delta \hat{x}_a^+(L))_{15 \times 1}^{(1)} \\ \mathbf{0}_{2 \times 1} \end{pmatrix}_{17 \times 1} \quad (3.59)$$

The transition at the beginning of the third epoch from one known/one unknown to two unknown ground objects follows the same pattern as incorporating the first unknown ground object. Now

$$(\mathbf{P}(0))^{(3)} = \begin{bmatrix} (\mathbf{P}(L))_{17 \times 17}^{(2)} & \mathbf{P}_{17 \times 2}^{(3)} \\ (\mathbf{p}_{2 \times 17}^{(3)})^T & \mathbf{\Pi}_{2 \times 2} \end{bmatrix}_{19 \times 19} \quad (3.60)$$

where the elements of the matrix block $\mathbf{P}(0)_{17 \times 2}^{(3)}$ are obtained using Eqs. (3.50) and (3.51) as follows:

$$\begin{aligned} \mathbf{P}(0)_{16,1}^{(3)} &= \mathbf{E} \left(\delta x(L)_{p2}^{(2)} \cdot \delta x(0)_{p2}^{(3)} \right) \\ &= \mathbf{E} \left(\delta x(L)_{p2}^{(2)} \cdot (\delta x(L)^{(2)} + 2\delta z(L)^{(2)} - 5\delta \theta(L)^{(2)} \pm 2y_p \delta \phi(L)^{(2)} \mp y_p \delta \psi(L)^{(2)} + \xi) \right) \\ &= \mathbf{P}(L)_{1,1}^{(2)} + 2\mathbf{P}(L)_{3,1}^{(2)} - 5\mathbf{P}(L)_{8,1}^{(2)} \pm 2y_p \mathbf{P}(L)_{7,1}^{(2)} \mp y_p \mathbf{P}(L)_{9,1}^{(2)} \end{aligned}$$

$$\begin{aligned}
\mathbf{P}(0)_{16,2}^{(3)} &= \mathbf{E} \left(\delta y(L)_{p2}^{(2)} \cdot \delta x(0)_{p2}^{(3)} \right) \\
&= \mathbf{E} \left(\delta y(L)_{p2}^{(2)} \cdot (\delta x(L)^{(2)} + 2\delta z(L)^{(2)} - 5\delta\theta(L)^{(2)} \pm 2y_p\delta\phi(L)^{(2)} \mp y_p\delta\psi(L)^{(2)} + \xi) \right) \\
&= \mathbf{P}(L)_{1,2}^{(2)} + 2\mathbf{P}(L)_{3,2}^{(2)} - 5\mathbf{P}(L)_{8,2}^{(2)} \pm 2y_p\mathbf{P}(L)_{7,2}^{(2)} \mp y_p\mathbf{P}(L)_{9,2}^{(2)} \\
&\quad \vdots \\
\mathbf{P}(0)_{16,i}^{(3)} &= \mathbf{P}(L)_{1,i}^{(2)} + 2\mathbf{P}(L)_{3,i}^{(2)} - 5\mathbf{P}(L)_{8,i}^{(2)} \pm 2y_p\mathbf{P}(L)_{7,i}^{(2)} \mp y_p\mathbf{P}(L)_{9,i}^{(2)}
\end{aligned}$$

for $i=1, \dots, 17$

Similarly,

$$\mathbf{P}(0)_{17,i}^{(3)} = \mathbf{P}(L)_{2,i}^{(2)} + \mathbf{P}(L)_{7,i}^{(2)} + 2\mathbf{P}(L)_{9,i}^{(2)} \pm y_p\mathbf{P}(L)_{3,i}^{(2)} \mp 2y_p\mathbf{P}(L)_{8,i}^{(2)} + y_p^2\mathbf{P}(L)_{7,i}^{(2)}$$

for $i=1, \dots, 17$

The first and second diagonal terms of the matrix block $\mathbf{\Pi}(0)_{2 \times 2}^{(3)}$ are the respective uncertainty in the x and y position of the new ground object, and they are obtained using Eqs. (3.50) and (3.51) as follows:

$$\mathbf{\Pi}(0)_{1,1}^{(3)} = \mathbf{P}(0)_{16,16}^{(3)}$$

where

$$\begin{aligned}
\mathbf{P}(0)_{16,16}^{(3)} &= \mathbf{E} \left(\delta x(0)_{p2}^{(3)} \cdot \delta x(0)_{p2}^{(3)} \right) \\
&= \mathbf{E} \left((\delta x(L)^{(2)} + 2\delta z(L)^{(2)} - 5\delta\theta(L)^{(2)} \pm 2y_p\delta\phi(L)^{(2)} \mp y_p\delta\psi(L)^{(2)} + \xi) \cdot (\delta x(L)^{(2)} \right. \\
&\quad \left. + 2\delta z(L)^{(2)} - 5\delta\theta(L)^{(2)} \pm 2y_p\delta\phi(L)^{(2)} \mp y_p\delta\psi(L)^{(2)} + \xi) \right) \\
&= \mathbf{P}(L)_{1,1}^{(2)} + 4\mathbf{P}(L)_{3,3}^{(2)} + 25\mathbf{P}(L)_{8,8}^{(2)} + 4\mathbf{P}(L)_{1,3}^{(2)} - 10\mathbf{P}(L)_{1,8}^{(2)} - 20\mathbf{P}(L)_{3,8}^{(2)} + 4y_p^2\mathbf{P}(L)_{7,7}^{(2)} \\
&\quad + y_p^2\mathbf{P}(L)_{9,9}^{(2)} \pm 4y_p\mathbf{P}(L)_{1,7}^{(2)} \mp 2y_p\mathbf{P}(L)_{1,9}^{(2)} \pm 8y_p\mathbf{P}(L)_{3,7}^{(2)} \mp 4y_p\mathbf{P}(L)_{3,9}^{(2)} \mp 20y_p\mathbf{P}(L)_{7,8}^{(2)} \\
&\quad \pm 10y_p\mathbf{P}(L)_{8,9}^{(2)} - 4y_p^2\mathbf{P}(L)_{7,9}^{(2)} + \sigma_\xi^2
\end{aligned}$$

$$\mathbf{\Pi}(0)_{2,2}^{(3)} = \mathbf{P}(0)_{17,17}^{(3)}$$

where

$$\mathbf{P}(0)_{17,17}^{(3)} = \mathbf{E} \left(\delta y(0)_{p2}^{(3)} \cdot \delta y(0)_{p2}^{(3)} \right)$$

$$\begin{aligned}
&= \mathbf{E} \left((\delta y(L)^{(2)} + \delta \phi(L)^{(2)} + 2\delta \psi(L)^{(2)} \pm y_p \delta z(L)^{(2)} \mp 2y_p \delta \theta(L)^{(2)} + y_p^2 \delta \phi(L)^{(2)} + \eta) \cdot \right. \\
&\quad \left. (\delta y(L)^{(2)} + \delta \phi(L)^{(2)} + 2\delta \psi(L)^{(2)} \pm y_p \delta z(L)^{(2)} \mp 2y_p \delta \theta(L)^{(2)} + y_p^2 \delta \phi(L)^{(2)} + \eta) \right) \\
&= \mathbf{P}(L)_{2,2}^{(2)} + \mathbf{P}(L)_{7,7}^{(2)} + 4\mathbf{P}(L)_{9,9}^{(2)} + 2\mathbf{P}(L)_{2,7}^{(2)} + 4\mathbf{P}(L)_{2,9}^{(2)} + 4\mathbf{P}(L)_{7,9}^{(2)} \pm 2y_p \mathbf{P}(L)_{3,7}^{(2)} \\
&\quad \mp 4y_p \mathbf{P}(L)_{7,8}^{(2)} + 2y_p^2 \mathbf{P}(L)_{2,7}^{(2)} \pm 2y_p^3 \mathbf{P}(L)_{3,7}^{(2)} \mp 4y_p^3 \mathbf{P}(L)_{7,8}^{(2)} + 2y_p^2 \mathbf{P}(L)_{7,7}^{(2)} + y_p^4 \mathbf{P}(L)_{7,7}^{(2)} \\
&\quad \pm 4y_p \mathbf{P}(L)_{3,9}^{(2)} \mp 8y_p \mathbf{P}(L)_{8,9}^{(2)} + 4y_p^2 \mathbf{P}(L)_{7,9}^{(2)} \pm y_p \mathbf{P}(L)_{2,3}^{(2)} \mp 2y_p \mathbf{P}(L)_{2,8}^{(2)} \pm y_p \mathbf{P}(L)_{2,3}^{(2)} \\
&\quad + y_p^2 \mathbf{P}(L)_{3,3}^{(2)} - 2y_p^2 \mathbf{P}(L)_{3,8}^{(2)} \mp 2y_p \mathbf{P}(L)_{2,8}^{(2)} - 2y_p^2 \mathbf{P}(L)_{3,8}^{(2)} + 4y_p^2 \mathbf{P}(L)_{8,8}^{(2)} + \sigma_\eta^2
\end{aligned}$$

Similarly the off-diagonal terms of the matrix $\mathbf{\Pi}(0)_{2 \times 2}^{(3)}$ are obtained as follows:

$$\mathbf{\Pi}(0)_{1,2}^{(3)} = \mathbf{\Pi}(0)_{2,1}^{(3)} = \mathbf{P}(0)_{16,17}^{(3)}$$

where

$$\begin{aligned}
\mathbf{P}(0)_{16,17}^{(3)} &= \mathbf{E} \left(\delta x(0)_{p2}^{(3)} \cdot \delta y(0)_{p2}^{(3)} \right) \\
&= \mathbf{E} \left((\delta x(L)^{(2)} + 2\delta z(L)^{(2)} - 5\delta \theta(L)^{(2)} \pm 2y_p \delta \phi(L)^{(2)} \mp y_p \delta \psi(L)^{(2)} + \xi) \cdot (\delta y(L)^{(2)} \right. \\
&\quad \left. + \delta \phi(L)^{(2)} + 2\delta \psi(L)^{(2)} \pm y_p \delta z(L)^{(2)} \mp 2y_p \delta \theta(L)^{(2)} + y_p^2 \delta \phi(L)^{(2)} + \eta) \right) \\
&= \mathbf{P}(L)_{1,2}^{(2)} + 2\mathbf{P}(L)_{3,2}^{(2)} - 5\mathbf{P}(L)_{8,2}^{(2)} + \mathbf{P}(L)_{1,7}^{(2)} + 2\mathbf{P}(L)_{3,7}^{(2)} - 5\mathbf{P}(L)_{7,8}^{(2)} + 2\mathbf{P}(L)_{1,9}^{(2)} + 4\mathbf{P}(L)_{3,9}^{(2)} \\
&\quad - 10\mathbf{P}(L)_{8,9}^{(2)} \pm y_p \mathbf{P}(L)_{1,3}^{(2)} \mp 2y_p \mathbf{P}(L)_{1,8}^{(2)} + y_p^2 \mathbf{P}(L)_{1,7}^{(2)} \pm 2y_p \mathbf{P}(L)_{3,3}^{(2)} \mp 4y_p \mathbf{P}(L)_{3,8}^{(2)} \\
&\quad + 2y_p^2 \mathbf{P}(L)_{3,7}^{(2)} \mp 5y_p \mathbf{P}(L)_{3,8}^{(2)} \pm 10y_p \mathbf{P}(L)_{8,8}^{(2)} - 5y_p^2 \mathbf{P}(L)_{7,8}^{(2)} \pm 2y_p \mathbf{P}(L)_{2,7}^{(2)} \pm 2y_p \mathbf{P}(L)_{7,7}^{(2)} \\
&\quad \pm 4y_p \mathbf{P}(L)_{7,9}^{(2)} + 2y_p^2 \mathbf{P}(L)_{3,7}^{(2)} - 4y_p^2 \mathbf{P}(L)_{7,8}^{(2)} \pm 2y_p^3 \mathbf{P}(L)_{7,7}^{(2)} \mp y_p \mathbf{P}(L)_{2,9}^{(2)} \mp y_p \mathbf{P}(L)_{7,9}^{(2)} \\
&\quad \mp 2y_p \mathbf{P}(L)_{9,9}^{(2)} - y_p^2 \mathbf{P}(L)_{3,9}^{(2)} + 2y_p^2 \mathbf{P}(L)_{8,9}^{(2)} \mp y_p^3 \mathbf{P}(L)_{7,9}^{(2)}
\end{aligned}$$

In the previous epoch, the unknown object's position was (x_{p2}, y_{p2}) , but when it transitioned to being the closer ground object, all of its cross-covariances goes with it. Because $(\mathbf{P}(0))_{(16,16)}^{(3)}$ and $(\mathbf{P}(0))_{(17,17)}^{(3)}$ show the uncertainty of the closest object to the aircraft, the entirety of $(\mathbf{P}(0))_{15 \times 15}^{(3)}$ is directly translated to the upper-diagonal section of the new covariance matrix. Substituting \mathbf{H}_{uu} for \mathbf{H}_{ku} , and using the $\mathbf{A}_{ad19 \times 19}$ dynamics matrix, the covariance was propagated according to Eqs. (3.53)-(3.56). These matrices were used for the remainder of the measurement epochs.

Likewise, the state estimate is transitioned by augmenting the state estimate at the last measurement step ($L = 2$) with zeros as

$$(\delta\hat{x}^+(0))^{(3)} = \begin{pmatrix} (\delta\hat{x}^+(L))_{17 \times 1}^{(2)} \\ \mathbf{0}_{2 \times 1} \end{pmatrix}_{19 \times 1} \quad (3.61)$$

The transitions from the third to the last epoch, when the Kalman Filter completes a time block using two unknown ground objects, and begins to use a new unknown ground object, is done in a slightly different way.

$$(\mathbf{P}(0))^{(n)} = \begin{bmatrix} (\mathbf{P}(L))_{15 \times 15}^{(n-1)} & \mathbf{P}_{15 \times 4}^{(n)} \\ (\mathbf{P}_{4 \times 15}^{(n)})^T & \mathbf{\Pi}_{4 \times 4} \end{bmatrix}_{19 \times 19} \quad (3.62)$$

$n = 4, \dots, N - 1$

where the elements of the matrix $\mathbf{P}_{15 \times 4}^{(n)}$ are obtained using Eqs. (3.50) and (3.51) as follows:

$$\mathbf{P}(0)_{16,i}^{(n)} = \mathbf{P}(L)_{18,i}^{(n-1)}$$

$$\mathbf{P}(0)_{17,i}^{(n)} = \mathbf{P}(L)_{19,i}^{(n-1)}$$

$$\begin{aligned} \mathbf{P}(0)_{18,i}^{(n)} &= \mathbf{E} \left(\delta x(L)_{p2}^{(n-1)} \cdot \delta x(0)_{p2}^{(n)} \right) \\ &= \mathbf{E} \left(\delta x(L)_{p2}^{(n-1)} \cdot (\delta x(L)^{(n-1)} + 2\delta z(L)^{(n-1)} - 5\delta\theta(L)^{(n-1)} \pm 2y_p\delta\phi(L)^{(n-1)} \mp y_p\delta\psi(L)^{(n-1)} \right. \\ &\quad \left. + \xi) \right) \\ &= \mathbf{P}(L)_{1,i}^{(n-1)} + 2\mathbf{P}(L)_{3,i}^{(n-1)} - 5\mathbf{P}(L)_{8,i}^{(n-1)} \pm 2y_p\mathbf{P}(L)_{7,i}^{(n-1)} \mp y_p\mathbf{P}(L)_{9,i}^{(n-1)} \\ \mathbf{P}(0)_{19,i}^{(n)} &= \mathbf{E} \left(\delta y(0)_{p2}^{(n)} \cdot \delta y(L)_{p2}^{(n-1)} \right) \\ &= \mathbf{E} \left((\delta y(L)^{(n-1)} + \delta\phi(L)^{(n-1)} + 2\delta\psi(L)^{(n-1)} \pm y_p\delta z(L)^{(n-1)} \mp 2y_p\delta\theta(L)^{(n-1)} + y_p^2\delta\phi(L)^{(n-1)} \right. \\ &\quad \left. + \eta) \cdot \delta y(L)_{p2}^{(n-1)} \right) \\ &= \mathbf{P}(L)_{2,i}^{(n-1)} + \mathbf{P}(L)_{7,i}^{(n-1)} + 2\mathbf{P}(L)_{9,i}^{(n-1)} \pm y_p\mathbf{P}(L)_{3,i}^{(n-1)} \mp 2y_p\mathbf{P}(L)_{8,i}^{(n-1)} + y_p^2\mathbf{P}(L)_{7,i}^{(n-1)} \end{aligned}$$

for $i=1, \dots, 15$

The first and second diagonal terms of the matrix $\mathbf{\Pi}(0)_{4 \times 4}^{(n)}$ are the respective uncertainty in the x and y position of the first ground object, and they are obtained by transplanting the uncertainty in the x and y position of the second ground object from the previous epoch as:

$$\mathbf{P}(0)_{16,16}^{(n)} = \mathbf{\Pi}(0)_{1,1}^{(n)} = \mathbf{P}(L)_{18,18}^{(n-1)}$$

$$\mathbf{P}(0)_{17,17}^{(n)} = \mathbf{\Pi}(0)_{2,2}^{(n)} = \mathbf{P}(L)_{19,19}^{(n-1)}$$

The third and fourth diagonal terms of the matrix $\mathbf{\Pi}(0)_{4 \times 4}^{(n)}$ are the respective uncertainty in the x and y position of the second ground object, and they are obtained by using Eqs. (3.50) and (3.51) as follows:

$$\mathbf{\Pi}(0)_{3,3}^{(n)} = \mathbf{P}(0)_{18,18}^{(n)}$$

where

$$\begin{aligned} \mathbf{P}(0)_{18,18}^{(n)} &= \mathbf{E} \left(\delta x(0)_{p2}^{(n)} \cdot \delta x(0)_{p2}^{(n)} \right) \\ &= \mathbf{E} \left((\delta x(L)^{(n-1)} + 2\delta z(L)^{(n-1)} - 5\delta\theta(L)^{(n-1)} \pm 2y_p\delta\phi(L)^{(n-1)} \mp y_p\delta\psi(L)^{(n-1)} + \xi) \right. \\ &\quad \cdot (\delta x(L)^{(n-1)} + 2\delta z(L)^{(n-1)} - 5\delta\theta(L)^{(n-1)} \pm 2y_p\delta\phi(L)^{(n-1)} (\delta x(L)^{(n-1)} + 2\delta z(L)^{(n-1)} \\ &\quad \left. - 5\delta\theta(L)^{(n-1)} + \xi) \right) \\ &= \mathbf{P}(L)_{1,1}^{(n-1)} + 4\mathbf{P}(L)_{3,3}^{(n-1)} + 25\mathbf{P}(L)_{8,8}^{(n-1)} + 4\mathbf{P}(L)_{1,3}^{(n-1)} - 10\mathbf{P}(L)_{1,8}^{(n-1)} - 20\mathbf{P}(L)_{3,8}^{(n-1)} \\ &\quad + 4y_p^2\mathbf{P}(L)_{7,7}^{(n-1)} + y_p^2\mathbf{P}(L)_{9,9}^{(n-1)} \pm 4y_p\mathbf{P}(L)_{1,7}^{(n-1)} \mp 2y_p\mathbf{P}(L)_{1,9}^{(n-1)} \pm 8y_p\mathbf{P}(L)_{3,7}^{(n-1)} \\ &\quad \mp 4y_p\mathbf{P}(L)_{3,9}^{(n-1)} \mp 20y_p\mathbf{P}(L)_{7,8}^{(n-1)} \pm 10y_p\mathbf{P}(L)_{8,9}^{(n-1)} - 4y_p^2\mathbf{P}(L)_{7,9}^{(n-1)} + \sigma_\xi^2 \end{aligned}$$

$$\mathbf{\Pi}(0)_{4,4}^{(n)} = \mathbf{P}(0)_{19,19}^{(n)}$$

where

$$\begin{aligned} \mathbf{P}(0)_{19,19}^{(n)} &= \mathbf{E} \left(\delta y(0)_{p2}^{(n)} \cdot \delta y(0)_{p2}^{(n)} \right) \\ &= \mathbf{E} \left((\delta y(L)^{(n-1)} + \delta\phi(L)^{(n-1)} + 2\delta\psi(L)^{(n-1)} \pm y_p\delta z(L)^{(n-1)} \mp 2y_p\delta\theta(L)^{(n-1)} + y_p^2\delta\phi(L)^{(n-1)} \right. \\ &\quad \left. + \eta) \cdot (\delta y(L)^{(n-1)} + \delta\phi(L)^{(n-1)} + 2\delta\psi(L)^{(n-1)} \pm y_p\delta z(L)^{(n-1)} \mp 2y_p\delta\theta(L)^{(n-1)} \right. \end{aligned}$$

$$\begin{aligned}
& + y_p^2 \delta \phi(L)^{(n-1)} + \eta) \Big) \\
& = \mathbf{P}(L)_{2,2}^{(n-1)} + \mathbf{P}(L)_{7,7}^{(n-1)} + 4\mathbf{P}(L)_{9,9}^{(n-1)} + 2\mathbf{P}(L)_{2,7}^{(n-1)} + 4\mathbf{P}(L)_{2,9}^{(n-1)} + 4\mathbf{P}(L)_{7,9}^{(n-1)} \\
& \quad \pm 2y_p \mathbf{P}(L)_{3,7}^{(n-1)} \mp 4y_p \mathbf{P}(L)_{7,8}^{(n-1)} + 2y_p^2 \mathbf{P}(L)_{2,7}^{(n-1)} \pm 2y_p^3 \mathbf{P}(L)_{3,7}^{(n-1)} \mp 4y_p^3 \mathbf{P}(L)_{7,8}^{(n-1)} \\
& \quad + 2y_p^2 \mathbf{P}(L)_{7,7}^{(n-1)} + y_p^4 \mathbf{P}(L)_{7,7}^{(n-1)} \pm 4y_p \mathbf{P}(L)_{3,9}^{(n-1)} \mp 8y_p \mathbf{P}(L)_{8,9}^{(n-1)} + 4y_p^2 \mathbf{P}(L)_{7,9}^{(n-1)} \\
& \quad \pm y_p \mathbf{P}(L)_{2,3}^{(n-1)} \mp 2y_p \mathbf{P}(L)_{2,8}^{(n-1)} \pm y_p \mathbf{P}(L)_{2,3}^{(n-1)} + y_p^2 \mathbf{P}(L)_{3,3}^{(n-1)} - 2y_p^2 \mathbf{P}(L)_{3,8}^{(n-1)} \\
& \quad \mp 2y_p \mathbf{P}(L)_{2,8}^{(n-1)} - 2y_p^2 \mathbf{P}(L)_{3,8}^{(n-1)} + 4y_p^2 \mathbf{P}(L)_{8,8}^{(n-1)} + \sigma_\eta^2
\end{aligned}$$

The off-diagonal terms of the matrix block $\mathbf{\Pi}(0)_{4 \times 4}^{(n)}$ are obtained as follows:

$$\begin{aligned}
\mathbf{\Pi}(0)_{1,2}^{(n)} &= \mathbf{\Pi}(0)_{2,1}^{(n)} = \mathbf{P}(L)_{18,19}^{(n-1)} \\
\mathbf{\Pi}(0)_{1,3}^{(n)} &= \mathbf{\Pi}(0)_{3,1}^{(n)} = \mathbf{P}(L)_{16,18}^{(n)}
\end{aligned}$$

where

$$\begin{aligned}
\mathbf{P}(L)_{16,18}^{(n)} &= \mathbf{E} \left(\delta x(L)_{p2}^{(n-1)} \cdot \delta x(0)_{p2}^{(n)} \right) \\
&= \mathbf{E} \left(\delta x(L)_{p2}^{(n-1)} \cdot (\delta x(L)^{(n-1)} + 2\delta z(L)^{(n-1)} - 5\delta \theta(L)^{(n-1)}) \right) \\
&= \mathbf{P}(L)_{18,1}^{(n-1)} + 2\mathbf{P}(L)_{18,3}^{(n-1)} - 5\mathbf{P}(L)_{18,8}^{(n-1)} \pm 2y_p \mathbf{P}(L)_{18,7}^{(n-1)} \mp y_p \mathbf{P}(L)_{18,9}^{(n-1)}
\end{aligned}$$

$$\mathbf{\Pi}(0)_{2,3}^{(n)} = \mathbf{\Pi}(0)_{3,2}^{(n)} = \mathbf{P}(L)_{17,18}^{(n)}$$

where

$$\begin{aligned}
\mathbf{P}(L)_{17,18}^{(n)} &= \mathbf{E} \left(\delta y(L)_{p2}^{(n-1)} \cdot \delta x(0)_{p2}^{(n)} \right) \\
&= \mathbf{E} \left(\delta y(L)_{p2}^{(n-1)} \cdot (\delta x(L)^{(n-1)} + 2\delta z(L)^{(n-1)} - 5\delta \theta(L)^{(n-1)} \pm 2y_p \delta \phi(L)^{(n-1)} \right. \\
&\quad \left. \mp y_p \delta \psi(L)^{(n-1)} + \xi) \right) \\
&= \mathbf{P}(L)_{19,1}^{(n-1)} + 2\mathbf{P}(L)_{19,3}^{(n-1)} - 5\mathbf{P}(L)_{19,8}^{(n-1)} \pm 2y_p \mathbf{P}(L)_{19,7}^{(n-1)} \mp y_p \mathbf{P}(L)_{19,9}^{(n-1)}
\end{aligned}$$

$$\mathbf{\Pi}(0)_{3,4}^{(n)} = \mathbf{\Pi}(0)_{4,3}^{(n)} = \mathbf{P}(L)_{18,19}^{(n)}$$

where

$$\begin{aligned}
\mathbf{P}(L)_{18,19}^{(n)} &= \mathbf{E} \left(\delta y(0)_{p2}^{(n)} \cdot \delta x(0)_{p2}^{(n)} \right) \\
&= \mathbf{E} \left((\delta y(L)^{(n-1)} + \delta \phi(L)^{(n-1)} + 2\delta \psi(L)^{(n-1)} \pm y_p \delta z(L)^{(n-1)} \mp 2y_p \delta \theta(L)^{(n-1)} \right.
\end{aligned}$$

$$\begin{aligned}
& + y_p^2 \delta \phi(L)^{(n-1)} + \eta) \cdot (\delta x(L)^{(n-1)} + 2\delta z(L)^{(n-1)} - 5\delta \theta(L)^{(n-1)} \pm 2y_p \delta \phi(L)^{(n-1)} \\
& \mp y_p \delta \psi(L)^{(n-1)} + \xi) \Big) \\
& = \mathbf{P}(L)_{1,2}^{(n-1)} + 2\mathbf{P}(L)_{2,3}^{(n-1)} - 5\mathbf{P}(L)_{2,8}^{(n-1)} + \mathbf{P}(L)_{1,7}^{(n-1)} + 2\mathbf{P}(L)_{3,7}^{(n-1)} - 5\mathbf{P}(L)_{7,8}^{(n-1)} + 2\mathbf{P}(L)_{1,9}^{(n-1)} \\
& + 4\mathbf{P}(L)_{3,9}^{(n-1)} - 10\mathbf{P}(L)_{8,9}^{(n-1)} \pm y_p \mathbf{P}(L)_{1,3}^{(n-1)} \mp 2y_p \mathbf{P}(L)_{1,8}^{(n-1)} + y_p^2 \mathbf{P}(L)_{1,7}^{(n-1)} \pm 2y_p \mathbf{P}(L)_{3,3}^{(n-1)} \\
& \mp 4y_p \mathbf{P}(L)_{3,8}^{(n-1)} + 2y_p^2 \mathbf{P}(L)_{3,7}^{(n-1)} \mp 5y_p \mathbf{P}(L)_{3,8}^{(n-1)} \pm 10y_p \mathbf{P}(L)_{8,8}^{(n-1)} - 5y_p^2 \mathbf{P}(L)_{7,8}^{(n-1)} \\
& \pm 2y_p \mathbf{P}(L)_{2,7}^{(n-1)} \pm 2y_p \mathbf{P}(L)_{7,7}^{(n-1)} \pm 4y_p \mathbf{P}(L)_{7,9}^{(n-1)} + 2y_p^2 \mathbf{P}(L)_{3,7}^{(n-1)} - 4y_p^2 \mathbf{P}(L)_{7,8}^{(n-1)} \\
& \pm 2y_p^3 \mathbf{P}(L)_{7,7}^{(n-1)} \mp y_p \mathbf{P}(L)_{2,9}^{(n-1)} \mp y_p \mathbf{P}(L)_{7,9}^{(n-1)} \mp 2y_p \mathbf{P}(L)_{9,9}^{(n-1)} - y_p^2 \mathbf{P}(L)_{3,9}^{(n-1)} + 2y_p^2 \mathbf{P}(L)_{8,9}^{(n-1)} \\
& \mp y_p^3 \mathbf{P}(L)_{7,9}^{(n-1)}
\end{aligned}$$

$$\mathbf{\Pi}(0)_{1,4}^{(n)} = \mathbf{\Pi}(0)_{4,1}^{(n)} = \mathbf{P}(L)_{16,19}^{(n)}$$

where

$$\begin{aligned}
\mathbf{P}(L)_{16,19}^{(n)} & = \mathbf{E} \left(\delta y(0)_{p2}^{(n)} \cdot \delta x(L)_{p2}^{(n-1)} \right) \\
& = \mathbf{E} \left((\delta y(L)^{(n-1)} + \delta \phi(L)^{(n-1)} + 2\delta \psi(L)^{(n-1)} \pm y_p \delta z(L)^{(n-1)} \mp 2y_p \delta \theta(L)^{(n-1)} \right. \\
& \quad \left. + y_p^2 \delta \phi(L)^{(n-1)} + \eta) \cdot \delta x(L)_{p2}^{(n-1)} \right) \\
& = \mathbf{P}(L)_{18,2}^{(n-1)} + \mathbf{P}(L)_{7,18}^{(n-1)} + 2\mathbf{P}(L)_{9,18}^{(n-1)} \pm y_p \mathbf{P}(L)_{3,18}^{(n-1)} \mp 2y_p \mathbf{P}(L)_{8,18}^{(n-1)} + y_p^2 \mathbf{P}(L)_{7,18}^{(n-1)}
\end{aligned}$$

$$\mathbf{\Pi}(0)_{2,4}^{(n)} = \mathbf{\Pi}(0)_{4,2}^{(n)} = \mathbf{P}(L)_{17,19}^{(n)}$$

where

$$\begin{aligned}
\mathbf{P}(L)_{17,19}^{(n)} & = \mathbf{E} \left(\delta y(0)_{p2}^{(n)} \cdot \delta y(L)_{p2}^{(n-1)} \right) \\
& = \mathbf{E} \left((\delta y(L)^{(n-1)} + \delta \phi(L)^{(n-1)} + 2\delta \psi(L)^{(n-1)} \pm y_p \delta z(L)^{(n-1)} \mp 2y_p \delta \theta(L)^{(n-1)} + y_p^2 \delta \phi(L)^{(n-1)} \right. \\
& \quad \left. + \eta) \cdot \delta y(L)_{p2}^{(n-1)} \right) \pm y_p \mathbf{P}(L)_{3,19}^{(n-1)} \\
& = \mathbf{P}(L)_{2,19}^{(n-1)} + \mathbf{P}(L)_{7,19}^{(n-1)} + 2\mathbf{P}(L)_{9,19}^{(n-1)} \mp 2y_p \mathbf{P}(L)_{8,19}^{(n-1)} + y_p^2 \mathbf{P}(L)_{7,19}^{(n-1)}
\end{aligned}$$

The state estimate transition for the fourth to the n th epochs is accomplished by

augmenting the first fifteen states of the previous epoch with the farthest ground feature

and zeros as follows

$$(\delta\hat{x}^+(L))^{(n+1)} = \begin{pmatrix} (\delta\hat{x}^+(L)_{15 \times 1})^{(n)} \\ (\delta\hat{x}^+(L)_{18})^{(n)} \\ (\delta\hat{x}^+(L)_{19})^{(n)} \\ \mathbf{0}_{2 \times 1} \end{pmatrix}_{19 \times 1} \quad (3.63)$$

Starting at epoch 4, the transitions for the remainder of the epochs followed Eqs. (3.62) and (3.63) for epoch 3, because there are no more known ground objects.

3.4.3 Summary. In summary, the KF is reinitialized at the beginning of each measurement epoch. The KF operates twice in each measurement epoch at a frequency of 0.2 [Hz] in 10 seconds. At the beginning of measurement epoch one, the exact state of the aircraft is known with very small uncertainties. The location of the two tracked ground features are known so the KF starts operation using the fifteen original states.

At the beginning of measurement epoch two, the first ground feature is dropped out of the FOV of the camera and the camera geolocates the first unknown ground feature, which becomes the second ground feature for the second measurement epoch. The INS provided state of the aircraft at the end of measurement epoch one is used to estimate the position of the newly acquired unknown ground feature. SLAM is achieved through the augmentation of the fifteen states state vector by two states (x and y position of the new ground feature) to a seventeen states state vector. Zeros are used for the augmentation because the derivative of position is zero.

In measurement epoch three and beyond, the errors in the position of the second unknown ground feature for the previous measurement epoch becomes the error in position of the first unknown ground feature. The INS provided state of the aircraft at the end of the previous measurement epoch is used to estimate the position of the newly acquired unknown ground feature. Because two unknown ground features are used from measurement epoch three and beyond, the KF operates with 19 states, which includes 15

original states and two states (x and y position of unknown ground feature) each from the two unknown ground features. SLAM is achieved through the augmentation of states at the beginning of each of these measurement epochs. Zeros are used for these augmentations because the derivative of position of the newly acquired unknown ground feature is zero.

4 Simulation Results

4.1 Introduction

This chapter shows simulation experiments that were run for the one hour duration. The chapter will start with plots showing the first three epochs of the first three navigation states for the INS. This information will then be followed by plots of the first three epochs of the aided INS. The effect of tracked ground features which are staggered is also discussed. Plots showing the remainder of the navigation states, for both the unaided and aided INS schemes are found in Appendix A.

4.2 Simulation

Simulation experiments were run to gauge the strength of the aiding action afforded by bearings only measurements using “bootstrapping” for cross country flight. The aim is to reduce the errors of the free INS as much as possible: the closer the KF-estimated and the true errors are, the better the aiding action is. To study the effects of using known and unknown ground features, the first three navigation states (position) estimation errors and standard deviations of the unaided (free) INS for the first three epochs are plotted in Figure 4.1. The error in the x position is of most concern and its uncertainty level after the duration of thirty seconds of flight is about 110 [cm], with a realized error in position of about 99 [cm]. For the same duration, the standard deviation of the aided INS and the difference in the error of the true and estimated x position are plotted in Figure 4.2. The uncertainty in the estimated x position (prediction of what the difference between the true and estimated errors will be) after the third epoch is about 25 [cm] (better than the free INS), with a realized error in position of about 27 [cm] (better than the free INS). It can be seen that with aiding, when the aircraft’s position is estimated by two known ground features, the errors in the position are almost negligible for the first epoch (first 10

seconds). For the second epoch (next 10 seconds), when aiding is achieved by using one known and one unknown geolocated ground feature, the errors start increasing because of the higher uncertainty added by the unknown feature's geolocation on the fly. With the lost of the last known ground feature and addition of another unknown feature, the uncertainty is even higher with the difference in the true and estimated error in position eventually falling outside the aided INS predicted standard deviation.

Next, the simulation results for the whole one hour flight for the free and aided INS are respectively plotted in Figures A.1 and A.2. The uncertainty in the x position for the free INS after one hour is about six and a half kilometers, with a realized error in position of about 6.02 [km] in Figure A.1. It can be seen from the plots that with aiding using the 9 mega pixel camera, the uncertainty in the x position is significantly reduced in Figure A.2. After a one hour duration, the uncertainty in x position is only about 693 [m] with a realized error in position of about 588 [m]. It is worth noting that from the third to the last epoch, even with the introduction of two unknown ground features as opposed to at least one known ground feature, the Kalman Filter learns and eventually reduce the estimation errors in the x position.

In the scenario where ground features are arranged in a straight line, though aiding was primarily achieved in the x position, the uncertainty and realized error in the y position are also significantly reduced from six and a half kilometers and 5.98 [km] to about 18.84 [m] and 1.78 [m] respectively. When the ground features are laterally staggered 10 [m] about the aircraft trajectory, Figure A.3, the uncertainty in the x and y positions remains almost the same. Beyond 10 [m] displacement, the KF is unstable. So, as long as the ground features are within the LOS of the camera, aiding in the x direction is not impacted, and there is little to no impact in the y direction.

There also are improvements in the other seven navigation states estimates, as shown in Figures A.2 through A.5. In Figures A.4 and A.5, the plots show how the KF closely

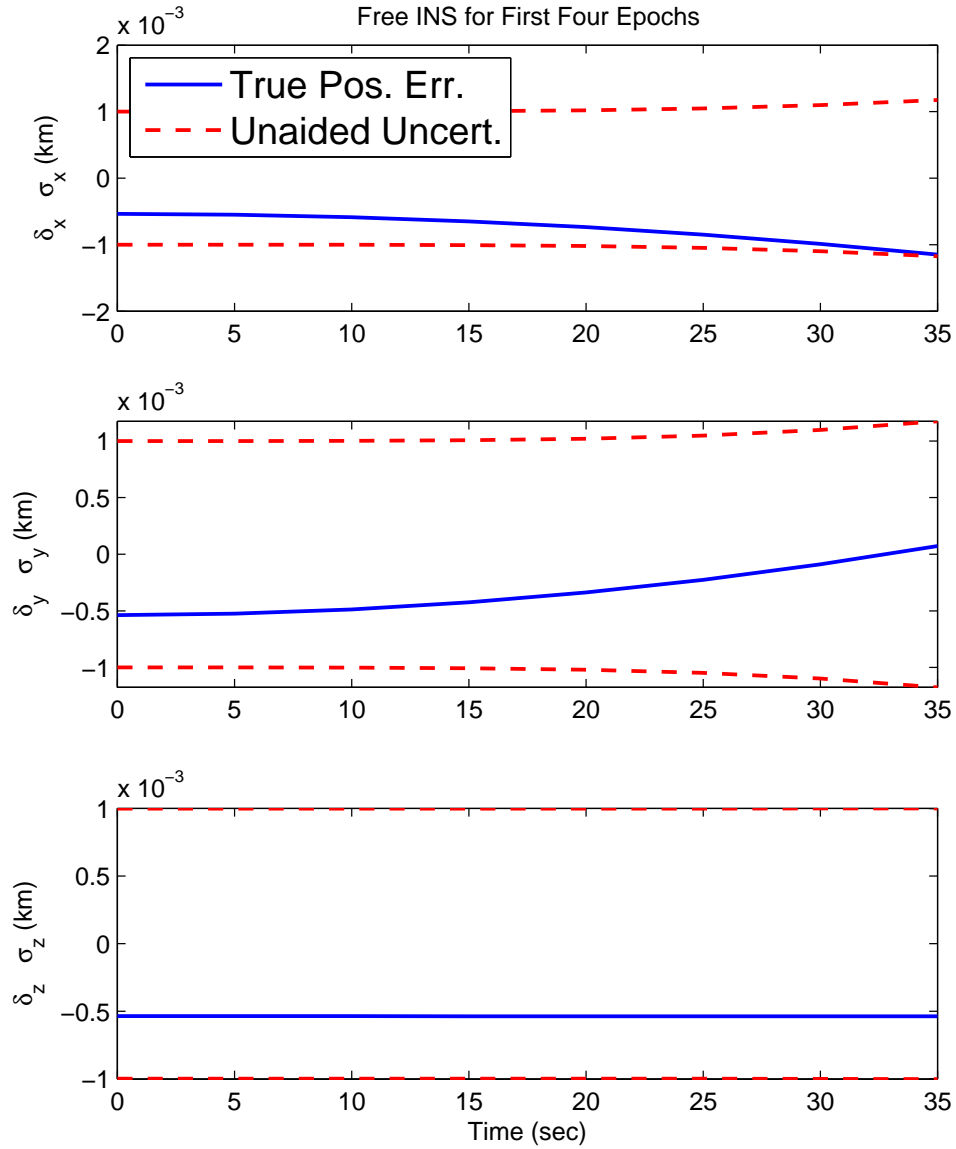


Figure 4.1: The development of the KF predicted standard deviation and realized position estimates of the unaided INS in the first three measurement epochs.

estimate the true error (again the aim is to closely track the true errors to eliminate their effect in the navigation process), thus achieving aiding action. This information is portrayed in Table 4.1.

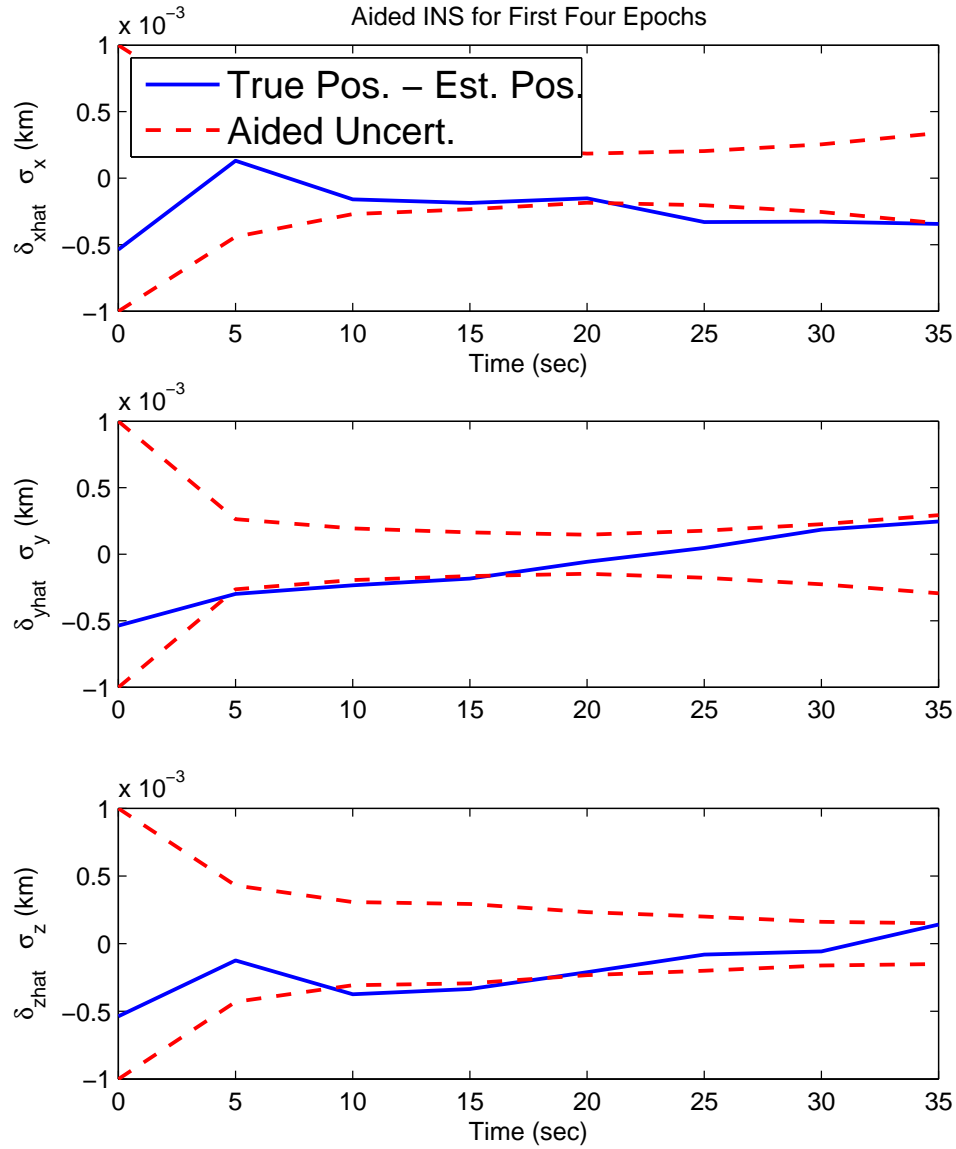


Figure 4.2: The development of the KF predicted standard deviation and realized position estimates of the aided INS for the first three measurement epochs.

The calculated first ground feature and geolocation of second ground feature are shown in Figure A.7. The x position of the first ground feature starts at one kilometer (because its position was exactly known) and it is calculated up to 360.61 [km] at the end of one hour. Its y position starts at zero and it is calculated up to about four and a half meters at the end of one hour. Likewise, the x position of the second ground feature starts

Table 4.1: The final values for the standard deviations and errors for the unaided navigation states. Also included are the final values for the standard deviations and errors for the aided navigation states in both the scenario when the ground features are in a straight line and when they are staggered.

Standard Deviation/Error	Unaided Final Value	Aided Final Value(Linear)	Aided Final Value(Staggered)
$\sigma_x (s.d)$	6.56 [km]	692.72 [m]	692.70 [m]
$\delta x (err)$	6.02 [km]	587.84 [m]	697.19 [m]
$\sigma_y (s.d)$	6.56 [km]	18.84 [m]	18.88 [m]
$\delta y (err)$	5.98 [km]	1.78 [m]	2.54 [m]
$\sigma_z (s.d)$	707.11 [m]	5.72 [m]	5.72 [m]
$\delta z (err)$	18.96 [m]	5.04 [m]	5.60 [m]
$\sigma_{v_x} (s.d)$	3.67×10^{-2} [m/s]	5.74×10^{-3} [m/s]	5.74×10^{-3} [m/s]
$\delta v_x (err)$	3.21×10^{-2} [m/s]	5.15×10^{-3} [m/s]	5.53×10^{-3} [m/s]
$\sigma_{v_y} (s.d)$	3.67×10^{-2} [m/s]	8.66×10^{-5} [m/s]	8.70×10^{-5} [m/s]
$\delta v_y (err)$	3.19×10^{-2} [m/s]	4.54×10^{-5} [m/s]	2.52×10^{-6} [m/s]
$\sigma_{v_z} (s.d)$	3.93×10^{-3} [m/s]	3.18×10^{-5} [m/s]	3.18×10^{-5} [m/s]
$\delta v_z (err)$	1.02×10^{-4} [m/s]	2.86×10^{-5} [m/s]	3.06×10^{-5} [m/s]
$\sigma_\phi (s.d)$	1.05×10^{-4} [rad]	1.09×10^{-5} [rad]	1.09×10^{-5} [rad]
$\delta\phi (err)$	7.82×10^{-5} [rad]	1.10×10^{-6} [rad]	1.38×10^{-6} [rad]
$\sigma_\theta (s.d)$	1.05×10^{-4} [rad]	3.27×10^{-5} [rad]	3.27×10^{-5} [rad]
$\delta\theta (err)$	7.82×10^{-5} [rad]	3.30×10^{-5} [rad]	2.94×10^{-5} [rad]
$\sigma_\psi (s.d)$	1.05×10^{-4} [rad]	5.85×10^{-5} [rad]	5.87×10^{-5} [rad]
$\delta\psi (err)$	7.82×10^{-5} [rad]	1.02×10^{-5} [rad]	1.66×10^{-5} [rad]

at two kilometers (because its position was exactly known) and it is calculated up to 361.60 [km] at the end of one hour. Its y position starts at zero and it is calculated up to

about five and a fifth meters at the end of one hour. Figures A.8 and A.9 shows the uncertainties of the first eight epochs of the first and second ground features. Each epoch consists of 2 bearing measurements which are sampled at a rate of 0.2 [Hz]. Each spike corresponds to the utilization of bearing measurements. During a measurement epoch the error increases. At the beginning of a new measurement epoch the knowledge from the previous epochs causes the errors to decrease.

The errors in the positions of the aircraft with the attendant uncertainties for the aided INS, and the two calculated ground features, are shown in Figure A.10. This shows the accuracy in the calculated ground features and how well they are used to estimate errors in the aircraft navigation process.

5 Conclusion

In [12] covariance analysis was performed and it was shown that the rate of growth of position uncertainty is significantly reduced when the aircraft continuously uses the measurement of the bearings of sequentially acquired unknown terrain features to aid the INS. In this paper the analysis is refined. The LOS errors that will be present when using an optical camera to aid the INS are accounted for. Furthermore, in this paper the Kalman Filter's design is provided and its performance is validated by simulation of the KF action. The on-board INS of an aircraft was aided by an optical camera used to take the bearing measurements of ground features. So long as the ground features are regularly spaced and are not more laterally displaced than 10 [m] about the aircraft's trajectory, the LOS of the camera, the INS aiding action is strong. It is a cyclic process where the aircraft uses its INS-provided ownship position to geolocate a ground object, then uses the bearing measurements of the very same ground feature to aid its INS.

The navigation state of most concern was the aircraft's position. For a one hour flight, it was shown that with INS aiding, the error in the aided INS navigation system provided position of the aircraft was significantly reduced from about 3.87 [km] with a KF predicted uncertainty of about 6.5 [km], to about 583 [m] with an uncertainty of 693 [m]. This validates our analysis and showed that INS aiding using vision is possible for long range flight. The practicality of this INS aiding scheme hinges on the robustness of the image registration scheme, in particular, in an outdoors setting. In [5], [6], and [7] these issues are addressed using the Scale-Invariant Feature Transform (SIFT) algorithms to detect images registered on an optical camera's focal plane.

Appendix A: Simulation Results

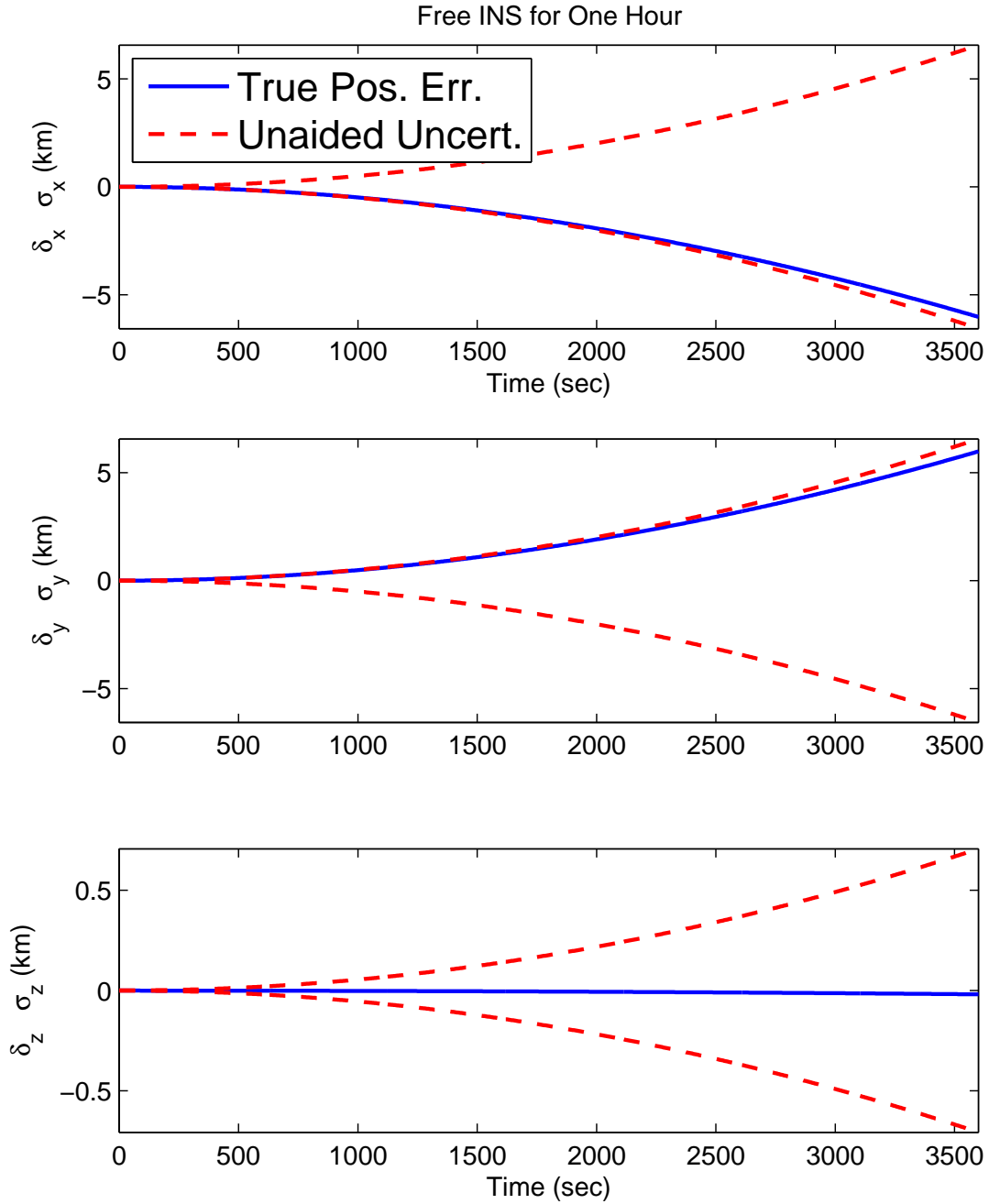


Figure A.1: The development of the KF predicted standard deviation and realized position estimate of the aided INS during a one hour flight.

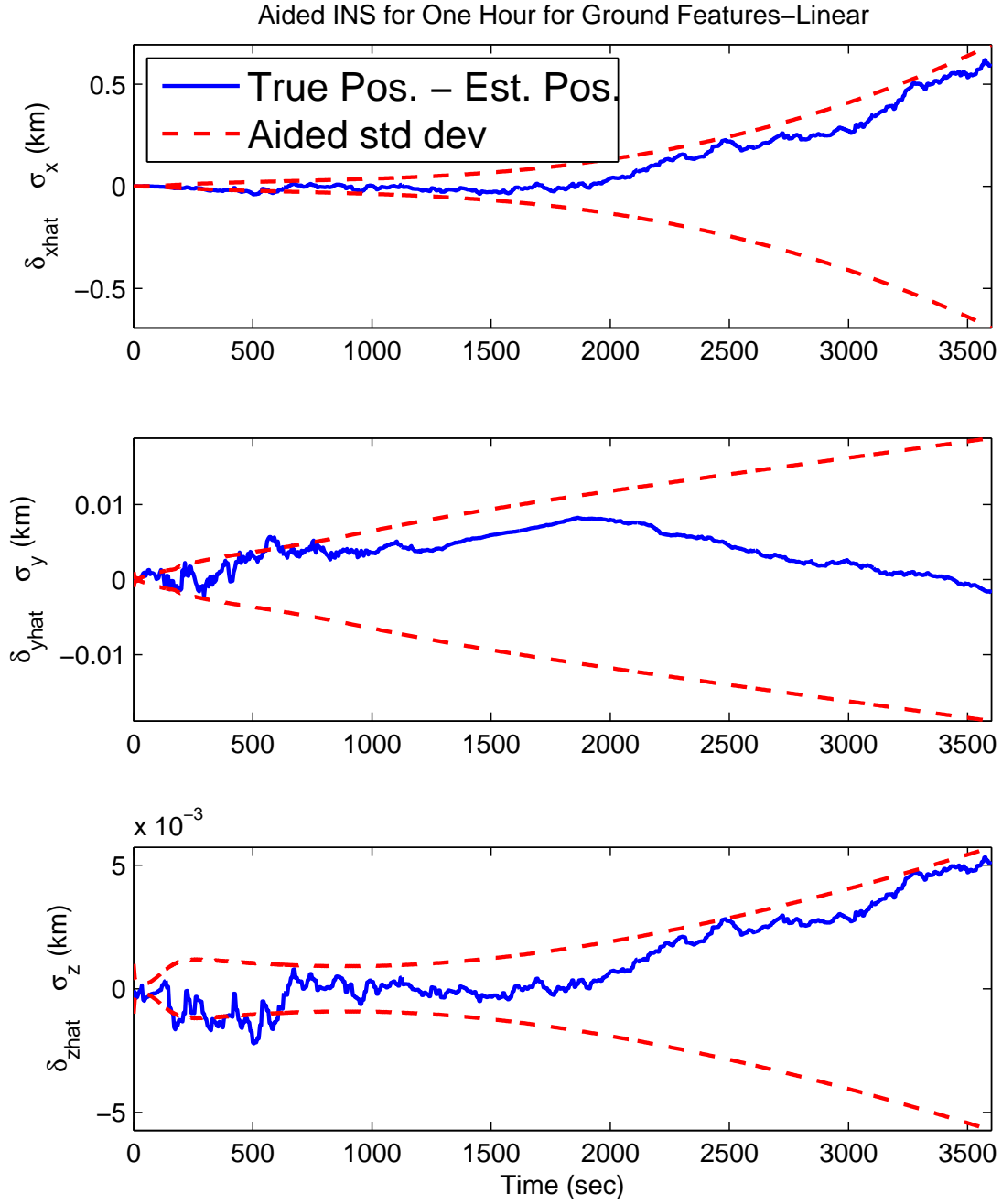


Figure A.2: The development of the KF predicted standard deviation and realized position estimates of the aided INS during a one hour flight for ground features arranged in a straight line.

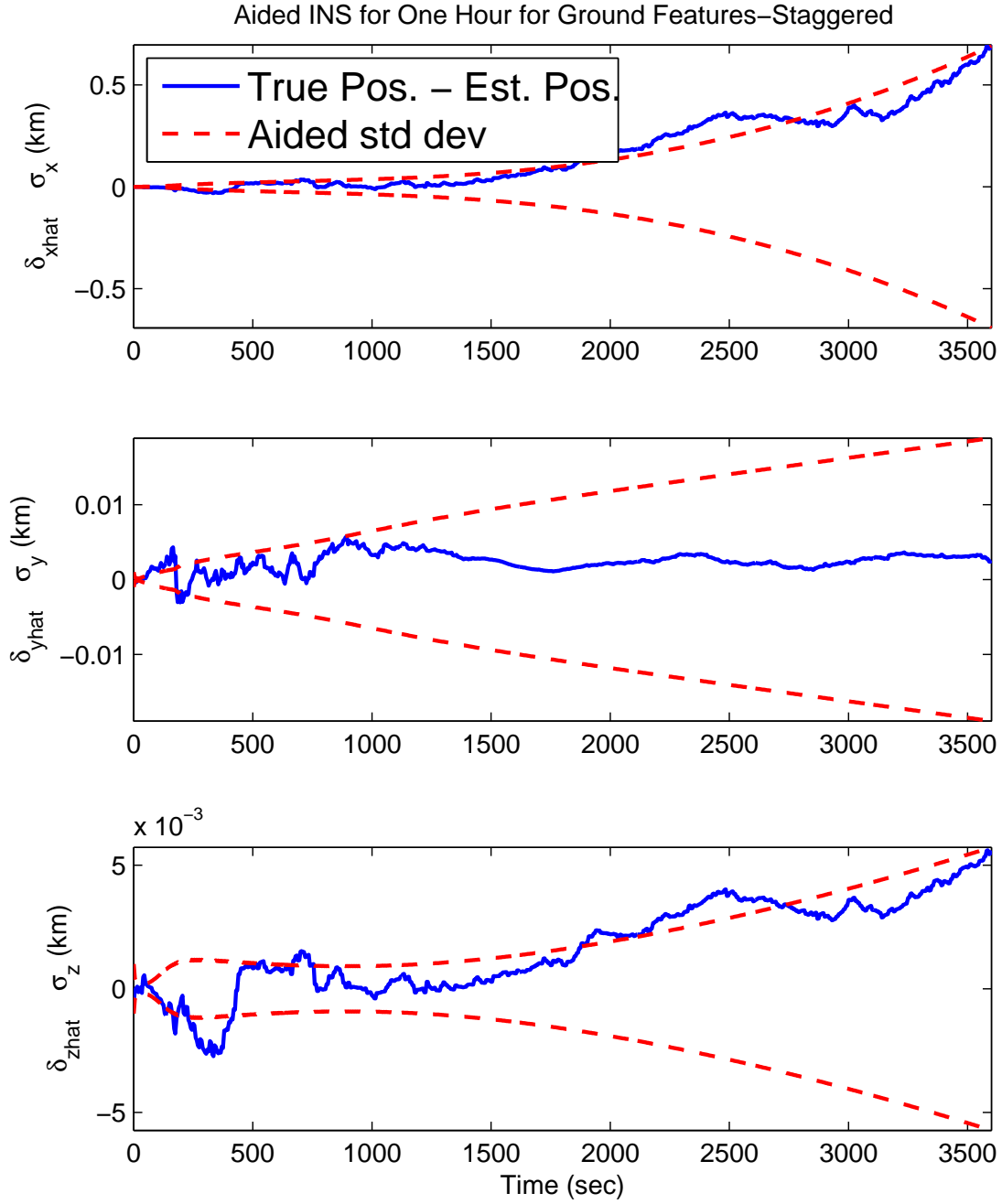


Figure A.3: The development of the KF predicted standard deviation and realized position estimates in the aided INS during a one hour flight for staggered ground features.

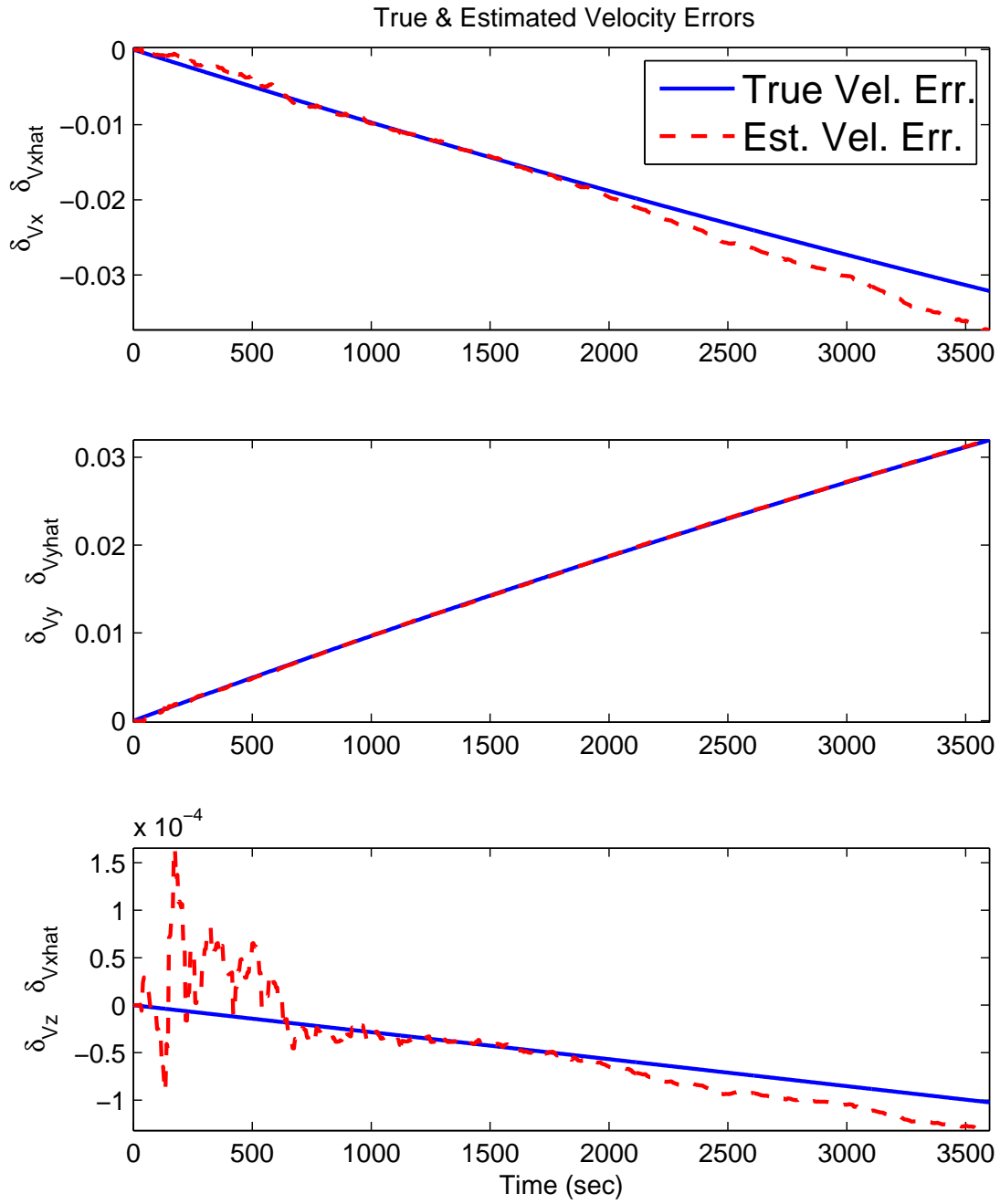


Figure A.4: The development of velocity estimates in the aided INS during a one hour flight.

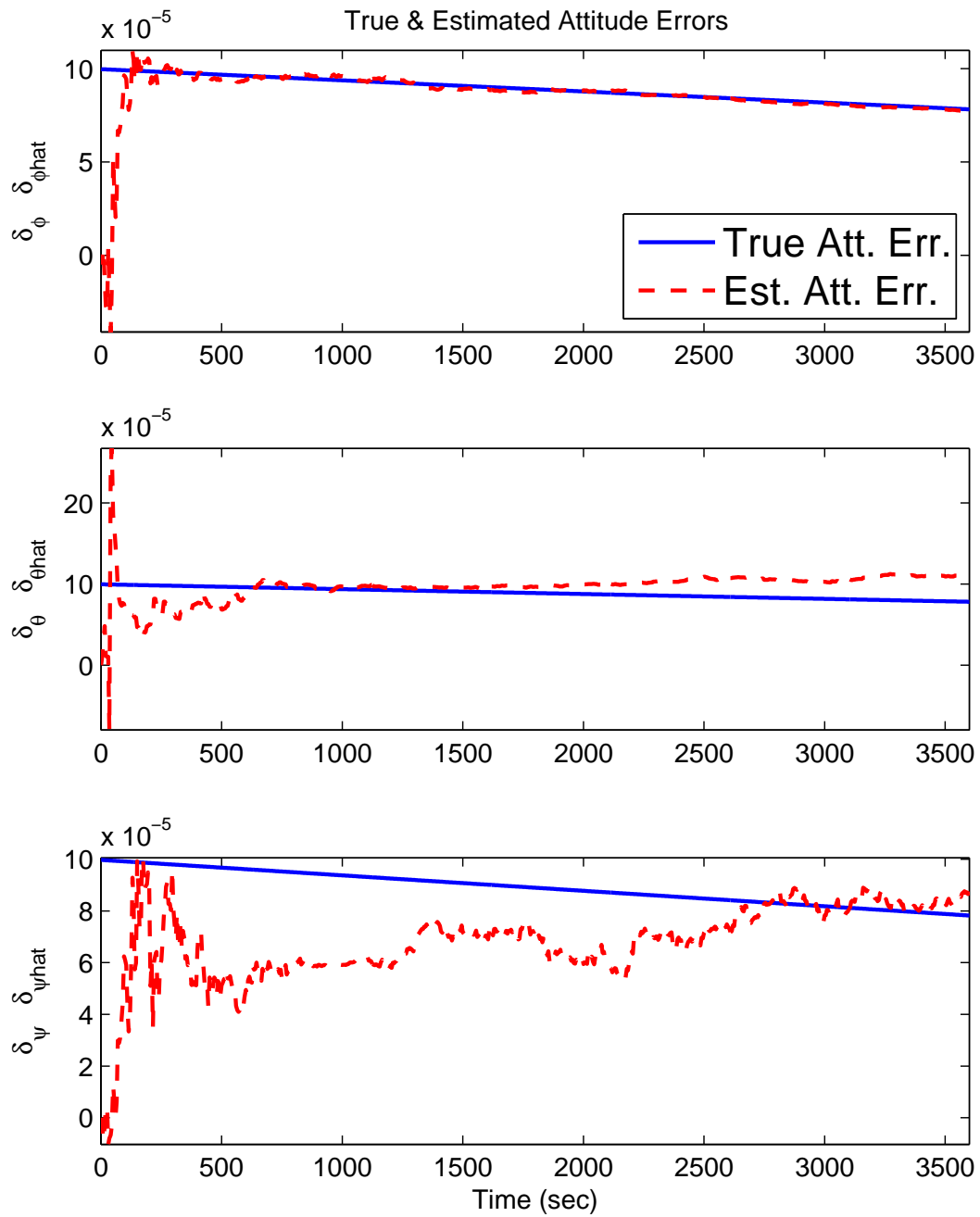


Figure A.5: The development of attitude estimates in the aided INS during a one hour flight.

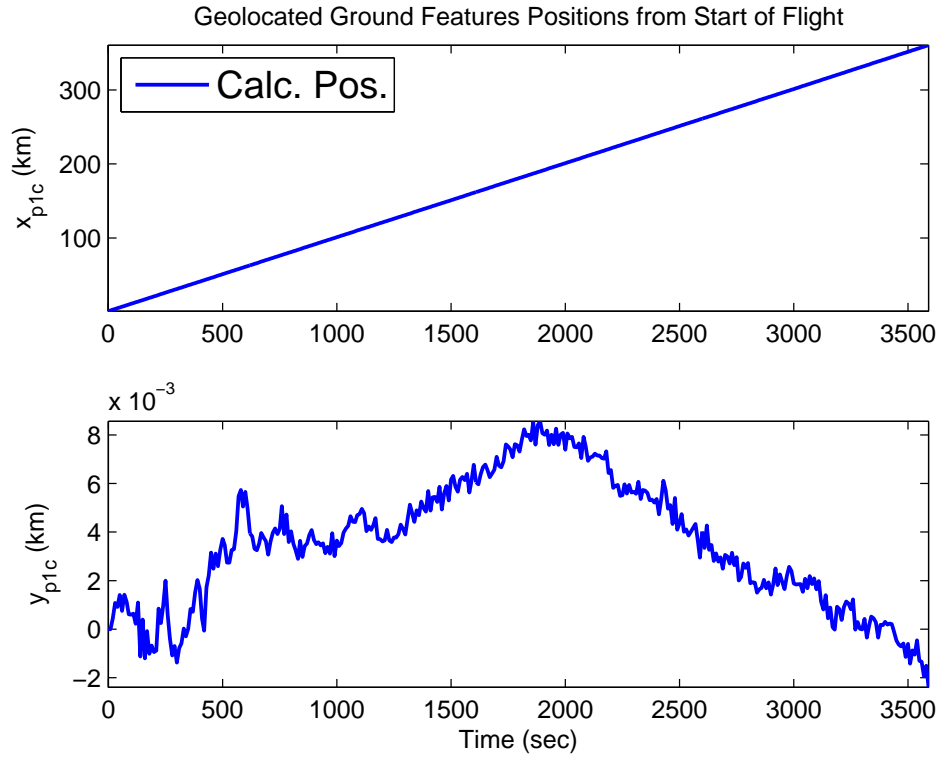


Figure A.6: The calculated position of the first ground feature.

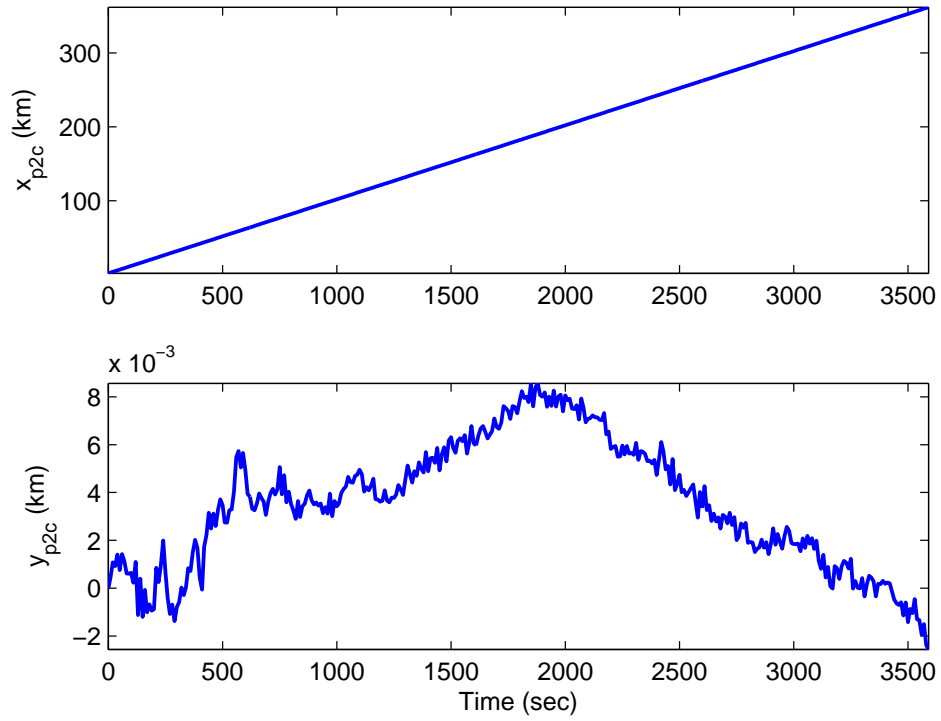


Figure A.7: The geolocated second ground feature's position.

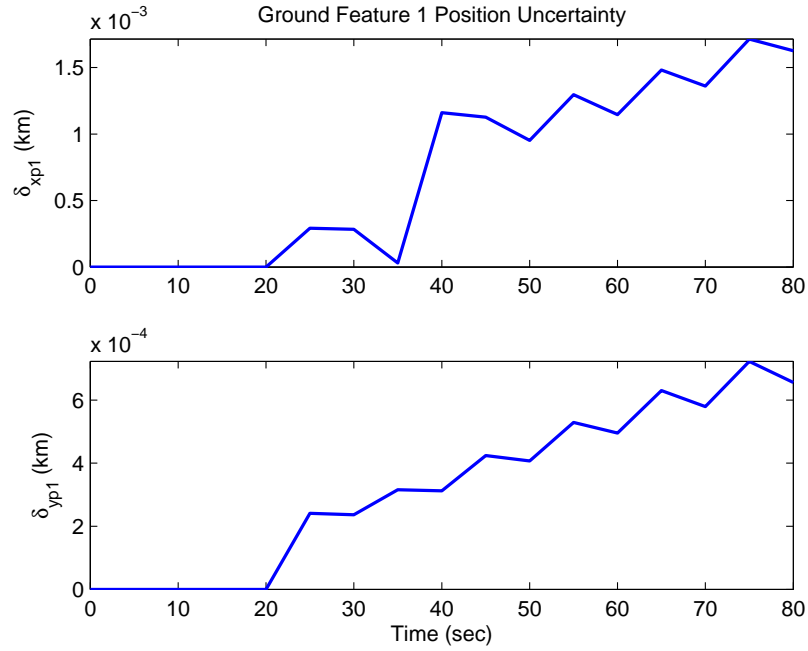


Figure A.8: A zoomed in view of the development of the KF predicted standard deviation of the first ground feature's position in first seven measurement epochs.

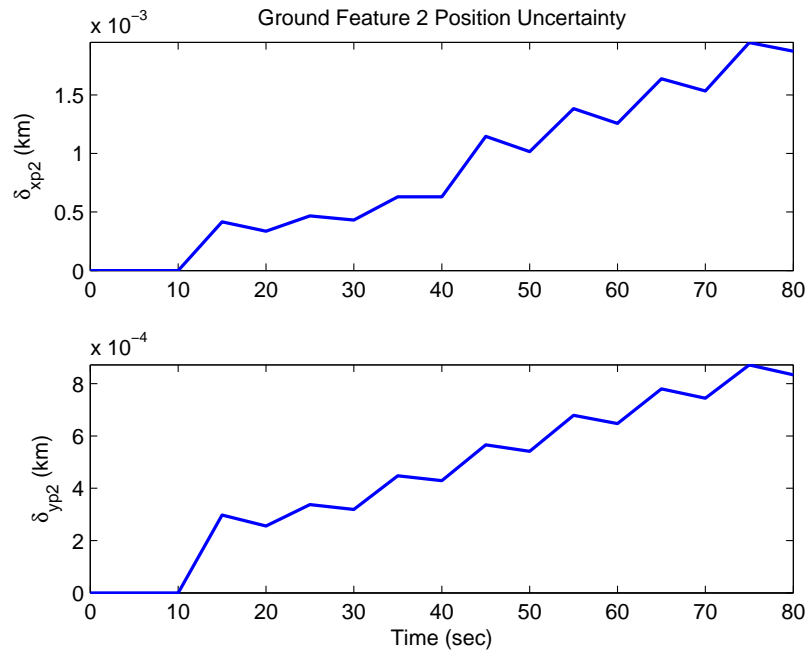


Figure A.9: A zoomed in view of the development of the KF predicted standard deviation of the second ground object's position in first seven measurement epochs.

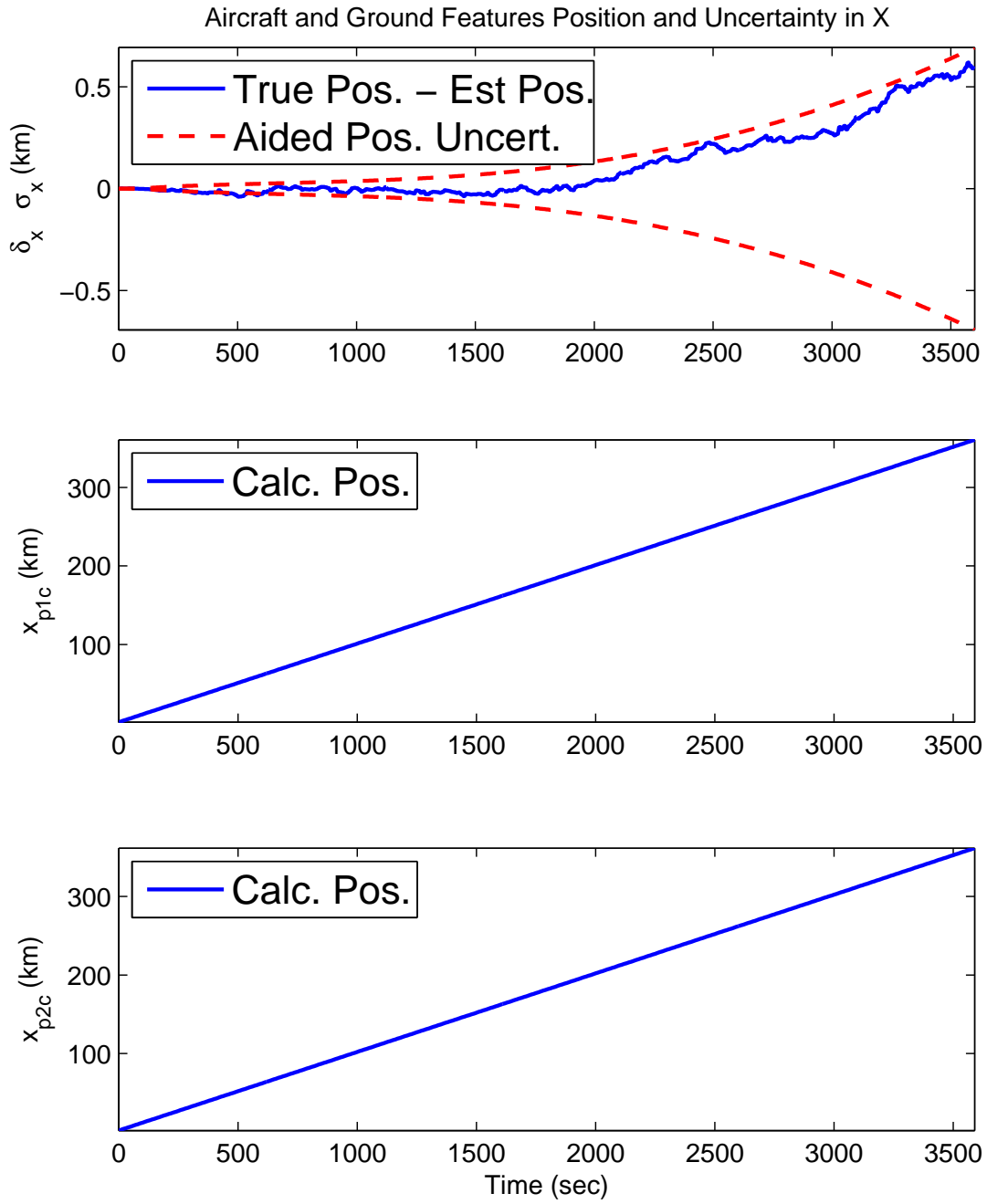


Figure A.10: Aircraft and ground objects' position estimates with KF predicted standard deviations.

Appendix B: Ground Feature Calculations

The calculation and geolocation of ground features used for aiding are shown in Tables B.1 - B.3 below:

Table B.1: Ground Features on X-Axis: X Position

Epoch #	x_{p1c}	x_{p2c}
1	1	2
2	2	$3 + \delta \hat{x}(L)$
$n(\geq 3)$	$n + \delta \hat{x}(L(n - 2))$	$n + 1 + \delta \hat{x}(L(n - 1))$

Table B.2: Ground Features on X-Axis: Y Position

Epoch #	y_{p1c}	y_{p2c}
1	0	0
2	0	$\delta \hat{y}(L)$
$n(\geq 3)$	$\delta \hat{y}(L(n - 2))$	$\delta \hat{y}(L(n - 1))$

Table B.3: Y Positions of Laterally Staggered Ground Features on Both Sides of X-Axis

Epoch #	y_{p1c}	y_{p2c}
1	$-y_p$	y_p
2	y_p	$-y_p + \delta \hat{y}(L)$
$n(\geq 3)$	$-y_p + \delta \hat{y}(L(n - 2))$	$y_p + \delta \hat{y}(L(n - 1))$

where n is the epoch number.

Bibliography

- [1] Bowditch, Nathaniel. *The American Practical Navigator*. National Imagery and Mapping Agency, Bethesda, MD, 2002.
- [2] Durrant-Whyte, H. and T. Bailey. “Simultaneous localization and mapping: part I”. *Robotics Automation Magazine, IEEE*, 13(2):99 –110, june 2006. ISSN 1070-9932.
- [3] Giebner, M. *Tightly-Coupled Image-Aided Inertial Navigation System via a Kalman Filter*. Master’s thesis, AFIT, WPAFB, OH, 2003.
- [4] Hartley, Richard and Andrew Zisserman. *Multiple View Geometry in Computer Vision*. Cambridge University Press, New York, NY, 2003.
- [5] Lowe, David G. “Object Recognition from Local Scale-Invariant Features”. *International Journal of Computer Vision*, 1150–1157, September 1999.
- [6] Lowe, David G. “Distinctive Image Features from Scale-Invariant Keypoints”. *International Journal of Computer Vision*, 60(2):91–110, 2004.
- [7] Lowe, David G. “Local Feature View Clustering for 3D Object Recognition”. *IEEE Conference on Computer Vision and Pattern Recognition*, 682–688, December 2001.
- [8] Maybeck, Peter S. *Stochastic Models, Estimation, and Control Volume 2*. Academic Press, New York, NY, 1983.
- [9] Pachter, M. and G. Mutlu. *Dynamics of Information Systems: Theory and Application*, chapter The Navigation Potential of Ground Feature Tracking, 287–303. Springer, 2010.
- [10] Pachter, M., A. Porter, and M. Polat. “INS Aiding Using Bearing-Only Measurements of an Unknown Ground Object”. *ION Journal Navigation*, 53(1):1–20, 2006.
- [11] Relyea, A. *Covariance Analysis of Vision Aided Navigation by Bootstrapping*. Master’s thesis, Air Force Institute of Technology, WPAFB, OH, March 2012.
- [12] Relyea, Andrew and Meir Pachter. “A Covariance Analysis of Vision-Aided Inertial Navigation: 3-D case”. 568–587. Bar Itzhack Symposium, Haifa, Israel, October 14-17, 2012.
- [13] Titterton, David and John Weston. *Strapdown Inertial Navigation Technology 2nd Edition*. The Institution of Engineering and Technology, London, UK, 2004.
- [14] Veth, M. *Fusion of Imaging and Inertial Sensors for Navigation*. Ph.D. thesis, Air Force Institute of Technology, WPAFB, OH, September 2006.

REPORT DOCUMENTATION PAGE			Form Approved OMB No. 0704-0188		
The public reporting burden for this collection of information is estimated to average 1 hour per response, including the time for reviewing instructions, searching existing data sources, gathering and maintaining the data needed, and completing and reviewing the collection of information. Send comments regarding this burden estimate or any other aspect of this collection of information, including suggestions for reducing this burden to Department of Defense, Washington Headquarters Services, Directorate for Information Operations and Reports (0704-0188), 1215 Jefferson Davis Highway, Suite 1204, Arlington, VA 22202-4302. Respondents should be aware that notwithstanding any other provision of law, no person shall be subject to any penalty for failing to comply with a collection of information if it does not display a currently valid OMB control number. PLEASE DO NOT RETURN YOUR FORM TO THE ABOVE ADDRESS.					
1. REPORT DATE (DD-MM-YYYY) 03-2013		2. REPORT TYPE Master's Thesis		3. DATES COVERED (From — To) May 2012 – Mar 2013	
4. TITLE AND SUBTITLE Inertial Navigation System Aiding Using Vision			5a. CONTRACT NUMBER		
			5b. GRANT NUMBER		
			5c. PROGRAM ELEMENT NUMBER		
6. AUTHOR(S) Quarmyne, James, O, 2Lt, USAF			5d. PROJECT NUMBER		
			5e. TASK NUMBER		
			5f. WORK UNIT NUMBER		
7. PERFORMING ORGANIZATION NAME(S) AND ADDRESS(ES) Air Force Institute of Technology Graduate School of Engineering and Management (AFIT/ENY) 2950 Hobson Way WPAFB OH 45433-7765			8. PERFORMING ORGANIZATION REPORT NUMBER AFIT-ENG-13-M-40		
9. SPONSORING / MONITORING AGENCY NAME(S) AND ADDRESS(ES) Dr. Robert A. Murphey Air Force Research Laboratory, Munitions Directorate AFRL/RWG 101 West Eglin Boulevard Eglin AFB, FL 32542-6810			10. SPONSOR/MONITOR'S ACRONYM(S) AFRL/RWG		
			11. SPONSOR/MONITOR'S REPORT NUMBER(S)		
12. DISTRIBUTION / AVAILABILITY STATEMENT APPROVED FOR PUBLIC RELEASE; DISTRIBUTION UNLIMITED					
13. SUPPLEMENTARY NOTES This material is declared a work of the U.S. Government and is not subject to copyright protection in the United States.					
14. ABSTRACT The aiding of an INS using measurements over time of the line of sight of ground features as they come into view of an onboard camera is investigated. The objective is to quantify the reduction in the navigation states' errors by using bearings-only measurements over time of terrain features in the aircraft's field of view. INS aiding is achieved through the use of a Kalman Filter. The design of the Kalman Filter is presented and it is shown that during a long range, wings level cruising flight at constant velocity and altitude, a 90% reduction in the aided INS-calculated navigation state errors compared to a free INS, is possible.					
15. SUBJECT TERMS INS Aiding, Bearings-Only Measurements, Kalman Filter, SLAM					
16. SECURITY CLASSIFICATION OF:			17. LIMITATION OF ABSTRACT UU	18. NUMBER OF PAGES 90	19a. NAME OF RESPONSIBLE PERSON Dr. Meir Pachter, ENG
a. REPORT U	b. ABSTRACT U	c. THIS PAGE U			19b. TELEPHONE NUMBER (Include Area Code) (937)255-3636, ext 7247